

# CITATION REPORT

List of articles citing

The interpretation of protein structures: estimation of static accessibility

DOI: 10.1016/0022-2836(71)90324-x  
Journal of Molecular Biology, 1971, 55, 379-400.

**Source:** <https://exaly.com/paper-pdf/10434853/citation-report.pdf>

**Version:** 2024-04-25

This report has been generated based on the citations recorded by exaly.com for the above article. For the latest version of this publication list, visit the link given above.

The third column is the impact factor (IF) of the journal, and the fourth column is the number of citations of the article.

| #    | Paper   | IF | Citations |
|------|---|----|-----------|
| 2319 | mkgridXf: Consistent Identification of Plausible Binding Sites Despite the Elusive Nature of Cavities and Grooves in Protein Dynamics.                      |    |           |
| 2318 | A New Mixed All-Atom/Coarse-Grained Model: Application to Melittin Aggregation in Aqueous Solution.   |    |           |
| 2317 | Explicit Solvent Hydration Benchmark for Proteins with Application to the PBSA Method.  |    |           |
| 2316 | Combined Molecular Dynamics and Density Functional Theory Study of AzobenzeneGraphene Interfaces.   |    |           |
| 2315 | Importance of Atomic Contacts in Vibrational Energy Flow in Proteins.   |    |           |
| 2314 | Chameleonic Dye Adapts to Various Environments Shining on Macrocycles or Peptide and Polysaccharide Aggregates.   |    |           |
| 2313 | .   |    |           |
| 2312 | 24 Bovine Pancreatic Ribonuclease. <b>1971</b> , 647-806  |    | 279       |
| 2311 | 21 Vertebrate Lysozymes. <b>1972</b> , 7, 665-868   |    | 246       |
| 2310 | [43] cyanuration. <b>1972</b> , 25, 506-14  |    | 1         |
| 2309 | Comparison of the effects of various detergents on antigen-antibody interaction. <b>1972</b> , 22, 210-212  |    | 65        |
| 2308 | Ionization behavior of the catalytic carboxyls of lysozyme. Effects of temperature. <b>1972</b> , 11, 1630-3  |    | 20        |
| 2307 | A study on the conformation and conformational stability of ribonuclease A and its peptic derivative, des-(121-124)-ribonuclease. <b>1972</b> , 11, 1980-90 |    | 61        |
| 2306 | Hydrogen exchange. <b>1972</b> , 41, 903-24   |    | 445       |
| 2305 | Cooperative conformational changes in globular proteins. <b>1972</b> , 11, 894-6  |    | 21        |
| 2304 | Kooperative Konformationsänderungen von globulären Proteinen. <b>1972</b> , 84, 931-944   |    | 12        |
| 2303 | Protein Structure and Stability: Conventional Wisdom and New Perspectives. <b>1973</b> , 38, 740-743  |    | 7         |

|      |   |     |     |
|------|---|-----|-----|
| 2302 | Environment and exposure to solvent of protein atoms. Lysozyme and insulin. <i>Journal of Molecular Biology</i> , <b>1973</b> , 79, 351-71  | 6.5 | 972 |
| 2301 | Structural and functional role of leucine residues in proteins. <i>Journal of Molecular Biology</i> , <b>1973</b> , 74, 263-83  | 6.5 | 113 |
| 2300 | Rat pancreatic ribonuclease. II. Amino acid sequence. <b>1973</b> , 310, 161-73   |     | 35  |
| 2299 | Insulin self-association. Spectrum changes and thermodynamics. <b>1973</b> , 12, 4385-91  |     | 47  |
| 2298 | Nucleation, rapid folding, and globular intrachain regions in proteins. <b>1973</b> , 70, 697-701   |     | 671 |
| 2297 | A model for solvent contributions to polypeptide and protein circular dichroism. <b>1974</b> , 13, 1557-62  |     | 11  |
| 2296 | Hydrophobic bonding and accessible surface area in proteins. <b>1974</b> , 248, 338-9   |     | 813 |
| 2295 | Protein densities from X-ray crystallographic coordinates. <b>1974</b> , 248, 447-9   |     | 34  |
| 2294 | Sorption equilibria between proteins and cation exchangers. <b>1974</b> , 89, 239-250   |     | 4   |
| 2293 | The effect of chloroplatinite on the <sup>1</sup> H NMR spectrum of ribonuclease. Solvent accessibility of methionine residues. <b>1974</b> , 359, 13-21  |     | 12  |
| 2292 | Electrostatic effects in myoglobin. Hydrogen ion equilibria in sperm whale ferrimyoglobin. <b>1974</b> , 13, 2967-74  |     | 195 |
| 2291 | Molecular basis of the antigenic difference between two closely related lysozymes of known sequence: effect of internal substitutions. <b>1974</b> , 11, 153-6  |     | 27  |
| 2290 | Structural principles of the globular organization of protein chains. A stereochemical theory of globular protein secondary structure. <i>Journal of Molecular Biology</i> , <b>1974</b> , 88, 857-72 | 6.5 | 304 |
| 2289 | Native collagen has a two-banded structure. <i>Journal of Molecular Biology</i> , <b>1974</b> , 83, 1-16  | 6.5 | 56  |
| 2288 | The interpretation of protein structures: total volume, group volume distributions and packing density. <i>Journal of Molecular Biology</i> , <b>1974</b> , 82, 1-14                                  | 6.5 | 812 |
| 2287 | Lysozyme Bibliography: 1922-1972. <b>1974</b> , 493-621   |     |     |
| 2286 | X-Ray Studies of Protein Interactions. <b>1974</b> , 43, 475-507  |     | 153 |
| 2285 | The amino acid sequence of dromedary pancreatic ribonuclease. <b>1975</b> , 147, 505-11   |     | 48  |

|      |   |     |      |
|------|---|-----|------|
| 2284 | Stopped-flow fluorescence studies on saccharide binding to lysozyme. <b>1975</b> , 149, 411-22  |     | 30   |
| 2283 | 2 Flavodoxins and Electron-Transferring Flavoproteins. <b>1975</b> , 12, 57-118   |     | 106  |
| 2282 | Immunological comparison of azurins of known amino acid sequence. Dependence of cross-reactivity upon sequence resemblance. <b>1975</b> , 5, 291-305  |     | 84   |
| 2281 | Assignment of the histidine 12-threonine 45 hydrogen-bonded proton in the NMR spectrum of ribonuclease A in H <sub>2</sub> O. <b>1975</b> , 14, 959-74  |     | 32   |
| 2280 | Structural invariants in protein folding. <b>1975</b> , 254, 304-8  |     | 834  |
| 2279 | Principles of protein-protein recognition. <b>1975</b> , 256, 705-8   |     | 913  |
| 2278 | 4 Lactate Dehydrogenase. <b>1975</b> , 11, 191-292  |     | 225  |
| 2277 | Energetics of ligand binding to proteins. <b>1975</b> , 29, 1-83  |     | 412  |
| 2276 | Evolution at two levels in humans and chimpanzees. <b>1975</b> , 188, 107-16  |     | 2211 |
| 2275 | The stability of globular proteins. <b>1975</b> , 3, 1-43   |     | 522  |
| 2274 | Tropomyosin coiled-coil interactions: evidence for an unstaggered structure. <i>Journal of Molecular Biology</i> , <b>1975</b> , 98, 293-304  | 6.5 | 653  |
| 2273 | Logical analysis of the mechanism of protein folding III. Prediction of the strong long-range interactions. <i>Journal of Molecular Biology</i> , <b>1975</b> , 94, 257-81                              | 6.5 | 18   |
| 2272 | Volume occupation, environment and accessibility in proteins. The problem of the protein surface. <i>Journal of Molecular Biology</i> , <b>1975</b> , 96, 721-32  | 6.5 | 129  |
| 2271 | Refinement of the structure of carp muscle calcium-binding parvalbumin by model building and difference Fourier analysis. <i>Journal of Molecular Biology</i> , <b>1975</b> , 91, 201-25                | 6.5 | 379  |
| 2270 | Experimental and theoretical aspects of protein folding. <b>1975</b> , 29, 205-300  |     | 746  |
| 2269 | Hydrogen exchange kinetics changes upon formation of the soybean trypsin inhibitor-trypsin complex. <b>1975</b> , 14, 3419-23   |     | 15   |
| 2268 | Hydrogen-tritium exchange kinetics of soybean trypsin inhibitor (Kunitz). Solvent accessibility in the folded conformation. <b>1975</b> , 14, 3413-9  |     | 34   |
| 2267 | Electrostatic effects in myoglobin. Application of the modified Tanford-Kirkwood theory to myoglobins from horse, California grey whale, harbor seal, and California sea lion. <b>1975</b> , 14, 1352-8 |     | 39   |

|      |  |     |      |
|------|--|-----|------|
| 2266 | Nuclear magnetic resonance studies of hemoglobin: functional state correlations and isotopic enrichment strategies. <b>1975</b> , 3, 221-87                                      |     | 45   |
| 2265 | The role of solvent interactions in protein conformation. <b>1975</b> , 3, 165-219   |     | 175  |
| 2264 | Stability and specificity of protein-protein interactions: the case of the trypsin-trypsin inhibitor complexes. <i>Journal of Molecular Biology</i> , <b>1976</b> , 100, 197-211 | 6.5 | 105  |
| 2263 | A simplified representation of protein conformations for rapid simulation of protein folding. <i>Journal of Molecular Biology</i> , <b>1976</b> , 104, 59-107                    | 6.5 | 933  |
| 2262 | On the conformation of proteins: the handedness of the beta-strand-alpha-helix-beta-strand unit. <i>Journal of Molecular Biology</i> , <b>1976</b> , 105, 367-82                 | 6.5 | 155  |
| 2261 | Concentration-dependent hydrogen exchange kinetics of 3H-labeled S-peptide in ribonuclease S. <i>Journal of Molecular Biology</i> , <b>1976</b> , 105, 409-26                    | 6.5 | 62   |
| 2260 | Surface area of globular proteins. <i>Journal of Molecular Biology</i> , <b>1976</b> , 105, 13-4   | 6.5 | 57   |
| 2259 | The protein chemistry of enzymes. <b>1976</b> , 62, E20-9  |     |      |
| 2258 | X-ray enzymology. <b>1976</b> , 62, E30-6  |     | 8    |
| 2257 | Immunologic comparison of pancreatic ribonucleases. <b>1976</b> , 13, 653-8  |     | 17   |
| 2256 | The nature of the accessible and buried surfaces in proteins. <i>Journal of Molecular Biology</i> , <b>1976</b> , 105, 1-12  | 6.5 | 1042 |
| 2255 | Role of subunit interfaces in the allosteric mechanism of hemoglobin. <b>1976</b> , 73, 3793-7   |     | 71   |
| 2254 | A neutron small-angle scattering study of hen egg-white lysozyme. <b>1976</b> , 32, 67-74  |     | 48   |
| 2253 | Amino acid sequence and immunological properties of chalchalaca egg white lysozyme. <b>1976</b> , 8, 59-78   |     | 56   |
| 2252 | Preferred backbone conformations of amino acid residues for solvent interaction. <b>1976</b> , 60, 481-6   |     | 14   |
| 2251 | The thermodynamic basis of the stability of proteins, nucleic acids, and membranes. <b>1976</b> , 30, 183-250  |     | 131  |
| 2250 | Effects of long range interactions on the conformational statistics of short polypeptide chains generated by a Monte Carlo method. <b>1977</b> , 66, 3418-3425                   |     | 34   |
| 2249 | Protein folding. <b>1977</b> , 10, 239-52  |     | 261  |

|      |  |        |
|------|--|--------|
| 2248 | Use of solvent cavity area and number of packed solvent molecules around a solute in regard to hydrocarbon solubilities and hydrophobic interactions. <b>1977</b> , 74, 4144-5 | 65     |
| 2247 | Hydrophobicity, hydrophilicity, and the radial and orientational distributions of residues in native proteins. <b>1977</b> , 74, 5248-51                                       | 44     |
| 2246 | Structural convergence during protein evolution. <b>1977</b> , 74, 2820-4  | 25     |
| 2245 | Solvent accessibilities in glycyl, alanyl and seryl dipeptides. <b>1977</b> , 167, 171-82  | 17     |
| 2244 | Salt effect on hydrophobic interactions in precipitation and chromatography of proteins: an interpretation of the lyotropic series. <b>1977</b> , 183, 200-15                  | 815    |
| 2243 | A study of the preferred environment of amino acid residues in globular proteins. <b>1977</b> , 184, 476-87  | 85     |
| 2242 | Dynamic solvent accessibility in the soybean trypsin inhibitor--trypsin complex. <i>Journal of Molecular Biology</i> , <b>1977</b> , 111, 509-15                               | 6.5 22 |
| 2241 | On the conformation of proteins: hydrophobic ordering of strands in beta-pleated sheets. <i>Journal of Molecular Biology</i> , <b>1977</b> , 115, 1-17                         | 6.5 56 |
| 2240 | Hydrophobic free energy and the denaturation of proteins. <b>1977</b> , 495, 110-8   | 11     |
| 2239 | Structural rules for globular proteins. <b>1977</b> , 16, 23-32  | 54     |
| 2238 | Regeln für Strukturen globulärer Proteine. <b>1977</b> , 89, 24-33   | 12     |
| 2237 | The molecular evolution of pancreatic ribonuclease. <b>1977</b> , 10, 49-71  | 54     |
| 2236 | Prediction of protein structure from amino acid sequence. <b>1978</b> , 271, 15-20   | 98     |
| 2235 | Haem exposure as the determinate of oxidation-reduction potential of haem proteins. <b>1978</b> , 275, 73-4  | 288    |
| 2234 | Hydrophobic character of amino acid residues in globular proteins. <b>1978</b> , 275, 673-4  | 251    |
| 2233 | Pseudo-dynamic contact surface areas: estimation of apolar bonding. <b>1978</b> , 533, 465-77  | 10     |
| 2232 | Structures of membrane proteins. <b>1978</b> , 42, 265-79  | 56     |
| 2231 | Comparison of various immunological methods for distinguishing among mammalian pancreatic ribonucleases of known amino acid sequence. <b>1978</b> , 10, 293-307                | 47     |

|      |   |     |     |
|------|---|-----|-----|
| 2230 | Large-angle X-ray diffuse scattering, a new method for investigating changes in the conformation of globular proteins in solutions. <b>1978</b> , 11, 473-477             |     | 22  |
| 2229 | Measurement of the strongly held water of lysozyme by drying. <b>1978</b> , 17, 291-314   |     | 9   |
| 2228 | Measurement of the strongly held water of myoglobin by drying. <b>1978</b> , 17, 1957-1972  |     | 2   |
| 2227 | Solvent accessibilities in the dimeric subunits of RNA and DNA. <b>1978</b> , 17, 2503-2518   |     | 15  |
| 2226 | Feinauflösende UV/VIS-Derivativspektrophotometrie höherer Ordnung. <b>1978</b> , 90, 840-854  |     | 38  |
| 2225 | Nature of steroid-glucocorticoid receptor interactions: thermodynamic analysis of the binding reaction. <b>1978</b> , 17, 3201-8  |     | 100 |
| 2224 | Hydrophobic (interaction) chromatography. <b>1978</b> , 60, 1-15  |     | 84  |
| 2223 | Solvent accessibility calculations for sperm whale ferrimyoglobin based on refined crystallographic data. <b>1978</b> , 81, 410-5   |     | 20  |
| 2222 | Discrete charge calculations of potentiometric titrations for globular proteins: sperm whale myoglobin, hemoglobin alpha chain, cytochrome c. <b>1978</b> , 81, 416-21    |     | 58  |
| 2221 | Packing of alpha-helices: geometrical constraints and contact areas. <i>Journal of Molecular Biology</i> , <b>1978</b> , 119, 537-55                                      | 6.5 | 342 |
| 2220 | Volume occupation, environment, and accessibility in proteins. Environment and molecular area of RNase-S. <i>Journal of Molecular Biology</i> , <b>1978</b> , 119, 415-41 | 6.5 | 73  |
| 2219 | A survey of atomic interactions in 21 proteins. <i>Journal of Molecular Biology</i> , <b>1978</b> , 118, 273-87   | 6.5 | 45  |
| 2218 | Computer analysis of protein-protein interaction. <i>Journal of Molecular Biology</i> , <b>1978</b> , 124, 323-42   | 6.5 | 242 |
| 2217 | A refined model of the sugar binding site of yeast hexokinase B. <i>Journal of Molecular Biology</i> , <b>1978</b> , 123, 207-19  | 6.5 | 126 |
| 2216 | Conformation of amino acid side-chains in proteins. <i>Journal of Molecular Biology</i> , <b>1978</b> , 125, 357-86   | 6.5 | 705 |
| 2215 | Glucose-induced conformational change in yeast hexokinase. <b>1978</b> , 75, 4848-52  |     | 286 |
| 2214 | Macromolecular shape and surface maps by solvent exclusion. <b>1978</b> , 75, 303-7   |     | 151 |
| 2213 | Physical methods for the study of myoglobin. <b>1978</b> , 52, 473-86   |     | 48  |

|      |   |     |
|------|---|-----|
| 2212 | Water, protein folding, and the genetic code. <b>1979</b> , 206, 575-7  | 168 |
| 2211 | Motions in proteins. <b>1979</b> , 33, 73-165   | 222 |
| 2210 | Model for the conformational analysis of hydrated peptides. Effect of hydration on the conformational stability of the terminally blocked residues of the 20 naturally occurring amino acids. <b>1979</b> , 18, 1565-1610 | 95  |
| 2209 | Solvent accessibility study on tRNAPhe. <b>1979</b> , 18, 2233-47   | 22  |
| 2208 | Flexibility of the pyranose ring in $\alpha$ - and $\beta$ -D-glucoses. <b>1979</b> , 18, 2993-3004   | 61  |
| 2207 | Staphylococcal nuclease reviewed: a prototypic study in contemporary enzymology. III. Correlation of the three-dimensional structure with the mechanisms of enzymatic action. <b>1979</b> , 23, 67-86                     | 61  |
| 2206 | Surface and inside volumes in globular proteins. <b>1979</b> , 277, 491-2   | 605 |
| 2205 | Solvent accessibility properties of complex proteins. <b>1979</b> , 280, 333-5  | 23  |
| 2204 | Incorporation of $^3\text{H}$ -thymidine in the nephron of <i>Gasterosteus aculeatus</i> L. and its stimulation by methyltestosterone. A high-speed scintillation autoradiographic study. <b>1979</b> , 201, 249-62       | 4   |
| 2203 | Complete amino acid sequence of the myoglobin from the Pacific spotted dolphin, <i>Stenella attenuata</i> graffmani. <b>1979</b> , 577, 454-63  | 11  |
| 2202 | Complete amino acid sequence of the myoglobin from the Pacific sei whale, <i>Balaenoptera borealis</i> . <b>1979</b> , 577, 464-74  | 7   |
| 2201 | Packing defects, cavities, volume fluctuations, and access to the interior of proteins. Including some general comments on surface area and protein structure. <b>1979</b> , 44, 47-63                                    | 143 |
| 2200 | Experimental studies of protein folding and unfolding. <b>1978</b> , 33, 231-97   | 434 |
| 2199 | Protein--water interactions. Heat capacity of the lysozyme--water system. <b>1979</b> , 18, 2654-61   | 145 |
| 2198 | Myoglobin semisynthesis: removal of the NH <sub>2</sub> -terminal valine of sperm whale myoglobin and its subsequent reincorporation. <b>1979</b> , 18, 3101-9  | 8   |
| 2197 | Electrostatic stabilization in myoglobin. Interactive free energies between individual sites. <b>1979</b> , 18, 4620-30   | 38  |
| 2196 | Electrostatic stabilization in myoglobin. pH dependence of summed electrostatic contributions. <b>1979</b> , 18, 4612-9   | 86  |
| 2195 | Amino acid sequence of pheasant lysozyme. Evolutionary change affecting processing of prelysozyme. <b>1979</b> , 18, 2744-52  | 50  |



|      |   |     |     |
|------|---|-----|-----|
| 2194 | Crystal structure of a bacterial protein proteinase inhibitor (Streptomyces subtilisin inhibitor) at 2.6 A resolution. <i>Journal of Molecular Biology</i> , <b>1979</b> , 131, 697-724                       | 6.5 | 84  |
| 2193 | Solvent-accessible surfaces of nucleic acids. <i>Journal of Molecular Biology</i> , <b>1979</b> , 132, 411-34   | 6.5 | 148 |
| 2192 | Structure of erythrocrucorin in different ligand states refined at 1.4 A resolution. <i>Journal of Molecular Biology</i> , <b>1979</b> , 127, 309-38  | 6.5 | 290 |
| 2191 | Shape and accessible surface area of globular proteins. <i>Journal of Molecular Biology</i> , <b>1979</b> , 127, 345-51   | 6.5 | 8   |
| 2190 | Packing of alpha-helices in globular proteins. Layer-structure of globin hydrophobic cores. <i>Journal of Molecular Biology</i> , <b>1979</b> , 134, 23-40  | 6.5 | 66  |
| 2189 | The symmetry of self-complementary surfaces. <i>Journal of Molecular Biology</i> , <b>1979</b> , 127, 31-8  | 6.5 | 19  |
| 2188 | Intermediates in the refolding of reduced ribonuclease A. <i>Journal of Molecular Biology</i> , <b>1979</b> , 129, 411-31   | 6.5 | 145 |
| 2187 | Dynamic information from protein crystallography. An analysis of temperature factors from refinement of the hen egg-white lysozyme structure. <i>Journal of Molecular Biology</i> , <b>1979</b> , 130, 231-52 | 6.5 | 139 |
| 2186 | Side-chain torsional potentials: effect of dipeptide, protein, and solvent environment. <b>1979</b> , 18, 1256-68   |     | 278 |
| 2185 | The translational friction coefficient of proteins. <b>1979</b> , 61, 103-24  |     | 49  |
| 2184 | Aliphatic groups of sperm whale myoglobin: <sup>13</sup> C NMR study. <b>1979</b> , 76, 1059-63   |     | 39  |
| 2183 | Association of proteins. <b>1979</b> , 46, 241-52   |     | 12  |
| 2182 | Thermodynamic and Related Studies of Water Interacting with Proteins. <b>1980</b> , 111-132   |     | 66  |
| 2181 | Hydrophobic basis of packing in globular proteins. <b>1980</b> , 77, 4643-7   |     | 166 |
| 2180 | Analytical approximation to the accessible surface area of proteins. <b>1980</b> , 77, 1736-40  |     | 157 |
| 2179 | Relation between enzymic catalysis and energy coupling. <b>1980</b> , 77, 5703-5  |     | 3   |
| 2178 | Model for haptoglobin heavy chain based upon structural homology. <b>1980</b> , 77, 3393-7  |     | 88  |
| 2177 | Evolution of the amino acid substitution in the mammalian myoglobin gene. <b>1980</b> , 15, 197-218   |     | 22  |

|      |  |     |     |
|------|--|-----|-----|
| 2176 | The electrostatic molecular potential of yeast tRNAPhe. III. The molecular potential and the steric accessibility associated with the phosphate groups. <b>1980</b> , 57, 233-243  |     | 22  |
| 2175 | Local hydrophobicity stabilizes secondary structures in proteins. <b>1980</b> , 19, 1617-28  |     | 67  |
| 2174 | Interactions of molecules with nucleic acids. III. Steric and electrostatic energy contours for the principal intercalation sites, prerequisites for binding, and the exclusion of essential metabolites from intercalation. <b>1980</b> , 19, 2067-89 |     | 27  |
| 2173 | Hydration of peptides. I. Calculation of accessible surface areas for several conformations of a cyclic dipeptide. <b>1980</b> , 87, 71-84   |     | 6   |
| 2172 | Hydration of peptides. II. Determination of the preferred sites of interactions of a cyclic dipeptide with water. <b>1980</b> , 87, 85-95  |     | 6   |
| 2171 | The pentaammineruthenium(III)-histidine complex in ribonuclease A as an optical probe of conformational change. <b>1980</b> , 624, 499-510   |     | 9   |
| 2170 | Hydrophobic packing and spatial arrangement of amino acid residues in globular proteins. <b>1980</b> , 623, 301-16   |     | 125 |
| 2169 | Correlation of IR spectroscopic, heat capacity, diamagnetic susceptibility and enzymatic measurements on lysozyme powder. <b>1980</b> , 284, 572-3   |     | 179 |
| 2168 | Role of Physical Forces in Hydrophobic Interaction Chromatography. <b>1980</b> , 9, 267-370  |     | 52  |
| 2167 | The effect of hGH on hypothalamic-pituitary-thyroid function in patients with pituitary dwarfism. <b>1980</b> , 93, 13-9   |     | 15  |
| 2166 | Proposed extensions to the TanfordKirkwood theory of protein titration. <b>1980</b> , 73, 1354-1358  |     | 4   |
| 2165 | Structure of a complex between yeast hexokinase A and glucose. II. Detailed comparisons of conformation and active site configuration with the native hexokinase B monomer and dimer. <i>Journal of Molecular Biology</i> , <b>1980</b> , 140, 211-30  | 6.5 | 236 |
| 2164 | Packing of alpha-helices onto beta-pleated sheets and the anatomy of alpha/beta proteins. <i>Journal of Molecular Biology</i> , <b>1980</b> , 143, 95-128  | 6.5 | 104 |
| 2163 | How different amino acid sequences determine similar protein structures: the structure and evolutionary dynamics of the globins. <i>Journal of Molecular Biology</i> , <b>1980</b> , 136, 225-70   | 6.5 | 633 |
| 2162 | The effect of a single amino acid substitution on the antigenic specificity of the loop region of lysozyme. <b>1980</b> , 17, 37-46  |     | 41  |
| 2161 | Activation volumes for the rotational motion of interior aromatic rings in globular proteins determined by high resolution 1H NMR at variable pressure. <b>1980</b> , 112, 280-4   |     | 96  |
| 2160 | A three-disulphide intermediate in refolding of reduced ribonuclease A with a folded conformation. <b>1980</b> , 118, 283-8  |     | 23  |
| 2159 | HYDROPHOBIC PROPERTIES OF INTERFERONS. <b>1980</b> , 350, 339-346  |     | 4   |

|      |   |         |
|------|---|---------|
| 2158 | Solvent effects and polar interactions in the structural stability and dynamics of globular proteins. <b>1980</b> , 32, 17-33   | 101     |
| 2157 | Solvent accessibility, protein surfaces, and protein folding. <b>1980</b> , 32, 35-47   | 36      |
| 2156 | Electrostatic stabilization in sperm whale and harbor seal myoglobins. Identification of groups primarily responsible for changes in anchoring of the A helix. <b>1980</b> , 32, 65-75  | 16      |
| 2155 | Volume changes of globular protein association. <b>1980</b> , 32, 86-7  | 3       |
| 2154 | Modeling water-protein interactions in a protein crystal. <b>1980</b> , 32, 87-8  |         |
| 2153 | Subunit interactions and the allosteric response in phosphorylase. <b>1980</b> , 32, 175-92   | 28      |
| 2152 | Energetics of subunit assembly and ligand binding in human hemoglobin. <b>1980</b> , 32, 331-46   | 72      |
| 2151 | Effect of a molecular dipole on the ionic strength dependence of a biomolecular rate constant. Identification of the site of reaction. <b>1980</b> , 29, 493-507  | 66      |
| 2150 | Charge-site communication in proteins: electrostatic heme linkage of azide binding by sperm whale myoglobin. <b>1980</b> , 19, 3039-47  | 21      |
| 2149 | Proton magnetic resonance study of <i>Streptomyces subtilisin</i> inhibitor. pH titration and assignments of individual tyrosyl resonances. <b>1981</b> , 20, 518-23  | 21      |
| 2148 | Tryptophanyl fluorescence heterogeneity of apomyoglobins. Correlation with the presence of two distinct structural domains. <b>1981</b> , 20, 792-9   | 63      |
| 2147 | Electrostatic contributions to the energetics of dimer-tetramer assembly in human hemoglobin: pH dependence and effect of specifically bound chloride ions. <b>1981</b> , 20, 7439-49   | 37      |
| 2146 | Ultraviolet difference spectroscopy of myoglobin: assignment of pK values of tyrosyl phenolic groups and the stability of the ferryl derivatives. <b>1981</b> , 20, 2028-35   | 43      |
| 2145 | The relationship between molecular weight and quaternary structure of globular proteins. <b>1981</b> , 207, 63-8  | 1       |
| 2144 | Hydrogen exchange from identified regions of the S-protein component of ribonuclease as a function of temperature, pH, and the binding of S-peptide. <i>Journal of Molecular Biology</i> , <b>1981</b> , 145, 835-51 <sup>6,5</sup> | 53      |
| 2143 | Comparative model-building of the mammalian serine proteases. <i>Journal of Molecular Biology</i> , <b>1981</b> , 153, 1027-42  | 6.5 280 |
| 2142 | Molecular electrostatic potential of the nucleic acids. <b>1981</b> , 14, 289-380   | 348     |
| 2141 | Affinities of amino acid side chains for solvent water. <b>1981</b> , 20, 849-55  | 750     |

|      |   |      |
|------|---|------|
| 2140 | Location of structural domains in protein. <b>1981</b> , 20, 6544-52  | 128  |
| 2139 | HYDROGEN BOND AND INTERNAL SOLVENT DYNAMICS OF BPTI PROTEIN*. <b>1981</b> , 367, 162-181  | 12   |
| 2138 | The anatomy and taxonomy of protein structure. <b>1981</b> , 34, 167-339  | 2607 |
| 2137 | Crystallographic refinement and atomic models of a human Fc fragment and its complex with fragment B of protein A from Staphylococcus aureus at 2.9- and 2.8-Å resolution. <b>1981</b> , 20, 2361-2370              | 1392 |
| 2136 | Can multiple low-density immunoabsorbents and 'negative' distance matrices help predict the three-dimensional structure of any globular protein?. <b>1981</b> , 199, 277-80   |      |
| 2135 | The pentaammineruthenium(III)histidine complex in ribonuclease A: application to the assignment of histidine proton resonances. <b>1981</b> , 112, 329-37   | 9    |
| 2134 | Steric accessibility of reactive centers in B-DNA. <b>1981</b> , 20, 49-62  | 45   |
| 2133 | The electrostatic molecular potential of tRNAPhe. V. The influence of counterion binding on the potential and the steric accessibility. <b>1981</b> , 20, 171-183   | 7    |
| 2132 | Location of domains in globular proteins. <b>1981</b> , 291, 85-7   | 66   |
| 2131 | Molecular dynamics of hydrogen bonds in bovine pancreatic trypsin inhibitor protein. <b>1981</b> , 294, 379-80  | 49   |
| 2130 | The flexibility during the juxtaposition of reacting groups and the upper limits of enzyme reactions. <b>1981</b> , 14, 277-81  | 23   |
| 2129 | Protein folding and the genetic code: an alternative quantitative model. <b>1981</b> , 91, 115-23   | 31   |
| 2128 | The internal dynamics of globular proteins. <b>1981</b> , 9, 293-349  | 418  |
| 2127 | Real-time color graphics in studies of molecular interactions. <b>1981</b> , 211, 661-6   | 213  |
| 2126 | Increase in apparent compressibility of cytochrome c upon oxidation. <b>1982</b> , 79, 815-9  | 91   |
| 2125 | Electronic distributions within protein phenylalanine aromatic rings are reflected by the three-dimensional oxygen atom environments. <b>1982</b> , 79, 4843-7  | 158  |
| 2124 | A computergraphical method of describing the shapes of subunit interfaces of oligomers. Analysis of the quaternary structure of concanavalin A and of prealbumin. <b>1982</b> , 205, 353-9                          | 5    |
| 2123 | New Potent Neuroleptic Drugs of Benzamide Derivatives. I. Crystal and Molecular Structure of N-[(2RS, 3RS)-1-Benzyl-2-methyl-3-pyrrolidinyl]-5-chloro-2-methoxy-4-methylaminobenzamide. <b>1982</b> , 55, 2321-2326 | 12   |

|      |  |         |
|------|--|---------|
| 2122 | Methylation of a Benzene Ring as a Chemical Signal. Marked Changes in the Pattern of Temperature Dependence of the Selectivity in Oxidation of a Pair of Associating Thiols. <b>1982</b> , 55, 2224-2232   | 15      |
| 2121 | Empirical calculations of peptide-water interactions. Structural aspects of hydration. <b>1981</b> , 63, 941-4   | 3       |
| 2120 | Prediction of the secondary and tertiary structures of interferon from four homologous amino acid sequences. <b>1982</b> , 4, 137-144  | 75      |
| 2119 | Production and subsequent second-order decomposition of protein disulfide anions lengthy collisions between proteins. <i>Journal of Molecular Biology</i> , <b>1982</b> , 159, 721-44  | 6.5 18  |
| 2118 | Analysis and prediction of the packing of alpha-helices against a beta-sheet in the tertiary structure of globular proteins. <i>Journal of Molecular Biology</i> , <b>1982</b> , 156, 821-62   | 6.5 128 |
| 2117 | Evolution of proteins formed by beta-sheets. I. Plastocyanin and azurin. <i>Journal of Molecular Biology</i> , <b>1982</b> , 160, 309-23   | 6.5 121 |
| 2116 | Amide protein exchange and surface conformation of the basic pancreatic trypsin inhibitor in solution. Studies with two-dimensional nuclear magnetic resonance. <i>Journal of Molecular Biology</i> , <b>1982</b> , 160, 343-61                                      | 6.5 305 |
| 2115 | Crystallographic refinement of Japanese quail ovomucoid, a Kazal-type inhibitor, and model building studies of complexes with serine proteases. <i>Journal of Molecular Biology</i> , <b>1982</b> , 158, 515-37  | 6.5 135 |
| 2114 | Refined crystal structure of the potato inhibitor complex of carboxypeptidase A at 2.5 A resolution. <i>Journal of Molecular Biology</i> , <b>1982</b> , 160, 475-98   | 6.5 252 |
| 2113 | Effects of binding of S-peptide and 2'-cytidine monophosphate on hydrogen exchange from the S-protein component of ribonuclease S. The amide protons of serine 123 and valine 124. <i>Journal of Molecular Biology</i> , <b>1982</b> , 160, 517-30                   | 6.5 13  |
| 2112 | Building models of globular protein molecules from their amino acid sequences. I. Theory. <i>Journal of Molecular Biology</i> , <b>1982</b> , 155, 53-62   | 6.5 47  |
| 2111 | Shape and surface features of globular proteins. <b>1982</b> , 15, 314-320   | 26      |
| 2110 | Crystal structure determinations of coenzyme analogue and substrate complexes of liver alcohol dehydrogenase: binding of 1,4,5,6-tetrahydronicotinamide adenine dinucleotide and trans-4-(N,N-dimethylamino)cinnamaldehyde to the enzyme. <b>1982</b> , 21, 4895-908 | 87      |
| 2109 | Analysis of an allosteric binding site: the nucleoside inhibitor site of phosphorylase alpha. <b>1982</b> , 21, 2036-48  | 50      |
| 2108 | Anion binding and pH-dependent electrostatic effects in ribonuclease. <b>1982</b> , 21, 4989-99  | 111     |
| 2107 | On the disordered activation domain in trypsinogen: chemical labelling and low-temperature crystallography. <b>1982</b> , 38, 1462-1472  | 171     |
| 2106 | Hydrophobic contribution to the binding of actinomycin D to deoxyguanosines. <b>1982</b> , 21, 2473-2476   | 1       |
| 2105 | A method to compute the volume of a molecule. <b>1982</b> , 6, 133-135   | 28      |

|      |   |       |
|------|---|-------|
| 2104 | The three-dimensional structure of antibodies. <b>1982</b> , 3, 160-6   | 70    |
| 2103 | Computer representation of molecular surfaces. <b>1982</b> , 6, 485-99  | 5     |
| 2102 | Hydrogen exchange and the dynamic structure of proteins. <b>1982</b> , 48, 135-60   | 302   |
| 2101 | Intron-exon splice junctions map at protein surfaces. <b>1982</b> , 299, 180-2  | 144   |
| 2100 | Cooperative motion and hydrogen exchange stability in protein beta-sheets. <b>1982</b> , 299, 754-6   | 17    |
| 2099 | A voltage-gated ion channel model inferred from the crystal structure of alamethicin at 1.5-A resolution. <b>1982</b> , 300, 325-30   | 685   |
| 2098 | Interior turns in globular proteins. <b>1983</b> , 304, 654-7   | 47    |
| 2097 | DOCKER, an interactive program for simulating protein receptor and substrate interactions. <b>1983</b> , 16, 432-437  | 18    |
| 2096 | Contrast variation of the small-angle neutron scattering of globular particles: the influence of hydrogen exchange. <b>1983</b> , 39, 706-711   | 12    |
| 2095 | The refined structure of the selenoenzyme glutathione peroxidase at 0.2-nm resolution. <b>1983</b> , 133, 51-69   | 543   |
| 2094 | Protein conformation and proton nuclear-magnetic-resonance chemical shifts. <b>1983</b> , 137, 445-54   | 199   |
| 2093 | Analytical molecular surface calculation. <b>1983</b> , 16, 548-558   | 1954  |
| 2092 | Structural studies of horse liver alcohol dehydrogenase: coenzyme, substrate and inhibitor binding. <b>1983</b> , 18 Suppl 1, 73-81   | 14    |
| 2091 | <sup>1</sup> H-NMR study on the tautomerism of the imidazole ring of histidine residues. II. Microenvironments of histidine-12 and histidine-119 of bovine pancreatic ribonuclease A. <b>1983</b> , 742, 586-96 | 44    |
| 2090 | Correlation between chemical modification and surface accessibility in yeast phenylalanine transfer RNA. <b>1983</b> , 22, 1145-66  | 39    |
| 2089 | Improved technique for calculating X-ray scattering intensity of biopolymers in solution: Evaluation of the form, volume, and surface of a particle. <b>1983</b> , 22, 1507-1522                                | 76    |
| 2088 | Dictionary of protein secondary structure: pattern recognition of hydrogen-bonded and geometrical features. <b>1983</b> , 22, 2577-637  | 11842 |
| 2087 | Enzyme immobilization on palmityl-sepharose. <b>1983</b> , 25, 2617-29  | 14    |

|      |   |     |       |
|------|---|-----|-------|
| 2086 | CHARMM: A program for macromolecular energy, minimization, and dynamics calculations. <b>1983</b> , 4, 187-217  |     | 13044 |
| 2085 | Interactions of molecules with nucleic acids. VII. Evaluation and presentation of steric contours and molecules in bonding sites. <b>1983</b> , 4, 366-378  |     | 10    |
| 2084 | Generation of molecular surfaces for graphic display. <b>1983</b> , 1, 9-12   |     | 44    |
| 2083 | Interactive modelling of enzyme-inhibitor complexes at merck macromolecular modeling graphics facility. <b>1983</b> , 8, 1-11   |     | 8     |
| 2082 | Proteins and polypeptides computer graphics for space-filling model representations. <b>1983</b> , 7, 67-74   |     | 7     |
| 2081 | Comparison of AMP and NADH binding to glycogen phosphorylase b. <i>Journal of Molecular Biology</i> , <b>1983</b> , 170, 529-65   | 6.5 | 48    |
| 2080 | Comparison of the structures of cro and lambda repressor proteins from bacteriophage lambda. <i>Journal of Molecular Biology</i> , <b>1983</b> , 169, 757-69  | 6.5 | 82    |
| 2079 | X-ray analysis of the eye lens protein gamma-II crystallin at 1.9 A resolution. <i>Journal of Molecular Biology</i> , <b>1983</b> , 170, 175-202  | 6.5 | 303   |
| 2078 | Integrating the equations of motion. <i>Journal of Molecular Biology</i> , <b>1983</b> , 168, 617-20  | 6.5 | 17    |
| 2077 | Molecular dynamics of native protein. II. Analysis and nature of motion. <i>Journal of Molecular Biology</i> , <b>1983</b> , 168, 621-57  | 6.5 | 188   |
| 2076 | Refined crystal structure of carboxypeptidase A at 1.54 A resolution. <i>Journal of Molecular Biology</i> , <b>1983</b> , 168, 367-87   | 6.5 | 386   |
| 2075 | Structure of oxidized poplar plastocyanin at 1.6 A resolution. <i>Journal of Molecular Biology</i> , <b>1983</b> , 169, 521-63  | 6.5 | 544   |
| 2074 | Protein folding by restrained energy minimization and molecular dynamics. <i>Journal of Molecular Biology</i> , <b>1983</b> , 170, 723-64   | 6.5 | 296   |
| 2073 | Structure and refinement of penicillopepsin at 1.8 A resolution. <i>Journal of Molecular Biology</i> , <b>1983</b> , 163, 299-361   | 6.5 | 399   |
| 2072 | Refined 2 A X-ray crystal structure of porcine pancreatic kallikrein A, a specific trypsin-like serine proteinase. Crystallization, structure determination, crystallographic refinement, structure and its comparison with bovine trypsin. <i>Journal of Molecular Biology</i> , <b>1983</b> , 164, 237-82   | 6.5 | 224   |
| 2071 | Refined 2.5 A X-ray crystal structure of the complex formed by porcine kallikrein A and the bovine pancreatic trypsin inhibitor. Crystallization, Patterson search, structure determination, refinement, structure and comparison with its components and with the bovine trypsin-pancreatic trypsin inhibitor complex. <i>Journal of Molecular Biology</i> , <b>1983</b> , 164, 237-82 | 6.5 | 197   |
| 2070 | H NMR studies of the Fc region of human IgG1 and IgG3 immunoglobulins: assignment of histidine resonances in the CH3 domain and identification of IgG3 protein carrying G3m(st) allotypes. <b>1983</b> , 20, 141-8  |     | 26    |
| 2069 | Solvent-accessible surfaces of proteins and nucleic acids. <b>1983</b> , 221, 709-13  |     | 2405  |

|      |  |         |
|------|--|---------|
| 2068 | Role of hydrophobic effects and polar groups in steroid-mineralocorticoid receptor interactions. <b>1983</b> , 19, 1639-45   | 3       |
| 2067 | Ion-pairs in proteins. <i>Journal of Molecular Biology</i> , <b>1983</b> , 168, 867-85   | 6.5 599 |
| 2066 | Unfolding pathway of myoglobin. Evidence for a multistate process. <b>1983</b> , 22, 4165-70   | 63      |
| 2065 | Computer Representation of Molecular Surfaces. <b>1983</b> , 3, 21-29  | 21      |
| 2064 | Van der waals surfaces in molecular modeling: implementation with real-time computer graphics. <b>1983</b> , 222, 1325-7   | 84      |
| 2063 | Electrostatic free energy of lysozyme. <b>1983</b> , 44, 293-8   | 26      |
| 2062 | Structural domains in proteins and their role in the dynamics of protein function. <b>1983</b> , 42, 21-78   | 239     |
| 2061 | Waterlogged molecules. <b>1983</b> , 222, 1087-93  | 114     |
| 2060 | Molecular dynamics of phenylalanine transfer RNA. <b>1983</b> , 1, 357-69  | 32      |
| 2059 | Hydrogen exchange and structural dynamics of proteins and nucleic acids. <b>1983</b> , 16, 521-655   | 1075    |
| 2058 | Calculation of volume fluctuation for globular protein models. <b>1983</b> , 80, 622-6   | 46      |
| 2057 | Dynamics of a small globular protein in terms of low-frequency vibrational modes. <b>1983</b> , 80, 3696-700   | 628     |
| 2056 | Characterization of the distribution of internal motions in the basic pancreatic trypsin inhibitor using a large number of internal NMR probes. <b>1983</b> , 16, 1-57 | 230     |
| 2055 | Oligosaccharide conformation and protein saccharide interactions in solution. <b>1983</b> , 55, 577-588  | 18      |
| 2054 | Correlation of exons with structural domains in alcohol dehydrogenase.. <b>1984</b> , 3, 1307-1310   | 56      |
| 2053 | Determination of the solvent accessibility of specific aromatic residues in gamma-crystallin by photo-CIDNP NMR measurements. <b>1984</b> , 3, 127-35                  | 8       |
| 2052 | Phenylalanine transfer RNA: molecular dynamics simulation. <b>1984</b> , 223, 1189-91  | 50      |
| 2051 | A model for the non-specific binding of catabolite gene activator protein to DNA. <b>1984</b> , 12, 8475-87  | 18      |



|      |   |     |
|------|---|-----|
| 2050 | A new theoretical index of biochemical reactivity combining steric and electrostatic factors. An application to yeast tRNAPhe. <b>1984</b> , 19, 171-81   | 47  |
| 2049 | Computer representation of molecular surfaces. <b>1984</b> , 2, 8-13  | 25  |
| 2048 | Structure and stability of proteins: The role of solvent. <b>1984</b> , 10, 1-7   | 3   |
| 2047 | Novel stereospecificity of the L-arabinose-binding protein. <b>1984</b> , 310, 381-6  | 267 |
| 2046 | The apolar surface area of amino acids and its empirical correlation with hydrophobic free energy. <b>1984</b> , 111, 247-60  | 65  |
| 2045 | The refined 2.2-A (0.22-nm) X-ray crystal structure of the ternary complex formed by bovine trypsinogen, valine-valine and the Arg15 analogue of bovine pancreatic trypsin inhibitor. <b>1984</b> , 144, 185-90 | 77  |
| 2044 | Interactions of molecules with nucleic acids. IX. Evaluation and presentation of electrostatic contours on a steric surface with the removal of hidden lines. <b>1984</b> , 5, 89-103                           | 6   |
| 2043 | Buried surface area, conformational entropy, and protein stability. <b>1984</b> , 23, 1605-20   | 58  |
| 2042 | Sequential hydration of dry proteins: a direct difference IR investigation of sequence homologs lysozyme and alpha- lactalbumin. <b>1984</b> , 23, 1647-66  | 57  |
| 2041 | Calculation of the thermodynamic quantities of solvation for lysozyme and beta-lactoglobulin A in guanidinium chloride. <b>1984</b> , 23, 1943-50   | 5   |
| 2040 | Differential electrostatic stabilization of A-, B-, and Z-forms of DNA. <b>1984</b> , 23, 2743-59   | 30  |
| 2039 | Interaction of proteins with Triton X-100-substituted sepharose 4B. <b>1984</b> , 26, 565-72  | 9   |
| 2038 | Protein structure and function, from a colloidal to a molecular view. <b>1984</b> , 49, 1-55  | 65  |
| 2037 | Spatial constraints and group behaviour in globular proteins. <b>1984</b> , 106, 25-40  | 2   |
| 2036 | Strategies for increasing the stability of enzymes. <b>1984</b> , 434, 1-6  | 11  |
| 2035 | Diffusion-collision model for the folding kinetics of the lambda-repressor operator-binding domain. <b>1984</b> , 1, 1243-55  | 32  |
| 2034 | Electrostatic modification of protein surfaces: effect on hemoglobin ligation and solubility. <b>1984</b> , 23, 1457-61   | 13  |
| 2033 | Independent folding of the carboxyl-terminal fragment 228-316 of thermolysin. <b>1984</b> , 23, 5512-9  | 22  |

|      |   |     |     |
|------|---|-----|-----|
| 2032 | Crystallographic investigations of nicotinamide adenine dinucleotide binding to horse liver alcohol dehydrogenase. <b>1984</b> , 23, 5982-96  |     | 236 |
| 2031 | Conformational transitions of thioredoxin in guanidine hydrochloride. <b>1984</b> , 23, 5095-102  |     | 52  |
| 2030 | Reaction of myoglobin with phenylhydrazine: a molecular doorstop. <b>1984</b> , 23, 2-4   |     | 192 |
| 2029 | Structure of satellite tobacco necrosis virus after crystallographic refinement at 2.5 Å resolution. <i>Journal of Molecular Biology</i> , <b>1984</b> , 177, 735-67  | 6.5 | 105 |
| 2028 | An analysis of incorrectly folded protein models. Implications for structure predictions. <i>Journal of Molecular Biology</i> , <b>1984</b> , 177, 787-818  | 6.5 | 267 |
| 2027 | Crystal structure at 2.6 Å resolution of the complex of subtilisin BPN' with streptomyces subtilisin inhibitor. <i>Journal of Molecular Biology</i> , <b>1984</b> , 178, 389-414  | 6.5 | 88  |
| 2026 | Solvent accessible surface area and excluded volume in proteins. Analytical equations for overlapping spheres and implications for the hydrophobic effect. <i>Journal of Molecular Biology</i> , <b>1984</b> , 178, 63-89 | 6.5 | 550 |
| 2025 | Structural evidence for ligand-induced sequential conformational changes in glyceraldehyde 3-phosphate dehydrogenase. <i>Journal of Molecular Biology</i> , <b>1984</b> , 178, 743-72                                     | 6.5 | 39  |
| 2024 | On the environment of ionizable groups in globular proteins. <i>Journal of Molecular Biology</i> , <b>1984</b> , 173, 515-21  | 6.5 | 140 |
| 2023 | Refined structure of cytochrome c3 at 1.8 Å resolution. <i>Journal of Molecular Biology</i> , <b>1984</b> , 172, 109-39   | 6.5 | 280 |
| 2022 | Intrahelical hydrogen bonding of serine, threonine and cysteine residues within alpha-helices and its relevance to membrane-bound proteins. <i>Journal of Molecular Biology</i> , <b>1984</b> , 175, 75-81                | 6.5 | 235 |
| 2021 | Increase in surface area due to atomic scale roughness. <b>1984</b> , 800, 309-311  |     | 3   |
| 2020 | Water structure of a hydrophobic protein at atomic resolution: Pentagon rings of water molecules in crystals of crambin. <b>1984</b> , 81, 6014-8   |     | 299 |
| 2019 | Chapter 1 The energetics and specificity of enzyme-substrate interactions. <b>1984</b> , 1-54   |     | 13  |
| 2018 | Allosteric interactions of glycogen phosphorylase b. A crystallographic study of glucose 6-phosphate and inorganic phosphate binding to di-imidate-cross-linked phosphorylase b. <b>1984</b> , 218, 45-60                 |     | 31  |
| 2017 | Genetic engineering in the Precambrian: structure of the chicken triosephosphate isomerase gene. <b>1985</b> , 5, 3497-506  |     | 68  |
| 2016 | Automatic recognition of domains in globular proteins. <b>1985</b> , 115, 430-40  |     | 13  |
| 2015 | Dielectric Properties of Biomacromolecules: Some Aspects of Relevance to Biological Systems. <b>1985</b> , 4, 389-418   |     | 4   |

|      |  |     |
|------|--|-----|
| 2014 | pH-dependent processes in proteins. <b>1985</b> , 18, 91-197   | 150 |
| 2013 | Structural invariants of antigen binding: comparison of immunoglobulin VL-VH and VL-VL domain dimers. <b>1985</b> , 82, 4592-6                           | 81  |
| 2012 | Crystallographic structure of an active, sequence-engineered ribonuclease. <b>1985</b> , 82, 6423-6  | 16  |
| 2011 | Influence of solvent accessibility and intermolecular contacts on atomic mobilities in hemerythrins. <b>1985</b> , 82, 1104-7                            | 68  |
| 2010 | A comparison of the structure and dynamics of avian pancreatic polypeptide hormone in solution and in the crystal. <b>1985</b> , 13, 77-88               | 51  |
| 2009 | Analysis of the factors and implications of an empirical method for estimating the stability of mutant human haemoglobins. <b>1985</b> , 117, 19-46      | 2   |
| 2008 | Structure of large fragment of Escherichia coli DNA polymerase I complexed with dTMP. <b>1985</b> , 313, 762-6   | 836 |
| 2007 | Sulphate sequestered in the sulphate-binding protein of Salmonella typhimurium is bound solely by hydrogen bonds. <b>1985</b> , 314, 257-60              | 409 |
| 2006 | Depth-buffer algorithms for molecular modelling. <b>1985</b> , 3, 19-24  | 58  |
| 2005 | Computer modeling studies of the structure of a repressor. <b>1985</b> , 18, 3-14  | 5   |
| 2004 | Structural studies of a protein using the assigned back-bone carbonyl carbon-13 NMR resonances. <b>1985</b> , 126, 549-562                               | 11  |
| 2003 | Hierarchic organization of globular proteins: Experimental studies on thermolysin. <b>1985</b> , 8, 57-66  | 4   |
| 2002 | On the interaction of small molecules with hemoproteins: Sperm whale myoglobin. <b>1985</b> , 5, 516-526   | 1   |
| 2001 | Microcalorimetric studies of the heats of solution of bovine myelin basic protein. <b>1985</b> , 831, 242-8  | 3   |
| 2000 | Ionization of tyrosine residues in horse-heart ferricytochrome c and its guanidinated and acetylated-guanidinated derivatives. <b>1985</b> , 828, 325-35 | 4   |
| 1999 | The crystal and molecular structure of the third domain of silver pheasant ovomucoid (OMSVP3). <b>1985</b> , 147, 387-95                                 | 103 |
| 1998 | Conformational fluctuations in alpha-chymotrypsinogen A powders. <b>1985</b> , 41, 91-3  | 6   |
| 1997 | Reaction pathway for the quaternary structure change in hemoglobin. <b>1985</b> , 24, 509-26   | 45  |

|      |   |      |
|------|---|------|
| 1996 | Domain characteristics of the carboxyl-terminal fragment 206B16 of thermolysin: pH and ionic strength dependence of conformation. <b>1985</b> , 24, 767-782 | 15   |
| 1995 | Molecular-dynamics simulation of phenylalanine transfer RNA. I. Methods and general results. <b>1985</b> , 24, 1169-88                                      | 23   |
| 1994 | Solvent accessibility studies of $\beta$ -bends and application to cyclic hexapeptides. <b>1985</b> , 24, 1205-1214   | 1    |
| 1993 | Fast approximations for accessible surface area and molecular volume of protein segments. <b>1985</b> , 24, 2511-9  | 12   |
| 1992 | Van der Waals volume fragmental constants. <b>1985</b> , 116, 415-419   | 38   |
| 1991 | Determinants of molecular reactivity as criteria for predicting toxicity: problems and approaches. <b>1985</b> , 61, 147-62                                 | 9    |
| 1990 | Nature of the Charge Distribution in Proteins. II. Effect of Atomic Partial Charges on Ionic Charges. <b>1985</b> , 54, 4042-4046                           | 8    |
| 1989 | Intrinsic and extrinsic factors in protein antigenic structure. <b>1985</b> , 229, 932-40   | 460  |
| 1988 | Calculation of molecular volumes and areas for structures of known geometry. <b>1985</b> , 115, 440-64  | 156  |
| 1987 | Construction of a model for the three-dimensional structure of human renal renin. <b>1985</b> , 7, 13-26  | 73   |
| 1986 | Domains in proteins: definitions, location, and structural principles. <b>1985</b> , 115, 420-30  | 58   |
| 1985 | How hydrophobic is tryptophan?. <b>1985</b> , 10, 268   | 9    |
| 1984 | Hydrophobicity of amino acid residues in globular proteins. <b>1985</b> , 229, 834-8  | 983  |
| 1983 | A procedure for calculating thermodynamic functions of cavity formation from the pure solvent simulation data. <b>1985</b> , 83, 2421-2425                  | 90   |
| 1982 | Choice of peptide and peptide length for the generation of antibodies reactive with the intact protein. <b>1985</b> , 182, 81-4                             | 12   |
| 1981 | Quantitative Analysis by Derivative Electronic Spectroscopy. <b>1985</b> , 21, 311-418  | 52   |
| 1980 | Theory for the folding and stability of globular proteins. <b>1985</b> , 24, 1501-9   | 1022 |
| 1979 | Amino acid side-chain partition energies and distribution of residues in soluble proteins. <b>1985</b> , 47, 61-70  | 180  |

|      |   |     |      |
|------|---|-----|------|
| 1978 | Refined structure of alpha-lytic protease at 1.7 A resolution. Analysis of hydrogen bonding and solvent structure. <i>Journal of Molecular Biology</i> , <b>1985</b> , 184, 479-502                                     | 6.5 | 158  |
| 1977 | Hydrogen kinetics of peptide amide protons at the bovine pancreatic trypsin inhibitor protein-solvent interface. <i>Journal of Molecular Biology</i> , <b>1985</b> , 185, 405-19  | 6.5 | 64   |
| 1976 | Folding of thermolysin fragments. Identification of the minimum size of a carboxyl-terminal fragment that can fold into a stable native-like structure. <i>Journal of Molecular Biology</i> , <b>1985</b> , 182, 331-40 | 6.5 | 38   |
| 1975 | Edward C. Heath, 1926-1984. <b>1985</b> , 10, 267-268   |     |      |
| 1974 | Protein modelling using computer graphics. <b>1985</b> , 2, 125-136   |     | 0    |
| 1973 | Haemoglobin: the surface buried between the alpha 1 beta 1 and alpha 2 beta 2 dimers in the deoxy and oxy structures. <i>Journal of Molecular Biology</i> , <b>1985</b> , 183, 267-70                                   | 6.5 | 41   |
| 1972 | Electron density calculations as an extension of protein structure refinement. Streptomyces griseus protease A at 1.5 A resolution. <i>Journal of Molecular Biology</i> , <b>1985</b> , 182, 555-66                     | 6.5 | 44   |
| 1971 | Mechanism of surface peptide proton exchange in bovine pancreatic trypsin inhibitor. Salt effects and O-protonation. <i>Journal of Molecular Biology</i> , <b>1985</b> , 185, 421-30                                    | 6.5 | 44   |
| 1970 | A molecular dynamics study of the C-terminal fragment of the L7/L12 ribosomal protein. Secondary structure motion in a 150 picosecond trajectory. <i>Journal of Molecular Biology</i> , <b>1985</b> , 183, 461-77       | 6.5 | 143  |
| 1969 | Refinement of a molecular model for lamprey hemoglobin from Petromyzon marinus. <i>Journal of Molecular Biology</i> , <b>1985</b> , 184, 147-64   | 6.5 | 76   |
| 1968 | Refined structure of alkaline phosphatase from Escherichia coli at 2.8 A resolution. <i>Journal of Molecular Biology</i> , <b>1985</b> , 186, 417-33  | 6.5 | 211  |
| 1967 | Formation of an infinite beta-sheet arrangement dominates the crystallization behavior of lambda-type antibody light chains. <i>Journal of Molecular Biology</i> , <b>1985</b> , 186, 475-8                             | 6.5 | 22   |
| 1966 | Domain association in immunoglobulin molecules. The packing of variable domains. <i>Journal of Molecular Biology</i> , <b>1985</b> , 186, 651-63  | 6.5 | 349  |
| 1965 | Molecular mechanics and molecular shape. <b>1985</b> , 124, 93-106  |     | 15   |
| 1964 | Study of ethanol-lysozyme interactions using neutron diffraction. <b>1985</b> , 24, 5862-9  |     | 45   |
| 1963 | Turns in peptides and proteins. <b>1985</b> , 37, 1-109   |     | 1372 |
| 1962 | The influence of tertiary structure on secondary structure prediction. <b>1985</b> , 188, 59-62   |     | 15   |
| 1961 | Surface accessibility of aromatic residues in human lysozyme using photochemically induced dynamic nuclear polarization NMR spectroscopy. <b>1985</b> , 185, 248-52   |     | 11   |

|      |  |     |     |
|------|--|-----|-----|
| 1960 | Guanidine hydrochloride induced equilibrium unfolding of mutant forms of iso-1-cytochrome c with replacement of proline-71. <b>1986</b> , 25, 6952-8   |     | 34  |
| 1959 | The structure of spherical viruses. <b>1986</b> , 48, 1-36   |     | 47  |
| 1958 | Static accessibility model of protein antigenicity: the case of scorpion neurotoxin. <b>1986</b> , 25, 6748-54   |     | 28  |
| 1957 | Location of antigenic epitopes on antibody molecules. <i>Journal of Molecular Biology</i> , <b>1986</b> , 189, 715-21  | 6.5 | 56  |
| 1956 | Three-dimensional structure of catalase from <i>Penicillium vitale</i> at 2.0 A resolution. <i>Journal of Molecular Biology</i> , <b>1986</b> , 188, 49-61   | 6.5 | 147 |
| 1955 | Mn <sup>2+</sup> -probe ESR method for the analyses of the dissociation of charged residues on the surface of immunoglobulins. <b>1986</b> , 23, 285-90  |     | 7   |
| 1954 | Identification of protein sequence homology by consensus template alignment. <i>Journal of Molecular Biology</i> , <b>1986</b> , 188, 233-58   | 6.5 | 270 |
| 1953 | New hydrophilicity scale derived from high-performance liquid chromatography peptide retention data: correlation of predicted surface residues with antigenicity and X-ray-derived accessible sites. <b>1986</b> , 25, 5425-32 |     | 890 |
| 1952 | Location of continuous antigenic determinants in the protruding regions of proteins.. <b>1986</b> , 5, 409-413   |     | 211 |
| 1951 | Theoretical methods for obtaining free energies of biomolecular equilibria in aqueous solutions. <b>1986</b> , 127, 64-78  |     | 7   |
| 1950 | Orientation of amino acid side chains: intraprotein and solvent interactions. <b>1986</b> , 127, 183-96  |     | 8   |
| 1949 | Observation of internal motility of proteins by nuclear magnetic resonance in solution. <b>1986</b> , 131, 307-26  |     | 39  |
| 1948 | The opsin family of proteins. <b>1986</b> , 238, 625-42  |     | 244 |
| 1947 | Antigenic determinants in proteins coincide with surface regions accessible to large probes (antibody domains). <b>1986</b> , 83, 226-30   |     | 251 |
| 1946 | Distribution of ions around DNA, probed by energy transfer. <b>1986</b> , 83, 3267-71  |     | 38  |
| 1945 | Computer Simulation and the Design of New Biological Molecules. <b>1986</b> , 27, 211-215  |     | 51  |
| 1944 | Molecular dynamics simulations of cooling in laser-excited heme proteins. <b>1986</b> , 83, 8982-6   |     | 253 |
| 1943 | Evolutionary origin of autoreactive determinants (autogens). <b>1986</b> , 83, 2521-5  |     | 19  |

|      |   |     |
|------|---|-----|
| 1942 | Redox pathways in electron-transfer proteins: correlations between reactivities, solvent exposure, and unpaired-spin-density distributions. <b>1986</b> , 83, 3693-7  | 26  |
| 1941 | Molecular models for the putative dimer of sea lamprey hemoglobin. <b>1986</b> , 83, 8487-91  | 16  |
| 1940 | Enthalpies of transfer for proteins from aqueous to water-alcohol solutions: a test for models of residues exposed to solvent. <b>1986</b> , 25, 119-34   | 2   |
| 1939 | Molecular cartography of globular proteins with application to antigenic sites. <b>1986</b> , 25, 863-83  | 55  |
| 1938 | Peptide-bond distortions and the curvature of alpha-helices. <b>1986</b> , 25, 1087-93  | 31  |
| 1937 | Shape complementarity at the hemoglobin alpha 1 beta 1 subunit interface. <b>1986</b> , 25, 1229-47   | 190 |
| 1936 | Estimation of the stability of globular proteins. <b>1986</b> , 25, 1623-1633   | 38  |
| 1935 | Calculations on the effect of methylation on the electrostatic stability of the B- and Z-conformers of DNA. <b>1986</b> , 25, 1697-715  | 18  |
| 1934 | The distribution of charged groups in proteins. <b>1986</b> , 25, 1717-33   | 119 |
| 1933 | Comparison between the unfolding rate and structural fluctuations in native lysozyme--effects of denaturants, ligand binding, and intrachain cross-linking on hydrogen exchange and unfolding kinetics. <b>1986</b> , 25, 1981-96 | 7   |
| 1932 | Membrane structure and biologic activity of adrenocorticotropin (ACTH) and melanotropin (MSH) peptides. Estimation of structural parameters including the influence of the helix dipole moment. <b>1986</b> , 69, 1685-1698       | 15  |
| 1931 | Hydrophobicity and amphiphilicity in protein structure. <b>1986</b> , 31, 11-7  | 61  |
| 1930 | Plotting protein surfaces. <b>1986</b> , 4, 93-96   | 6   |
| 1929 | Comprehensive molecular modelling system. <b>1986</b> , 4, 134-142  | 9   |
| 1928 | Measurement of protein surface shape by solid angles. <b>1986</b> , 4, 3-6  | 95  |
| 1927 | The role of non-covalent forces in micelle formation by vicilin from <i>Vicia faba</i> . The effect of pH variations on protein interactions. <b>1986</b> , 20, 305-318   | 9   |
| 1926 | Solute and mobile phase contributions to retention in hydrophobic interaction chromatography of proteins. <b>1986</b> , 359, 131-46   | 179 |
| 1925 | Computer simulation of protein adsorption and chromatography. <b>1986</b> , 365, 205-212  | 6   |

|      |  |      |
|------|--|------|
| 1924 | Mutant forms of staphylococcal nuclease with altered patterns of guanidine hydrochloride and urea denaturation. <b>1986</b> , 1, 81-9  | 240  |
| 1923 | An algorithm for determining the conformation of polypeptide segments in proteins by systematic search. <b>1986</b> , 1, 146-63  | 246  |
| 1922 | Solvation of amino acid residues in water and urea-water mixtures: Volumes and heat capacities of 20 amino acids in water and in 8 molar urea at 25°C. <b>1986</b> , 15, 109-128   | 125  |
| 1921 | Solvation energy in protein folding and binding. <b>1986</b> , 319, 199-203  | 1673 |
| 1920 | Continuous and discontinuous protein antigenic determinants. <b>1986</b> , 322, 747-8  | 471  |
| 1919 | New potent neuroleptic drugs of benzamide derivatives. III. Structures of YM-09151-1, N-[(2RS,3SR)-1-benzyl-2-methyl-3-pyrrolidinyl]-5-chloro-2-methoxy-4-methylaminobenzamide hydrochloride, and its monohydrate. <b>1986</b> , 42, 117-121 | 1    |
| 1918 | The refined structure of beef liver catalase at 2.5 Å resolution. <b>1986</b> , 42, 497-515  | 90   |
| 1917 | Effects of temperature on food proteins and its implications on functional properties. <b>1986</b> , 23, 323-95  | 76   |
| 1916 | Calculation of electrostatic interactions in proteins. <b>1986</b> , 130, 413-36   | 63   |
| 1915 | Loops in globular proteins: a novel category of secondary structure. <b>1986</b> , 234, 849-55   | 509  |
| 1914 | Three-dimensional structure of an antigen-antibody complex at 2.8 Å resolution. <b>1986</b> , 233, 747-53  | 1132 |
| 1913 | A static accessibility model of protein antigenicity. <b>1987</b> , 2, 379-89  |      |
| 1912 | The passive electrical properties of biological systems: their significance in physiology, biophysics and biotechnology. <b>1987</b> , 32, 933-70  | 607  |
| 1911 | Atomic structure of thymidylate synthase: target for rational drug design. <b>1987</b> , 235, 448-55   | 311  |
| 1910 | Molecular structure of troponin C and its implications for the Ca <sup>2+</sup> triggering of muscle contraction. <b>1987</b> , 139, 610-32  | 15   |
| 1909 | Structure of the reaction center from Rhodospirillum rubrum R-26: membrane-protein interactions. <b>1987</b> , 84, 6438-42   | 240  |
| 1908 | Accessible surface areas as a measure of the thermodynamic parameters of hydration of peptides. <b>1987</b> , 84, 3086-90  | 687  |
| 1907 | Molecular structure of mammalian neuropeptide Y: analysis by molecular cloning and computer-aided comparison with crystal structure of avian homologue. <b>1987</b> , 84, 2532-6   | 173  |



|      |  |     |      |
|------|--|-----|------|
| 1906 | Tertiary templates for proteins. Use of packing criteria in the enumeration of allowed sequences for different structural classes. <i>Journal of Molecular Biology</i> , <b>1987</b> , 193, 775-91           | 6.5 | 1366 |
| 1905 | Interior and surface of monomeric proteins. <i>Journal of Molecular Biology</i> , <b>1987</b> , 196, 641-56  | 6.5 | 784  |
| 1904 | Rubredoxin from <i>Desulfovibrio gigas</i> . A molecular model of the oxidized form at 1.4 Å resolution. <i>Journal of Molecular Biology</i> , <b>1987</b> , 197, 525-41                                     | 6.5 | 109  |
| 1903 | A model for electrostatic effects in proteins. <i>Journal of Molecular Biology</i> , <b>1987</b> , 197, 122-130  | 6.5 | 38   |
| 1902 | Rat submaxillary gland serine protease, tonin. Structure solution and refinement at 1.8 Å resolution. <i>Journal of Molecular Biology</i> , <b>1987</b> , 195, 373-96  | 6.5 | 121  |
| 1901 | Crystal and molecular structures of the complex of alpha-chymotrypsin with its inhibitor turkey ovomucoid third domain at 1.8 Å resolution. <i>Journal of Molecular Biology</i> , <b>1987</b> , 195, 397-418 | 6.5 | 235  |
| 1900 | Chemistry of antibody binding to a protein. <b>1987</b> , 235, 1184-90   |     | 230  |
| 1899 | Correlation of co-ordinated amino acid substitutions with function in viruses related to tobacco mosaic virus. <i>Journal of Molecular Biology</i> , <b>1987</b> , 193, 693-707                              | 6.5 | 219  |
| 1898 | Canonical structures for the hypervariable regions of immunoglobulins. <i>Journal of Molecular Biology</i> , <b>1987</b> , 196, 901-17   | 6.5 | 1195 |
| 1897 | Correlation among sites of limited proteolysis, enzyme accessibility and segmental mobility. <b>1987</b> , 211, 185-9  |     | 59   |
| 1896 | The hydration of protein secondary structures. <b>1987</b> , 213, 423-7  |     | 25   |
| 1895 | Structure and dynamics of water surrounding biomolecules. <b>1987</b> , 16, 93-114   |     | 250  |
| 1894 | Hydrophobicity scales and computational techniques for detecting amphipathic structures in proteins. <i>Journal of Molecular Biology</i> , <b>1987</b> , 195, 659-85   | 6.5 | 566  |
| 1893 | Computer studies of interactions between macromolecules. <b>1987</b> , 49, 29-63   |     | 41   |
| 1892 | Folding and association of proteins. <b>1987</b> , 49, 117-237   |     | 571  |
| 1891 | Refined crystal structure of dogfish M4 apo-lactate dehydrogenase. <i>Journal of Molecular Biology</i> , <b>1987</b> , 198, 445-67   | 6.5 | 178  |
| 1890 | Analysis of side-chain orientations in homologous proteins. <i>Journal of Molecular Biology</i> , <b>1987</b> , 196, 175-88  |     | 128  |
| 1889 | Hydrogen exchange kinetics of surface peptide amides in bovine pancreatic trypsin inhibitor. <i>Journal of Molecular Biology</i> , <b>1987</b> , 193, 793-802  | 6.5 | 36   |

|      |   |     |     |
|------|---|-----|-----|
| 1888 | Crystal structure of a deletion mutant of a tyrosyl-tRNA synthetase complexed with tyrosine. <i>Journal of Molecular Biology</i> , <b>1987</b> , 194, 287-97  | 6.5 | 106 |
| 1887 | Structure of the C-terminal domain of the ribosomal protein L7/L12 from <i>Escherichia coli</i> at 1.7 Å. <i>Journal of Molecular Biology</i> , <b>1987</b> , 195, 555-79   | 6.5 | 186 |
| 1886 | Structural studies of mutants of the lysozyme of bacteriophage T4. The temperature-sensitive mutant protein Thr157----Ile. <i>Journal of Molecular Biology</i> , <b>1987</b> , 197, 315-29                        | 6.5 | 57  |
| 1885 | Trypsinogen-trypsin transition: a molecular dynamics study of induced conformational change in the activation domain. <b>1987</b> , 26, 5153-62   |     | 58  |
| 1884 | How much do we know about the Bohr effect of hemoglobin?. <b>1987</b> , 26, 6299-305  |     | 79  |
| 1883 | Local structural features around the C-terminal segment of <i>Streptomyces subtilisin</i> inhibitor studied by carbonyl carbon nuclear magnetic resonances three phenylalanyl residues. <b>1987</b> , 26, 1068-75 |     | 36  |
| 1882 | Crystal and molecular structure of the serine proteinase inhibitor CI-2 from barley seeds. <b>1987</b> , 26, 261-9  |     | 244 |
| 1881 | Solvent exchange of buried water and hydrogen exchange of peptide NH groups hydrogen bonded to buried waters in bovine pancreatic trypsin inhibitor. <b>1987</b> , 26, 5163-72                                    |     | 27  |
| 1880 | Column liquid chromatography of integral membrane proteins. <b>1987</b> , 418, 223-43   |     | 20  |
| 1879 | An application of algebraic topology to solid modeling in molecular biology. <b>1987</b> , 3, 72-81   |     | 9   |
| 1878 | Distribution of termite (Isoptera) species in southwestern Kenya in relation to land use and the morphology of their galleries. <b>1987</b> , 3-3, 69   |     | 12  |
| 1877 | Structural disorder in proteins. A comparison of myoglobin and erythrocyruorin. <b>1987</b> , 14, 337-48  |     | 13  |
| 1876 | Estimation of uncertainties in X-ray refinement results by use of perturbed structures. <b>1987</b> , 2, 1-12   |     | 25  |
| 1875 | Continuous compact protein domains. <b>1987</b> , 2, 90-110   |     | 27  |
| 1874 | Intron/exon structure of the human gene for the muscle isozyme of glycogen phosphorylase. <b>1987</b> , 2, 177-87   |     | 73  |
| 1873 | Modeling the biochemical differences between rabbit muscle and human liver phosphorylase. <b>1987</b> , 2, 225-35   |     | 23  |
| 1872 | Electrostatic interaction of a solute with a continuum. Improved description of the cavity and of the surface cavity bound charge distribution.. <b>1987</b> , 8, 778-787   |     | 327 |
| 1871 | Local sequence patterns of hydrophobicity and solvent accessibility in soluble globular proteins. <b>1987</b> , 26, 17-26   |     | 13  |

|      |  |      |
|------|--|------|
| 1870 | Prediction of protein–ligand interactions: the complex of porcine pancreatic elastase with a valine-derived benzoxazinone. <b>1987</b> , 26, 1207-25   |      |
| 1869 | Computergestütztes Moleküldesign (CAMD) –ein Überblick. <b>1987</b> , 99, 413-428  | 18   |
| 1868 | Purification strategies for Sendai virus membrane proteins. <b>1987</b> , 397, 165-74  | 12   |
| 1867 | Protein antigenicity: a static surface property. <b>1987</b> , 8, 26-31  | 74   |
| 1866 | Surface fractality as a guide for studying protein-protein interactions. <b>1987</b> , 5, 30-34  | 47   |
| 1865 | Protein surface area and retention in hydrophobic interaction chromatography. <b>1987</b> , 24, 646-650  | 37   |
| 1864 | Inhibition of phosphorylcholine binding to antibodies using synthetic peptides. <b>1987</b> , 325, 168-71  | 5    |
| 1863 | Structure of a mutant of tyrosyl-tRNA synthetase with enhanced catalytic properties. <b>1987</b> , 326, 416-8  | 26   |
| 1862 | Structure of the human class I histocompatibility antigen, HLA-A2. <b>1987</b> , 329, 506-12   | 3084 |
| 1861 | Stabilization of charges on isolated ionic groups sequestered in proteins by polarized peptide units. <b>1987</b> , 329, 561-4   | 110  |
| 1860 | Isoleucyl-tRNA synthetase from baker's yeast and from Escherichia coli MRE 600. Discrimination of 20 amino acids in aminoacylation of tRNA(Ile)-C-C-A(3'NH <sub>2</sub> ). <b>1987</b> , 169, 33-9 | 29   |
| 1859 | Isoleucyl-tRNA synthetase from baker's yeast and from Escherichia coli MRE 600. Discrimination of 20 amino acids in aminoacylation of tRNA(Ile)-C-C-A. <b>1988</b> , 173, 27-34                    | 32   |
| 1858 | Protein stabilization via hydrophilization. Covalent modification of trypsin and alpha-chymotrypsin. <b>1988</b> , 173, 147-54   | 81   |
| 1857 | Isoleucyl-tRNA-Synthetase: Ein Enzym mit mehreren Katalysewegen, variabel in Spezifität und Energieverbrauch. <b>1988</b> , 100, 795-811   | 4    |
| 1856 | Identification of regions of potential flexibility in protein structures: folding units and correlations with intron positions. <b>1988</b> , 27, 23-40  | 18   |
| 1855 | Frictional models for stochastic simulations of proteins. <b>1988</b> , 27, 1001-14  | 119  |
| 1854 | Molecular dynamics of structural transitions and intercalation in DNA. <b>1988</b> , 27, 1239-48   | 15   |
| 1853 | Isoleucyl-tRNA Synthetase: An Enzyme with Several Catalytic Cycles Displaying Variation in Specificity and Energy Consumption. <b>1988</b> , 27, 773-788   | 6    |

|      |   |     |
|------|---|-----|
| 1852 | A basic library of microcomputer programs to obtain immunologically relevant information from protein sequences. <b>1988</b> , 22, 165-81 |     |
| 1851 | Calculating the electrostatic potential of molecules in solution: Method and error assessment. <b>1988</b> , 9, 327-335                   | 948 |
| 1850 | Shape characterization of some molecular model surfaces. <b>1988</b> , 9, 554-563   | 51  |
| 1849 | On the appearance and role of a spacer group in the protein amino acids. <b>1988</b> , 27, 147-53   | 1   |
| 1848 | A rapid approximation to the solvent accessible surface areas of atoms. <b>1988</b> , 1, 103-116  | 258 |
| 1847 | The importance of purity in the crystallization of DNA binding immunoglobulin Fab fragments. <b>1988</b> , 90, 153-159                    | 12  |
| 1846 | The polystyrene affinity of methylglycosides, deoxysugars and glucooligosaccharides. <b>1988</b> , 17, 347-358                            | 10  |
| 1845 | Energetics of charge-charge interactions in proteins. <b>1988</b> , 3, 32-52  | 258 |
| 1844 | Structural comparison of the prokaryotic ribosomal proteins L7/L12 and L30. <b>1988</b> , 3, 243-51                                       | 22  |
| 1843 | Criteria that discriminate between native proteins and incorrectly folded models. <b>1988</b> , 4, 19-30                                  | 173 |
| 1842 | Surface interactions of gamma-crystallins in the crystal medium in relation to their association in the eye lens. <b>1988</b> , 4, 137-47 | 28  |
| 1841 | Comparative molecular model building of two serine proteinases from cytotoxic T lymphocytes. <b>1988</b> , 4, 190-204                     | 75  |
| 1840 | Diffusion-collision model for the folding kinetics of myoglobin. <b>1988</b> , 4, 211-27  | 67  |
| 1839 | Refined structure of human carbonic anhydrase II at 2.0 A resolution. <b>1988</b> , 4, 274-82   | 465 |
| 1838 | Protein Folding: New Twists. <b>1988</b> , 6, 167-171   | 7   |
| 1837 | Protein structure. What's left out tells the story. <b>1988</b> , 334, 381  |     |
| 1836 | Hydrophobic stabilization in T4 lysozyme determined directly by multiple substitutions of Ile 3. <b>1988</b> , 334, 406-10                | 356 |
| 1835 | Structure of antibody hypervariable loops reproduced by a conformational search algorithm. <b>1988</b> , 335, 564-8                       | 193 |

|      |  |     |     |
|------|--|-----|-----|
| 1834 | A peptide model of a protein folding intermediate. <b>1988</b> , 336, 42-8   |     | 273 |
| 1833 | The MIDAS display system. <b>1988</b> , 6, 13-27   |     | 852 |
| 1832 | Combined use of spectroscopic and energy calculation methods for the determination of peptide conformation in solution. <b>1988</b> , 31, 101-6  |     | 18  |
| 1831 | Determination of cyclopeptide conformations in solution using NMR data and conformational energy calculations. <b>1988</b> , 31, 163-73  |     | 14  |
| 1830 | Interdomain mobility of enzymes and its functional role. <b>1988</b> , 47, 289-295   |     | 2   |
| 1829 | Crystallization of mutant lysozymes from bacteriophage T4. <b>1988</b> , 90, 160-167   |     | 12  |
| 1828 | Application of the periodic bond chain (PBC) theory to the analysis of the molecular packing in protein crystals. <b>1988</b> , 90, 245-258  |     | 18  |
| 1827 | Structure-stability relationship in proteins: fundamental tasks and strategy for the development of stabilized enzyme catalysts for biotechnology. <b>1988</b> , 23, 235-81                              |     | 96  |
| 1826 | Structural comparison of two serine proteinase-protein inhibitor complexes: Eglin-C-subtilisin Carlsberg and Cl-2-subtilisin Novo. <b>1988</b> , 27, 6582-6598   |     | 331 |
| 1825 | Modification of trypsin-solubilized cytochrome b5, apocytochrome b5, and liposome-bound cytochrome b5 by diethylpyrocarbonate. <b>1988</b> , 261, 55-63  |     | 8   |
| 1824 | Conservation of the putative receptor attachment site in picornaviruses. <b>1988</b> , 164, 373-82   |     | 130 |
| 1823 | A simple ELISA for the classification of monoclonal antibodies according to their recognition of native epitopes. <b>1988</b> , 106, 203-9   |     | 12  |
| 1822 | Analysis of immunoglobulin domain interactions. Evidence for a dominant role of salt bridges. <i>Journal of Molecular Biology</i> , <b>1988</b> , 203, 799-802   | 6.5 | 21  |
| 1821 | Advances in bioconcentration prediction. <b>1988</b> , 17, 1551-1574   |     | 42  |
| 1820 | The extended polarizable continuum model for calculation of solvent effects. <b>1988</b> , 179, 353-366  |     | 22  |
| 1819 | Combinatorial cassette mutagenesis as a probe of the informational content of protein sequences. <b>1988</b> , 241, 53-7   |     | 317 |
| 1818 | Structure analysis of bovine lens calf gamma-II crystallin: residue assignments of the five histidine CE1 resonances observed by proton-nuclear magnetic resonance spectroscopy. <b>1988</b> , 7, 777-88 |     | 2   |
| 1817 | Evolutionary and functional relationships between the basic and acidic beta-crystallins. <b>1988</b> , 46, 375-403   |     | 46  |

|      |   |     |     |
|------|---|-----|-----|
| 1816 | A simple formula for solvent-accessible areas of amino acid side-chains. <b>1988</b> , 156, 792-5   |     | 2   |
| 1815 | Solvent effect in protein crystals. A neutron diffraction analysis of solvent and ion density. <i>Journal of Molecular Biology</i> , <b>1988</b> , 201, 741-9   | 6.5 | 47  |
| 1814 | The use of thermally activated tritium atoms for structural-biological investigations: the topography of the TMV protein-accessible surface of the virus. <i>Journal of Molecular Biology</i> , <b>1988</b> , 201, 567-74 | 6.5 | 33  |
| 1813 | The 2 Å resolution structure of the sulfate-binding protein involved in active transport in <i>Salmonella typhimurium</i> . <i>Journal of Molecular Biology</i> , <b>1988</b> , 200, 163-80                               | 6.5 | 181 |
| 1812 | Surface, subunit interfaces and interior of oligomeric proteins. <i>Journal of Molecular Biology</i> , <b>1988</b> , 204, 155-64  | 6.5 | 590 |
| 1811 | Helix signals in proteins. <b>1988</b> , 240, 1632-41   |     | 630 |
| 1810 | A supertensor formalism for solute-continuum solvent interactions with an arbitrarily shaped cavity. II. Preliminary applications to model systems. <b>1988</b> , 88, 5021-5026   |     | 15  |
| 1809 | DNA stem-loop structures in oligopurine-oligopyrimidine triplexes. <b>1988</b> , 16, 11795-809  |     | 26  |
| 1808 | The chemistry and mechanism of antibody binding to protein antigens. <b>1988</b> , 43, 1-98   |     | 160 |
| 1807 | On the Approximation of Solvent Effects on the Conformation and Dynamics of Cyclosporin A by Stochastic Dynamics Simulation Techniques. <b>1988</b> , 1, 369-383  |     | 59  |
| 1806 | Sugar and signal-transducer binding sites of the <i>Escherichia coli</i> galactose chemoreceptor protein. <b>1988</b> , 242, 1290-5   |     | 342 |
| 1805 | Determination of Protein Structures in Solution Using Nmr Data and Impact. <b>1988</b> , 2, 41-61   |     | 23  |
| 1804 | Tertiary structure of plant RuBisCO: domains and their contacts. <b>1988</b> , 241, 71-4  |     | 142 |
| 1803 | Accurate simulation of protein dynamics in solution. <b>1988</b> , 85, 7557-61  |     | 394 |
| 1802 | Duck lens epsilon-crystallin and lactate dehydrogenase B4 are identical: a single-copy gene product with two distinct functions. <b>1988</b> , 85, 7114-8   |     | 104 |
| 1801 | The electrostatic fields in the active-site clefts of actinidin and papain. <b>1988</b> , 254, 235-8  |     | 33  |
| 1800 | The Study of Partition Coefficients. The Prediction of LogP Value Based on Molecular Structure. <b>1988</b> , 61, 2701-2706   |     | 7   |
| 1799 | References. <b>1988</b> , 19, 197-216   |     |     |

|      |  |     |
|------|--|-----|
| 1798 | The outline structure of the T-cell alpha beta receptor.. <b>1988</b> , 7, 3745-3755   | 420 |
| 1797 | Nobel lecture. The photosynthetic reaction centre from the purple bacterium <i>Rhodospseudomonas viridis</i> .. <b>1989</b> , 8, 2149-2170                       | 508 |
| 1796 | Hydrophobic organization of membrane proteins. <b>1989</b> , 245, 510-3  | 299 |
| 1795 | Effects of buried ionizable amino acids on the reduction potential of recombinant myoglobin. <b>1989</b> , 243, 69-72  | 141 |
| 1794 | Electrostatic interactions in proteins. A theoretical analysis of lysozyme ionization. <b>1989</b> , 999, 1-6  | 42  |
| 1793 | Dynamic space structure of the Leu-enkephalin molecule in DMSO solution. <b>1989</b> , 998, 204-9  | 19  |
| 1792 | Calculation of Molecular Volumes from Molecular Fragments via Valence Electron Indices. <b>1989</b> , 8, 11-16   | 6   |
| 1791 | The photosynthetic reaction centre from the purple bacterium <i>Rhodospseudomonas viridis</i> . <b>1989</b> , 9, 383-419   | 10  |
| 1790 | Some aspects of the organization and evolution of the genetic code. <b>1989</b> , 29, 191-201  | 69  |
| 1789 | Electronic and structural features of $\gamma$ -aminobutyric acid (GABA) and four of its direct agonists. <b>1989</b> , 195, 65-77                               | 21  |
| 1788 | Molecular mechanics and molecular shape. <b>1989</b> , 195, 147-158  | 2   |
| 1787 | Ring-opened analogues of Ambroxol : Synthesis and Structure-Odour relationships. <b>1989</b> , 72, 1278-1283   | 15  |
| 1786 | Das photosynthetische Reaktionszentrum des Purpurbakteriums <i>Rhodospseudomonas viridis</i> (Nobel-Vortrag). <b>1989</b> , 101, 872-892                         | 89  |
| 1785 | Ca <sup>2+</sup> binding cyclic octapeptides having an alternating Ser and a hydrophobic amino acid in the sequence. <b>1989</b> , 28, 1235-46                   | 8   |
| 1784 | Superoxide dismutase: fluctuations in the structure and solvation of the active site channel studied by molecular dynamics simulation. <b>1989</b> , 28, 2085-96 | 26  |
| 1783 | Reversible binding of substance P to artificial lipid membranes studied by capacitance minimization techniques. <b>1989</b> , 34, 103-14                         | 29  |
| 1782 | Calorimetric measurement of the enthalpy of dissolution of diketopiperazine in water as a function of temperature. <b>1989</b> , 139, 279-290                    | 31  |
| 1781 | Thermodynamics of dissolution of solid cyclic dipeptides containing hydrophobic side groups. <b>1989</b> , 21, 903-913   | 44  |

|      |  |        |
|------|--|--------|
| 1780 | A fast algorithm for generating smooth molecular dot surface representations. <b>1989</b> , 7, 109-12, 101   | 16     |
| 1779 | Excess enthalpies and apparent molar volumes of some N-methyl substituted amino acids in aqueous solutions. <b>1989</b> , 18, 131-142  | 6      |
| 1778 | Shape group theory of van der Waals surfaces. <b>1989</b> , 3, 43-71   | 17     |
| 1777 | Discrete characterization of cross-sections of molecular surfaces. <b>1989</b> , 75, 333-352   | 14     |
| 1776 | Electrostatic interactions in proteins: Calculations of the electrostatic term of free energy and the electrostatic potential field. <b>1989</b> , 17, 287   | 24     |
| 1775 | Electrostatic interactions in the assembly of Escherichia coli aspartate transcarbamylase. <b>1989</b> , 5, 66-77  | 12     |
| 1774 | Treatment of electrostatic effects in macromolecular modeling. <b>1989</b> , 5, 78-92  | 335    |
| 1773 | The crystal structure of the ternary complex of staphylococcal nuclease, Ca <sup>2+</sup> , and the inhibitor pdTp, refined at 1.65 Å. <b>1989</b> , 5, 183-201  | 233    |
| 1772 | Amino acid substitutions that increase the thermal stability of the lambda Cro protein. <b>1989</b> , 5, 202-10  | 87     |
| 1771 | Molecular dynamics effects on protein electrostatics. <b>1989</b> , 5, 313-21  | 57     |
| 1770 | A molecular dynamics analysis of protein structural elements. <b>1989</b> , 5, 337-54  | 40     |
| 1769 | Use of restrained molecular dynamics in water to determine three-dimensional protein structure: prediction of the three-dimensional structure of Ecballium elaterium trypsin inhibitor II. <b>1989</b> , 6, 405-17 | 64     |
| 1768 | The surface area of monomeric proteins: significance of power law behavior. <b>1989</b> , 6, 418-23  | 13     |
| 1767 | Alternative packing arrangements in the hydrophobic core of lambda repressor. <b>1989</b> , 339, 31-6  | 376    |
| 1766 | Three-dimensional crystal structures of Escherichia coli met repressor with and without corepressor. <b>1989</b> , 341, 705-10   | 175    |
| 1765 | Crystal structure of muconolactone isomerase at 3.3 Å resolution. <i>Journal of Molecular Biology</i> , <b>1989</b> , 205, 557-71  | 6.5 29 |
| 1764 | On the molecular nature of "restrictive" antigenic elements present on major histocompatibility complex (MHC) proteins. <b>1989</b> , 140, 145-58  | 3      |
| 1763 | DNA B to D transition can be explained in terms of hydration economy of the minor groove atoms. <i>Journal of Molecular Biology</i> , <b>1989</b> , 210, 399-409   | 6.5 13 |



|      |   |     |     |
|------|---|-----|-----|
| 1762 | Protein engineering of disulfide bonds in subtilisin BPN'. <b>1989</b> , 28, 4807-15  |     | 150 |
| 1761 | The Hydrophobicity Profile. <b>1989</b> , 625-633   |     | 10  |
| 1760 | Tertiary Structure Prediction. <b>1989</b> , 647-705  |     | 30  |
| 1759 | The Development of the Prediction of Protein Structure. <b>1989</b> , 193-316   |     | 56  |
| 1758 | Molecular dynamics of tryptophan in ribonuclease-T1. II. Correlations with fluorescence. <b>1989</b> , 56, 43-66  |     | 35  |
| 1757 | Approximate methods for solvent effects calculations on biomolecules. <b>1989</b> , 183, 403-419  |     | 13  |
| 1756 | In vitro cleavage of the Lathyrus nissolia isolectins. <b>1989</b> , 62, 181-189  |     | 6   |
| 1755 | Construction of side-chains in homology modelling. Application to the C-terminal lobe of rhizopuspepsin. <i>Journal of Molecular Biology</i> , <b>1989</b> , 210, 785-811   | 6.5 | 87  |
| 1754 | Periplasmic binding protein structure and function. Refined X-ray structures of the leucine/isoleucine/valine-binding protein and its complex with leucine. <i>Journal of Molecular Biology</i> , <b>1989</b> , 206, 171-91 | 6.5 | 234 |
| 1753 | Structure of the L-leucine-binding protein refined at 2.4 Å resolution and comparison with the Leu/Ile/Val-binding protein structure. <i>Journal of Molecular Biology</i> , <b>1989</b> , 206, 193-207                      | 6.5 | 98  |
| 1752 | Role of the hydrophobic effect in stability of site-specific protein-DNA complexes. <i>Journal of Molecular Biology</i> , <b>1989</b> , 209, 801-16   | 6.5 | 395 |
| 1751 | Biomedical science and the third world. Under the volcano. Trypanothione reductase. <b>1989</b> , 569, 193-200  |     | 9   |
| 1750 | Hidden thermodynamics of mutant proteins: a molecular dynamics analysis. <b>1989</b> , 244, 1069-72   |     | 259 |
| 1749 | Structure of Ca <sup>2+</sup> prothrombin fragment 1 including the conformation of the Gla domain. <b>1989</b> , 28, 6805-10  |     | 81  |
| 1748 | Electrostatic interactions in wild-type and mutant recombinant human myoglobins. <b>1989</b> , 28, 3771-81  |     | 98  |
| 1747 | Use of site-directed mutagenesis to destabilize native apomyoglobin relative to folding intermediates. <b>1989</b> , 28, 4415-22  |     | 117 |
| 1746 | Comparison of the Fc fragment from a human IgG1 and its CH2, pFc', and tFc' subfragments. A study using reductive methylation and <sup>13</sup> C NMR. <b>1989</b> , 28, 3250-7   |     | 8   |
| 1745 | Identification by proton nuclear magnetic resonance of the histidines in cytochrome b5 modified by diethyl pyrocarbonate. <b>1989</b> , 28, 7516-23   |     | 25  |

|      |  |     |
|------|--|-----|
| 1744 | A theoretical study of the acidification of the rhinovirus capsid. <b>1989</b> , 257, 403-7  | 8   |
| 1743 | Analysis of structure-function relationships of neuropeptide Y using molecular dynamics simulations and pharmacological activity and binding measurements. <b>1989</b> , 25, 295-313 | 28  |
| 1742 | Protein conformational prediction. <b>1989</b> , 14, 295-9   | 60  |
| 1741 | A relational database of protein structures designed for flexible enquiries about conformation. <b>1989</b> , 2, 431-42  | 40  |
| 1740 | Hydrophobic packing in T4 lysozyme probed by cavity-filling mutants. <b>1989</b> , 86, 8237-41   | 147 |
| 1739 | Crystallographic refinement of interleukin 1 beta at 2.0 A resolution. <b>1989</b> , 86, 9667-71   | 155 |
| 1738 | Unusually stable helix formation in short alanine-based peptides. <b>1989</b> , 86, 5286-90  | 691 |
| 1737 | Hydrophobic effect in protein folding and other noncovalent processes involving proteins. <b>1989</b> , 86, 8382-5   | 280 |
| 1736 | Topological distribution of four-alpha-helix bundles. <b>1989</b> , 86, 6592-6   | 175 |
| 1735 | Modeling antibody hypervariable loops: a combined algorithm. <b>1989</b> , 86, 9268-72   | 175 |
| 1734 | Experimental and Theoretical Studies of Albendazole, Oxibendazole, and Tioxidazole. <b>1990</b> , 76, 180  | 21  |
| 1733 | Lambda repressor: a model system for understanding protein-DNA interactions and protein stability. <b>1990</b> , 40, 1-61  | 55  |
| 1732 | Reverse hydrophobic effects relieved by amino-acid substitutions at a protein surface. <b>1990</b> , 344, 363-4  | 161 |
| 1731 | Surface areas of unfolded proteins. <b>1990</b> , 348, 397   |     |
| 1730 | The folding and solution conformation of penicillin G acylase. <b>1990</b> , 192, 133-41   | 41  |
| 1729 | Thermodynamic properties of globular proteins and the principle of stabilization of their native structure. <b>1990</b> , 1040, 346-54   | 23  |
| 1728 | A genetic screen to identify variants of bovine pancreatic trypsin inhibitor with altered folding energetics. <b>1990</b> , 7, 16-31   | 28  |
| 1727 | Computer analysis of mutations that affect antibody specificity. <b>1990</b> , 7, 93-8   | 24  |

|      |   |      |
|------|---|------|
| 1726 | A mutant T4 lysozyme (Val 131----Ala) designed to increase thermostability by the reduction of strain within an alpha-helix. <b>1990, 7, 198-204</b>                  | 79   |
| 1725 | Identification of protein folds: matching hydrophobicity patterns of sequence sets with solvent accessibility patterns of known structures. <b>1990, 7, 257-64</b>    | 92   |
| 1724 | Functionally acceptable substitutions in two alpha-helical regions of lambda repressor. <b>1990, 7, 306-16</b>  | 69   |
| 1723 | Functional interaction among catalytic residues in subtilisin BPN'. <b>1990, 7, 335-42</b>  | 67   |
| 1722 | Molecular interactions in protein crystals: solvent accessible surface and stability. <b>1990, 8, 1-5</b>   | 39   |
| 1721 | Crystallographic refinement of human serum retinol binding protein at 2A resolution. <b>1990, 8, 44-61</b>  | 282  |
| 1720 | Plastic adaptation toward mutations in proteins: structural comparison of thymidylate synthases. <b>1990, 8, 315-33</b>   | 133  |
| 1719 | Solvation of the active site of cytochrome P450-cam. <b>1990, 4, 199-204</b>  | 29   |
| 1718 | Case report 589: Use of Ostamer in fusion of lumbar spine, postoperative appearance. <b>1990, 19, 62-4</b>  | 0    |
| 1717 | A rapid method of protein structure alignment. <b>1990, 147, 517-51</b>   | 115  |
| 1716 | Thermodynamics of solvation of proteins in guanidine hydrochloride. <b>1990, 29, 1593-1598</b>  | 13   |
| 1715 | A molecular dynamics investigation of the elastomeric restoring force in elastin. <b>1990, 29, 1613-31</b>  | 71   |
| 1714 | Statistical descriptors for the size and shape of globular proteins. <b>1990, 29, 1745-54</b>   | 12   |
| 1713 | Analysis of side-chain conformational distributions in neutrophil peptide-5 NMR structures. <b>1990, 29, 1807-22</b>  | 8    |
| 1712 | Conformational sampling using high-temperature molecular dynamics. <b>1990, 29, 1847-62</b>   | 209  |
| 1711 | Fluctuation of the solvent-accessible surface area of tuna ferrocytochrome c. <b>1990, 29, 1877-83</b>  | 9    |
| 1710 | High temperature annealed molecular dynamics simulations as a tool for conformational sampling. Application to the bicyclic $\beta$ -cryptand. <b>1990, 11, 19-31</b> | 58   |
| 1709 | Macromodel—an integrated software system for modeling organic and bioorganic molecules using molecular mechanics. <b>1990, 11, 440-467</b>                            | 3405 |

|      |  |     |
|------|--|-----|
| 1708 | GEPOL: An improved description of molecular surfaces. I. Building the spherical surface set. <b>1990</b> , 11, 1047-1060   | 217 |
| 1707 | Protein interactions with immobilized transition metal ions: quantitative evaluations of variations in affinity and binding capacity. <b>1990</b> , 191, 160-8               | 64  |
| 1706 | A computational ab-initio model for the evaluation of thermodynamic functions for solvent transfer processes.. <b>1990</b> , 47, 25-34                                       | 21  |
| 1705 | A new tool for the qualitative and quantitative analysis of protein surfaces using B-spline and density of surface neighborhood. <b>1990</b> , 8, 133-40, 146                | 21  |
| 1704 | Molecular volumes and surfaces of biomacromolecules via GEPOL: a fast and efficient algorithm. <b>1990</b> , 8, 168-72, 151  | 85  |
| 1703 | A method to detect common features necessary for biological activity: Application of ANALOGS for aldose reductase inhibitors. <b>1990</b> , 3, 3-14                          | 1   |
| 1702 | Differential interaction of peptides and protein surface structures with free metal ions and surface-immobilized metal ions. <b>1990</b> , 500, 531-42                       | 47  |
| 1701 | High-performance liquid chromatography of insulin. Accessibility and flexibility. <b>1990</b> , 502, 325-36  | 6   |
| 1700 | Enthalpies of interaction of some N-acetyl amides of l-serine, l-threonine and l-hydroxyproline dissolved in N,N-dimethylformamide at 298.15 k. <b>1990</b> , 167, 65-72     | 13  |
| 1699 | Group additivity thermodynamics for dissolution of solid cyclic dipeptides into water. <b>1990</b> , 172, 11-20  | 84  |
| 1698 | 5.1.2 Methods of calculation and representation. 350-351   |     |
| 1697 | Interfaces, Protein Films, and Foams. <b>1990</b> , 34, 1-79   | 58  |
| 1696 | Solvation effects on the sequence variability of DNA double helical conformations. <b>1990</b> , 8, 187-98   | 7   |
| 1695 | Deciphering the message in protein sequences: tolerance to amino acid substitutions. <b>1990</b> , 247, 1306-10  | 443 |
| 1694 | Free energy of sickling: A simulation analysis. <b>1990</b> , 87, 8481-5   | 41  |
| 1693 | Residues in three conserved regions of the small subunit of ribulose-1,5-bisphosphate carboxylase/oxygenase are required for quaternary structure. <b>1990</b> , 87, 5768-72 | 28  |
| 1692 | Retention Studies and Protein Separation by Potential Barrier Chromatography. <b>1990</b> , 25, 207-242  | 2   |
| 1691 | Structural characterization of a partly folded apomyoglobin intermediate. <b>1990</b> , 249, 1544-8  | 680 |

|      |  |     |     |
|------|--|-----|-----|
| 1690 | Three-dimensional structure of cellobiohydrolase II from <i>Trichoderma reesei</i> . <b>1990</b> , 249, 380-6  |     | 593 |
| 1689 | Contribution of histidine residues to the conformational stability of ribonuclease T1 and mutant Glu-58----Ala. <b>1990</b> , 29, 7572-6   |     | 52  |
| 1688 | Molecular dynamics study of the structure and dynamics of a protein molecule in a crystalline ionic environment, <i>Streptomyces griseus</i> protease A. <b>1990</b> , 29, 8658-76                         |     | 56  |
| 1687 | Synthesis and biophysical characterization of engineered topographic immunogenic determinants with alpha alpha topology. <b>1990</b> , 29, 13-23   |     | 88  |
| 1686 | Bluetongue virus: surface exposure of VP7. <b>1990</b> , 16, 17-26   |     | 15  |
| 1685 | Common features of protein unfolding and dissolution of hydrophobic compounds. <b>1990</b> , 247, 559-61   |     | 396 |
| 1684 | Modelling allosteric processes in <i>E coli</i> aspartate transcarbamylase. <b>1990</b> , 72, 617-24   |     | 5   |
| 1683 | A precise analytical method for calculating the electrostatic energy of macromolecules in aqueous solution. <i>Journal of Molecular Biology</i> , <b>1990</b> , 216, 1045-66                               | 6.5 | 94  |
| 1682 | Excluded volume approximation to protein-solvent interaction. The solvent contact model. <b>1990</b> , 57, 1103-7  |     | 66  |
| 1681 | Crystallographic analysis of ribulose 1,5-bisphosphate carboxylase from spinach at 2.4 A resolution. Subunit interactions and active site. <i>Journal of Molecular Biology</i> , <b>1990</b> , 215, 113-60 | 6.5 | 285 |
| 1680 | Refined crystal structure of type III chloramphenicol acetyltransferase at 1.75 A resolution. <i>Journal of Molecular Biology</i> , <b>1990</b> , 213, 167-86  | 6.5 | 130 |
| 1679 | Comparison and accuracy of methodologies employed for analysis of hydrophathy, flexibility and secondary structure of proteins. <b>1990</b> , 129, 77-88   |     | 6   |
| 1678 | Refined structure of yeast apo-enolase at 2.25 A resolution. <i>Journal of Molecular Biology</i> , <b>1990</b> , 211, 235-48   |     | 92  |
| 1677 | Analysis of the structure of a common cold virus, human rhinovirus 14, refined at a resolution of 3.0 A. <i>Journal of Molecular Biology</i> , <b>1990</b> , 211, 763-801                                  | 6.5 | 114 |
| 1676 | X-ray analyses of aspartic proteinases. The three-dimensional structure at 2.1 A resolution of endothiapepsin. <i>Journal of Molecular Biology</i> , <b>1990</b> , 211, 919-41                             | 6.5 | 114 |
| 1675 | Refined structure of diene lactone hydrolase at 1.8 A. <i>Journal of Molecular Biology</i> , <b>1990</b> , 214, 497-525  | 6.5 | 114 |
| 1674 | Molecular structure of flavocytochrome b2 at 2.4 A resolution. <i>Journal of Molecular Biology</i> , <b>1990</b> , 212, 837-63   | 6.5 | 310 |
| 1673 | Crystal structure of thioredoxin from <i>Escherichia coli</i> at 1.68 A resolution. <i>Journal of Molecular Biology</i> , <b>1990</b> , 212, 167-84  | 6.5 | 532 |

|      |   |     |     |
|------|---|-----|-----|
| 1672 | Translational diffusion and intrinsic viscosity of globular proteins. Theoretical predictions using hydrated hydrodynamic models. Application to BPTI. <b>1990</b> , 12, 19-24  |     | 10  |
| 1671 | The importance of Val-157 hydrophobic interaction for papain inhibitory activity of an epoxysuccinyl amino acid derivative. A structure-activity relationship based on the crystal structure of the papain-E-64-c complex. <b>1990</b> , 263, 134-6 |     | 11  |
| 1670 | The influence of proline residues on alpha-helical structure. <b>1990</b> , 277, 185-8  |     | 113 |
| 1669 | "Hydration memory" of lysozyme: a misinterpretation. <b>1990</b> , 166, 1039-46   |     | 1   |
| 1668 | Hydrophobicity of amino acid subgroups in proteins. <b>1990</b> , 8, 6-13   |     | 126 |
| 1667 | Generation of a lysosomal enzyme targeting signal in the secretory protein pepsinogen. <b>1990</b> , 63, 281-91   |     | 143 |
| 1666 | Mapping of epitopes on the 86 kDa subunit of the Ku autoantigen. <b>1990</b> , 27, 973-80   |     | 28  |
| 1665 | An analysis of protein folding pathways. <b>1991</b> , 30, 3816-24  |     | 112 |
| 1664 | Molecular recognition. Conformational analysis of limited proteolytic sites and serine proteinase protein inhibitors. <i>Journal of Molecular Biology</i> , <b>1991</b> , 220, 507-30   | 6.5 | 340 |
| 1663 | Regulation of methionine biosynthesis in the Enterobacteriaceae. <b>1991</b> , 56, 145-85   |     | 48  |
| 1662 | Solvent denaturation and stabilization of globular proteins. <b>1991</b> , 30, 5974-85  |     | 242 |
| 1661 | Reconciling the magnitude of the microscopic and macroscopic hydrophobic effects. <b>1991</b> , 252, 106-9  |     | 459 |
| 1660 | Protein folding. <b>1991</b> , 1, 224-229   |     | 33  |
| 1659 | Atomic structure of adenosine deaminase complexed with a transition-state analog: understanding catalysis and immunodeficiency mutations. <b>1991</b> , 252, 1278-84  |     | 414 |
| 1658 | Crystal structure of the ternary complex of ribulose-1,5-bisphosphate carboxylase, Mg(II), and activator CO <sub>2</sub> at 2.3-Å resolution. <b>1991</b> , 30, 904-8   |     | 74  |
| 1657 | Hydroxyl radical footprinting. <b>1991</b> , 208, 380-413   |     | 179 |
| 1656 | The conserved, buried aspartic acid in oxidized <i>Escherichia coli</i> thioredoxin has a pK <sub>a</sub> of 7.5. Its titration produces a related shift in global stability. <b>1991</b> , 30, 7603-9  |     | 120 |
| 1655 | Extracting hydrophobic free energies from experimental data: relationship to protein folding and theoretical models. <b>1991</b> , 30, 9686-97  |     | 415 |

|      |  |     |     |
|------|--|-----|-----|
| 1654 | Toward a simplification of the protein folding problem: a stabilizing polyalanine alpha-helix engineered in T4 lysozyme. <b>1991</b> , 30, 2012-7  |     | 81  |
| 1653 | Crystal and molecular structure of human plasminogen kringle 4 refined at 1.9-A resolution. <b>1991</b> , 30, 10576-88   |     | 116 |
| 1652 | Neutron structure of subtilisin BPN': effects of chemical environment on hydrogen-bonding geometries and the pattern of hydrogen-deuterium exchange in secondary structure elements. <b>1991</b> , 30, 1211-21 |     | 23  |
| 1651 | Simulation analysis of the stability mutant R96H of T4 lysozyme. <b>1991</b> , 30, 3217-28   |     | 167 |
| 1650 | Linkage of thioredoxin stability to titration of ionizable groups with perturbed pKa. <b>1991</b> , 30, 7609-14  |     | 85  |
| 1649 | Probing the stability of a partly folded apomyoglobin intermediate by site-directed mutagenesis. <b>1991</b> , 30, 4113-8  |     | 169 |
| 1648 | Comparison of the structures of three carboxypeptidase A-phosphonate complexes determined by X-ray crystallography. <b>1991</b> , 30, 8171-80  |     | 107 |
| 1647 | Aromatic-aromatic interactions and protein stability. Investigation by double-mutant cycles. <i>Journal of Molecular Biology</i> , <b>1991</b> , 218, 465-75   | 6.5 | 288 |
| 1646 | Examination of phenylalanine microenvironments in proteins by second-derivative absorption spectroscopy. <b>1991</b> , 287, 33-40  |     | 34  |
| 1645 | Crystal structure of hevein at 2.8 A resolution. <b>1991</b> , 291, 307-9  |     | 48  |
| 1644 | Refined structure of the hirudin-thrombin complex. <i>Journal of Molecular Biology</i> , <b>1991</b> , 221, 583-601  | 6.5 | 336 |
| 1643 | Beta-breakers: an aperiodic secondary structure. <i>Journal of Molecular Biology</i> , <b>1991</b> , 221, 603-13   | 6.5 | 43  |
| 1642 | Serpin tertiary structure transformation. <i>Journal of Molecular Biology</i> , <b>1991</b> , 221, 615-21  | 6.5 | 148 |
| 1641 | In a staphylococcal nuclease mutant the side-chain of a lysine replacing valine 66 is fully buried in the hydrophobic core. <i>Journal of Molecular Biology</i> , <b>1991</b> , 221, 7-14                      | 6.5 | 151 |
| 1640 | Molecular basis of co-operativity in protein folding. <i>Journal of Molecular Biology</i> , <b>1991</b> , 222, 687-98  | 6.5 | 81  |
| 1639 | Solid model compounds and the thermodynamics of protein unfolding. <i>Journal of Molecular Biology</i> , <b>1991</b> , 222, 699-709  | 6.5 | 258 |
| 1638 | Construction of new ligand binding sites in proteins of known structure. I. Computer-aided modeling of sites with pre-defined geometry. <i>Journal of Molecular Biology</i> , <b>1991</b> , 222, 763-85        | 6.5 | 214 |
| 1637 | Mapping electrostatic interactions in macromolecular associations. <i>Journal of Molecular Biology</i> , <b>1991</b> , 221, 1453-60  | 6.5 | 72  |

|      |  |     |      |
|------|--|-----|------|
| 1636 | Mapping of isozymic differences in enolase. <b>1991</b> , 13, 97-100   |     | 25   |
| 1635 | Why proteins prefer interfaces. <b>1991</b> , 2, 183-202   |     | 299  |
| 1634 | Contribution to the thermodynamics of protein folding from the reduction in water-accessible nonpolar surface area. <b>1991</b> , 30, 4237-44  |     | 343  |
| 1633 | Protein adsorption in model systems. <b>1991</b> , 4, 37-51  |     | 45   |
| 1632 | Structure of bovine prothrombin fragment 1 refined at 2.25 Å resolution. <i>Journal of Molecular Biology</i> , <b>1991</b> , 220, 481-94   | 6.5 | 44   |
| 1631 | Computational method for the design of enzymes with altered substrate specificity. <i>Journal of Molecular Biology</i> , <b>1991</b> , 220, 495-506  | 6.5 | 61   |
| 1630 | Analysis of protein loop closure. Two types of hinges produce one motion in lactate dehydrogenase. <i>Journal of Molecular Biology</i> , <b>1991</b> , 220, 133-49                             | 6.5 | 150  |
| 1629 | Is the hydrophobic effect stabilizing or destabilizing in proteins? The contribution of disulphide bonds to protein stability. <i>Journal of Molecular Biology</i> , <b>1991</b> , 217, 389-98 | 6.5 | 157  |
| 1628 | The role of internal packing interactions in determining the structure and stability of a protein. <i>Journal of Molecular Biology</i> , <b>1991</b> , 219, 359-76                             | 6.5 | 198  |
| 1627 | Reaction mechanism of alkaline phosphatase based on crystal structures. Two-metal ion catalysis. <i>Journal of Molecular Biology</i> , <b>1991</b> , 218, 449-64                               | 6.5 | 821  |
| 1626 | X-ray crystal structure of the ferric sperm whale myoglobin: imidazole complex at 2.0 Å resolution. <i>Journal of Molecular Biology</i> , <b>1991</b> , 217, 409-12                            | 6.5 | 60   |
| 1625 | "Soft docking": matching of molecular surface cubes. <i>Journal of Molecular Biology</i> , <b>1991</b> , 219, 79-102   | 6.5 | 360  |
| 1624 | Analysis of structural design features in collagen. <i>Journal of Molecular Biology</i> , <b>1991</b> , 218, 209-19  | 6.5 | 81   |
| 1623 | Structural mechanism for glycogen phosphorylase control by phosphorylation and AMP. <i>Journal of Molecular Biology</i> , <b>1991</b> , 218, 233-60  | 6.5 | 220  |
| 1622 | Lysozyme and alpha-lactalbumin: structure, function, and interrelationships. <b>1991</b> , 41, 173-315   |     | 175  |
| 1621 | A method to identify protein sequences that fold into a known three-dimensional structure. <b>1991</b> , 253, 164-70   |     | 2411 |
| 1620 | Protein hydration and function. <b>1991</b> , 41, 37-172   |     | 679  |
| 1619 | Relative activities and stabilities of mutant <i>Escherichia coli</i> tryptophan synthase alpha subunits. <b>1991</b> , 173, 1886-93   |     | 21   |



|      |   |     |
|------|---|-----|
| 1618 | Histidine pKa shifts accompanying the inactivating Asp121----Asn substitution in a semisynthetic bovine pancreatic ribonuclease. <b>1991</b> , 88, 8116-20  | 33  |
| 1617 | Hydrophobic potentials from statistical analysis of protein structures. <b>1991</b> , 202, 20-31  | 6   |
| 1616 | Molecular modeling of antibody combining sites. <b>1991</b> , 203, 121-53   | 46  |
| 1615 | X-ray structure of trypanothione reductase from <i>Crithidia fasciculata</i> at 2.4-Å resolution. <b>1991</b> , 88, 8764-8  | 93  |
| 1614 | Three-dimensional structure of the <i>Escherichia coli</i> phosphocarrier protein IIIglc. <b>1991</b> , 88, 10382-6   | 95  |
| 1613 | Electrostatic effects in protein folding, stability, and function. <b>1991</b> , 202, 3-19  | 16  |
| 1612 | Hydration Thermodynamics of Biomolecules. II. Atomic Transfer Parameters of Amino Acids. <b>1991</b> , 60, 330-339  | 4   |
| 1611 | Defining antibody-antigen recognition: towards engineered antibodies and epitopes. <b>1991</b> , 7, 165-88  | 8   |
| 1610 | Clefts and binding sites in protein receptors. <b>1991</b> , 202, 126-56  | 14  |
| 1609 | Molecular interstitial skeleton. <b>1991</b> , 15, 37-45  | 8   |
| 1608 | Protein interactions with surface-immobilized metal ions: structure-dependent variations in affinity and binding capacity with temperature and urea concentration. <b>1991</b> , 42, 105-18           | 32  |
| 1607 | A molecular dynamics simulation of the C-terminal fragment of the L7/L12 ribosomal protein in solution. <b>1991</b> , 158, 501-512  | 21  |
| 1606 | Conformation and aggregation of M13 coat protein studied by molecular dynamics. <b>1991</b> , 41, 193-202   | 16  |
| 1605 | Improved AMYR program: an algorithm for the theoretical simulation of molecular associations, including geometrical and topological characterization of the dimers. <b>1991</b> , 9, 254-6            | 10  |
| 1604 | Influence of solute size and the non-polar interaction term on the selection of test solutes for the classification of stationary phase selectivity in gas chromatography. <b>1991</b> , 556, 457-484 | 33  |
| 1603 | A Molecular Modeling Approach to In vivo Efficacy of Triclabendazole. <b>1991</b> , 77, 998   | 12  |
| 1602 | Modelling of dispersion and repulsion interactions in liquids. <b>1991</b> , 227, 157-173   | 14  |
| 1601 | Convergent evolution of similar function in two structurally divergent enzymes. <b>1991</b> , 352, 172-4  | 164 |

|      |   |       |
|------|---|-------|
| 1600 | Metal ligand-induced alterations in the surface structures of lactoferrin and transferrin probed by interaction with immobilized copper(II) ions. <b>1991</b> , 536, 1-15 | 27    |
| 1599 | Atomic accessible and contact surfaces as restraints in the Hendrickson & Konnert refinement program. <b>1991</b> , 24, 941-946   | 3     |
| 1598 | MOLSCRIPT: a program to produce both detailed and schematic plots of protein structures. <b>1991</b> , 24, 946-950  | 11757 |
| 1597 | Global analysis of the time-resolved fluorescence of alpha-chymotrypsinogen A and alpha-chymotrypsin powders as a function of hydration. <b>1991</b> , 53, 57-63          | 11    |
| 1596 | Pair potential calculation of molecular associations: a vectorized version. <b>1991</b> , 66, 341-362   | 19    |
| 1595 | Incorporating solvent and ion screening into molecular dynamics using the finite-difference Poisson-Boltzmann method. <b>1991</b> , 12, 454-468                           | 120   |
| 1594 | Grid-search molecular accessible surface algorithm for solving the protein docking problem. <b>1991</b> , 12, 746-750   | 43    |
| 1593 | A vectorized algorithm for calculating the accessible surface area of macromolecules. <b>1991</b> , 12, 868-871   | 22    |
| 1592 | Detection of cavities in a set of interpenetrating spheres. <b>1991</b> , 12, 918-922   | 29    |
| 1591 | GEPOL: An improved description of molecular surfaces II. Computing the molecular area and volume. <b>1991</b> , 12, 1077-1088   | 211   |
| 1590 | A molecular dynamics study of thermodynamic and structural aspects of the hydration of cavities in proteins. <b>1991</b> , 31, 919-31                                     | 67    |
| 1589 | Solvent reorganization contribution to the transfer thermodynamics of small nonpolar molecules. <b>1991</b> , 31, 993-1008  | 215   |
| 1588 | Ribonuclease T1: Struktur, Funktion und Stabilität. <b>1991</b> , 103, 351-369  | 17    |
| 1587 | Molecular modeling of the weak glycine antagonist iso-THAO. <b>1991</b> , 30, 442-6   | 8     |
| 1586 | Monoclonal antibody 117,C-11 recognizes three exposed regions on the surface of the Lathyrus ochrus isolectin I. <b>1991</b> , 30, 47-51                                  | 2     |
| 1585 | Recent developments in molecular graphics: visualization of chemical structures and properties. <b>1991</b> , 7, 158-169  | 4     |
| 1584 | Photo-CIDNP study of the interaction between the glucocorticoid receptor DNA-binding domain and glucocorticoid response elements. <b>1991</b> , 1, 105-10                 | 10    |
| 1583 | VP2 is the major exposed protein on orbiviruses. <b>1991</b> , 121, 233-6   | 4     |

|      |  |      |
|------|--|------|
| 1582 | Comparative modeling of mammalian aspartate transcarbamylase. <b>1991</b> , 9, 191-206   | 28   |
| 1581 | Thiol protease-like active site found in the enzyme dienelactone hydrolase: localization using biochemical, genetic, and structural tools. <b>1991</b> , 9, 267-79                         | 32   |
| 1580 | Comparison of the crystal structure of bacteriophage T4 lysozyme at low, medium, and high ionic strengths. <b>1991</b> , 10, 10-21   | 52   |
| 1579 | Secondary structure-based profiles: use of structure-conserving scoring tables in searching protein sequence databases for structural similarities. <b>1991</b> , 10, 229-39               | 135  |
| 1578 | Variation of folded polypeptide surface area with probe size. <b>1991</b> , 10, 300-14   | 9    |
| 1577 | Protein-protein recognition analyzed by docking simulation. <b>1991</b> , 11, 271-80   | 134  |
| 1576 | Protein folding and association: insights from the interfacial and thermodynamic properties of hydrocarbons. <b>1991</b> , 11, 281-96  | 5087 |
| 1575 | Evolution of the Structural Representation of Sucrose [1]. <b>1991</b> , 43, 121-132   | 25   |
| 1574 | Theoretical study of simple pushpull ethylenes in solution. <b>1991</b> , 4, 141-148   | 28   |
| 1573 | Empirical methods for computing molecular partition coefficients. I. Upon the need to model the specific hydration of polar groups in fragment-based approaches. <b>1991</b> , 40, 299-316 | 8    |
| 1572 | Protein secondary structure preferences. <b>1991</b> , 8, 229-242  | 4    |
| 1571 | Modelling protein three-dimensional structure using tritium planigraphy. <b>1991</b> , 19, 283-6   | 4    |
| 1570 | Molecular packing and morphology of protein crystals. <b>1991</b> , 24, 105-110  | 14   |
| 1569 | Three-dimensional structure of human basic fibroblast growth factor, a structural homolog of interleukin 1 beta. <b>1991</b> , 88, 3446-50   | 226  |
| 1568 | Isoenthalpic and isoentropic temperatures and the thermodynamics of protein denaturation. <b>1991</b> , 88, 5154-8   | 96   |
| 1567 | The protein-folding problem: the native fold determines packing, but does packing determine the native fold?. <b>1991</b> , 88, 4195-9   | 87   |
| 1566 | Do interhelical side chain-backbone hydrogen bonds participate in formation of leucine zipper coiled coils?. <b>1991</b> , 88, 9488-92   | 21   |
| 1565 | The conformational analysis of serine protease inhibitors and its applications for drug design. <b>1992</b> , 5, 331-8   | 4    |

|      |  |     |
|------|--|-----|
| 1564 | Modelling of protein adsorption on polymeric surfaces. <b>1991</b> , 2, 91-111   | 14  |
| 1563 | References. <b>1992</b> , 1153-1478  |     |
| 1562 | Increasing the thermostability of a neutral protease by replacing positively charged amino acids in the N-terminal turn of alpha-helices. <b>1992</b> , 5, 165-70  | 27  |
| 1561 | Inverse protein folding problem: designing polymer sequences. <b>1992</b> , 89, 4163-7   | 141 |
| 1560 | Folding and function of a T4 lysozyme containing 10 consecutive alanines illustrate the redundancy of information in an amino acid sequence. <b>1992</b> , 89, 3751-5  | 97  |
| 1559 | Molecular Dynamics Simulations in Heterogeneous Dielectrics and Debye-Hückel Media - Application to the Protein Bovine Pancreatic Trypsin Inhibitor. <b>1992</b> , 8, 361-387                                  | 47  |
| 1558 | An unlikely sugar substrate site in the 1.65 Å structure of the human aldose reductase holoenzyme implicated in diabetic complications. <b>1992</b> , 257, 81-4  | 404 |
| 1557 | Complete folding of bovine pancreatic trypsin inhibitor with only a single disulfide bond. <b>1992</b> , 89, 1519-23   | 90  |
| 1556 | Kinetic role of nonnative species in the folding of bovine pancreatic trypsin inhibitor. <b>1992</b> , 89, 9900-4  | 97  |
| 1555 | Fuzzy molecular surfaces. <b>1992</b> , 9, 759-68  | 8   |
| 1554 | Heat capacity changes and hydrophobic interactions in the binding of FK506 and rapamycin to the FK506 binding protein. <b>1992</b> , 89, 4781-5  | 68  |
| 1553 | Molecular mimicry of hepatitis B surface antigen by an anti-idiotypic-derived synthetic peptide. <b>1992</b> , 89, 11900-4   | 56  |
| 1552 | Crystal structure of papain-E64-c complex. Binding diversity of E64-c to papain S2 and S3 subsites. <b>1992</b> , 287 ( Pt 3), 797-803   | 63  |
| 1551 | A model of the molten globule state from molecular dynamics simulations. <b>1992</b> , 89, 5142-6  | 144 |
| 1550 | Use of liquid hydrocarbon and amide transfer data to estimate contributions to thermodynamic functions of protein folding from the removal of nonpolar and polar surface from water. <b>1992</b> , 31, 3947-55 | 564 |
| 1549 | Structure of the Glutamyl-tRNA Synthetase [RNAGln] ATP Complex. <b>1992</b> , 225-245  | 8   |
| 1548 | Dissection of the functional role of structural elements of tyrosine-63 in the catalytic action of human lysozyme. <b>1992</b> , 31, 9212-9  | 29  |
| 1547 | Protein surface topology-probing by selective chemical modification and mass spectrometric peptide mapping. <b>1992</b> , 89, 5630-4   | 202 |

|      |   |     |
|------|---|-----|
| 1546 | Correlation of computed van der Waals and molecular volumes with apparent molar volumes (AMV) for amino acid, carbohydrate and sulfamate tasant molecules. Relationship between CoreyBaulingKoltun volumes (VCPK) and computed volumes. <b>1992</b> , 497-503 | 14  |
| 1545 | Three-dimensional structure of dimeric human recombinant macrophage colony-stimulating factor. <b>1992</b> , 258, 1358-62   | 173 |
| 1544 | Octan-1-ol/water partition coefficients of zwitterionic amino acids. Determination by centrifugal partition chromatography and factorization into steric/hydrophobic and polar components. <b>1992</b> , 79-84  | 73  |
| 1543 | Physicochemical Properties of Wheat Proteins in Relation to Functionality. <b>1992</b> , 36, 1-87   | 178 |
| 1542 | Heat capacity changes for protein-peptide interactions in the ribonuclease S system. <b>1992</b> , 31, 1421-6   | 106 |
| 1541 | The molecular basis of cooperativity in protein folding. Thermodynamic dissection of interdomain interactions in phosphoglycerate kinase. <b>1992</b> , 31, 250-6   | 102 |
| 1540 | Electrostatic fields in antibodies and antibody/antigen complexes. <b>1992</b> , 58, 203-24   | 83  |
| 1539 | Physicochemical and structural implications for molecular recognition in immobilized metal affinity chromatography. <b>1992</b> , 4, 14-24  | 5   |
| 1538 | A microscopic view of protein solvation. <b>1992</b> , 96, 7157-7159  | 26  |
| 1537 | Identification of effector-activating residues of Gs alpha. <b>1992</b> , 68, 911-22  | 175 |
| 1536 | Crystal structure of a soluble form of the human T cell coreceptor CD8 at 2.6 A resolution. <b>1992</b> , 68, 1145-62   | 257 |
| 1535 | The three-dimensional structure of HLA-B27 at 2.1 A resolution suggests a general mechanism for tight peptide binding to MHC. <b>1992</b> , 70, 1035-48   | 630 |
| 1534 | Three-dimensional structure of the beta subunit of E. coli DNA polymerase III holoenzyme: a sliding DNA clamp. <b>1992</b> , 69, 425-37   | 688 |
| 1533 | The pro region of BPTI facilitates folding. <b>1992</b> , 71, 841-51  | 132 |
| 1532 | Macromolecular graphics. <b>1992</b> , 2, 193-201   | 9   |
| 1531 | Folding kinetics of designer proteins. Application of the diffusion-collision model to a de novo designed four-helix bundle. <b>1992</b> , 63, 296-9  | 5   |
| 1530 | Thermodynamics of structural stability and cooperative folding behavior in proteins. <b>1992</b> , 43, 313-61   | 474 |
| 1529 | Molecular model of the cyclic GMP-binding domain of the cyclic GMP-gated ion channel. <b>1992</b> , 31, 4643-9  | 92  |

|      |  |     |      |
|------|--|-----|------|
| 1528 | Crystal structure of papain-succinyl-Gln-Val-Val-Ala-Ala-p-nitroanilide complex at 1.7-A resolution: noncovalent binding mode of a common sequence of endogenous thiol protease inhibitors. <b>1992</b> , 31, 11305-9      |     | 28   |
| 1527 | Identification of a reactive lysyl residue (Lys103) of recombinant human interleukin-1 beta. Mechanism of its reactivity and implication of its functional role in receptor binding. <b>1992</b> , 31, 2874-8              |     | 9    |
| 1526 | Crystal structure of recombinant murine adipocyte lipid-binding protein. <b>1992</b> , 31, 3484-92   |     | 107  |
| 1525 | Human growth hormone and extracellular domain of its receptor: crystal structure of the complex. <b>1992</b> , 255, 306-12   |     | 2117 |
| 1524 | Implications of a consensus recognition site for phosphatidylcholine separate from the active site in cobra venom phospholipases A2. <b>1992</b> , 31, 2887-96   |     | 33   |
| 1523 | Buried water in homologous serine proteases. <b>1992</b> , 31, 12785-91  |     | 105  |
| 1522 | Crystallographic structures of ribonuclease S variants with nonpolar substitution at position 13: packing and cavities. <b>1992</b> , 31, 12315-27   |     | 66   |
| 1521 | Use of a potential of mean force to analyze free energy contributions in protein folding. <b>1992</b> , 31, 6290-7   |     | 23   |
| 1520 | The folding of an enzyme. II. Substructure of barnase and the contribution of different interactions to protein stability. <i>Journal of Molecular Biology</i> , <b>1992</b> , 224, 783-804                                | 6.5 | 394  |
| 1519 | Thermal stabilities of mutant Escherichia coli tryptophan synthase alpha subunits. <b>1992</b> , 292, 34-41  |     | 17   |
| 1518 | Contribution of the hydrophobic effect to globular protein stability. <i>Journal of Molecular Biology</i> , <b>1992</b> , 226, 29-35   | 6.5 | 206  |
| 1517 | A 500 ps molecular dynamics simulation study of interleukin-1 beta in water. Correlation with nuclear magnetic resonance spectroscopy and crystallography. <i>Journal of Molecular Biology</i> , <b>1992</b> , 226, 239-50 | 6.5 | 166  |
| 1516 | Towards an understanding of the arginine-aspartate interaction. <i>Journal of Molecular Biology</i> , <b>1992</b> , 226, 251-62  | 6.5 | 98   |
| 1515 | Analysis of the heat capacity dependence of protein folding. <i>Journal of Molecular Biology</i> , <b>1992</b> , 227, 889-900  | 6.5 | 99   |
| 1514 | Structure of a hinge-bending bacteriophage T4 lysozyme mutant, Ile3-->Pro. <i>Journal of Molecular Biology</i> , <b>1992</b> , 227, 917-33   | 6.5 | 74   |
| 1513 | Orthogonal beta beta motifs in proteins. <i>Journal of Molecular Biology</i> , <b>1992</b> , 223, 845-51   | 6.5 | 19   |
| 1512 | Molecular dynamics simulations of helix denaturation. <i>Journal of Molecular Biology</i> , <b>1992</b> , 223, 1121-38   | 6.5 | 212  |
| 1511 | Internal motional averaging and three-dimensional structure determination by nuclear magnetic resonance. <i>Journal of Molecular Biology</i> , <b>1992</b> , 224, 1087-101   | 6.5 | 42   |

|      |  |     |     |
|------|--|-----|-----|
| 1510 | Design and structural analysis of alternative hydrophobic core packing arrangements in bacteriophage T4 lysozyme. <i>Journal of Molecular Biology</i> , <b>1992</b> , 224, 1143-59   | 6.5 | 120 |
| 1509 | The interdependence of protein surface topography and bound water molecules revealed by surface accessibility and fractal density measures. <i>Journal of Molecular Biology</i> , <b>1992</b> , 228, 13-22   | 6.5 | 116 |
| 1508 | Crystal packing in six crystal forms of pancreatic ribonuclease. <i>Journal of Molecular Biology</i> , <b>1992</b> , 228, 243-51   | 6.5 | 67  |
| 1507 | Refinement of an enzyme complex with inhibitor bound at partial occupancy. Hen egg-white lysozyme and tri-N-acetylchitotriose at 1.75 Å resolution. <i>Journal of Molecular Biology</i> , <b>1992</b> , 224, 613-28                                      | 6.5 | 161 |
| 1506 | Refined crystal structure of ascorbate oxidase at 1.9 Å resolution. <i>Journal of Molecular Biology</i> , <b>1992</b> , 224, 179-205   | 6.5 | 420 |
| 1505 | Modeling of the structure of bacteriorhodopsin. A molecular dynamics study. <i>Journal of Molecular Biology</i> , <b>1992</b> , 226, 837-50  | 6.5 | 46  |
| 1504 | High resolution functional analysis of antibody-antigen interactions. <i>Journal of Molecular Biology</i> , <b>1992</b> , 226, 851-65  | 6.5 | 203 |
| 1503 | Three-dimensional structure of the bifunctional enzyme phosphoribosylanthranilate isomerase: indoleglycerolphosphate synthase from <i>Escherichia coli</i> refined at 2.0 Å resolution. <i>Journal of Molecular Biology</i> , <b>1992</b> , 223, 477-507 | 6.5 | 96  |
| 1502 | Refined crystal structure of the influenza virus N9 neuraminidase-NC41 Fab complex. <i>Journal of Molecular Biology</i> , <b>1992</b> , 227, 122-48  | 6.5 | 203 |
| 1501 | Domain closure in mitochondrial aspartate aminotransferase. <i>Journal of Molecular Biology</i> , <b>1992</b> , 227, 197-213   | 6.5 | 172 |
| 1500 | Molecular basis of co-operativity in protein folding. III. Structural identification of cooperative folding units and folding intermediates. <i>Journal of Molecular Biology</i> , <b>1992</b> , 227, 293-306  | 6.5 | 172 |
| 1499 | Structure of oxidized bacteriophage T4 glutaredoxin (thioredoxin). Refinement of native and mutant proteins. <i>Journal of Molecular Biology</i> , <b>1992</b> , 228, 596-618  | 6.5 | 67  |
| 1498 | Ribose and glucose-galactose receptors. Competitors in bacterial chemotaxis. <i>Journal of Molecular Biology</i> , <b>1992</b> , 227, 418-40   | 6.5 | 29  |
| 1497 | X-ray structure refinement and comparison of three forms of mitochondrial aspartate aminotransferase. <i>Journal of Molecular Biology</i> , <b>1992</b> , 225, 495-517   | 6.5 | 192 |
| 1496 | Accurate modeling of protein conformation by automatic segment matching. <i>Journal of Molecular Biology</i> , <b>1992</b> , 226, 507-33   | 6.5 | 526 |
| 1495 | Evaluation of protein models by atomic solvation preference. <i>Journal of Molecular Biology</i> , <b>1992</b> , 225, 93-105   | 6.5 | 186 |
| 1494 | 1.7 Å X-ray structure of the periplasmic ribose receptor from <i>Escherichia coli</i> . <i>Journal of Molecular Biology</i> , <b>1992</b> , 225, 155-75  | 6.5 | 133 |
| 1493 | Relation between the convergence temperatures $T_h^*$ and $T_s^*$ in protein unfolding. <b>1992</b> , 89, 7110-3   |     | 51  |

|      |   |     |
|------|---|-----|
| 1492 | Ligand atom partial charges assignment for complementary electrostatic potentials. <b>1992</b> , 6, 461-74  | 9   |
| 1491 | A general algorithm for computing Voronoi volumes: Application to the hydrated crystal of myoglobin. <b>1992</b> , 42, 1515-1528  | 31  |
| 1490 | Quantum mechanical parametrization of a conformationally dependent hydrophobic index. <b>1992</b> , 44, 203-218   | 20  |
| 1489 | Empirical methods for computing molecular partition coefficients: II. Inclusion of conformational flexibility within fragmentBased approaches. <b>1992</b> , 44, 219-233  | 19  |
| 1488 | Calculation of the free energy of association for protein complexes. <b>1992</b> , 1, 169-81  | 274 |
| 1487 | Environment-specific amino acid substitution tables: tertiary templates and prediction of protein folds. <b>1992</b> , 1, 216-26  | 236 |
| 1486 | Atomic solvation parameters applied to molecular dynamics of proteins in solution. <b>1992</b> , 1, 227-35  | 453 |
| 1485 | The refined 1.9-A X-ray crystal structure of D-Phe-Pro-Arg chloromethylketone-inhibited human alpha-thrombin: structure analysis, overall structure, electrostatic properties, detailed active-site geometry, and structure-function relationships. <b>1992</b> , 1, 426-71 | 530 |
| 1484 | The molecular mechanism for the tetrameric association of glycogen phosphorylase promoted by protein phosphorylation. <b>1992</b> , 1, 472-93   | 41  |
| 1483 | Multiple alanine replacements within alpha-helix 126-134 of T4 lysozyme have independent, additive effects on both structure and stability. <b>1992</b> , 1, 761-76   | 59  |
| 1482 | Intramolecular interactions in pancreatic ribonucleases. <b>1992</b> , 1, 1050-60   | 7   |
| 1481 | Solution structure of the phosphocarrier protein HPr from <i>Bacillus subtilis</i> by two-dimensional NMR spectroscopy. <b>1992</b> , 1, 1363-76  | 59  |
| 1480 | Modeling the antigen combining site of an anti-dinitrophenyl antibody, ANO2. <b>1992</b> , 1, 1465-76   | 17  |
| 1479 | X-ray crystal structures of the oxidized and reduced forms of the rubredoxin from the marine hyperthermophilic archaeobacterium <i>Pyrococcus furiosus</i> . <b>1992</b> , 1, 1494-507  | 227 |
| 1478 | Functional implications of interleukin-1 beta based on the three-dimensional structure. <b>1992</b> , 12, 10-23   | 71  |
| 1477 | Subunit assembly and active site location in the structure of glutamate dehydrogenase. <b>1992</b> , 12, 75-86  | 206 |
| 1476 | Solvent structure in crystals of trypsin determined by X-ray and neutron diffraction. <b>1992</b> , 12, 203-22  | 88  |
| 1475 | The high-resolution crystal structure of porcine pepsinogen. <b>1992</b> , 13, 1-25   | 88  |




|      |   |     |
|------|---|-----|
| 1474 | Modeling microdomains: the surface area of globin helices. <b>1992</b> , 13, 327-35   | 1   |
| 1473 | Fast structure alignment for protein databank searching. <b>1992</b> , 14, 139-67   | 126 |
| 1472 | Some Disaccharide-derived Building Blocks of Potential Industrial Utility. <b>1992</b> , 44, 445-456  | 22  |
| 1471 | The structure of the E. coli recA protein monomer and polymer. <b>1992</b> , 355, 318-25  | 701 |
| 1470 | Crystal structure of the phosphotyrosine recognition domain SH2 of v-src complexed with tyrosine-phosphorylated peptides. <b>1992</b> , 358, 646-53                               | 651 |
| 1469 | Crystal structure of the met repressor-operator complex at 2.8 Å resolution reveals DNA recognition by beta-strands. <b>1992</b> , 359, 387-93                                    | 297 |
| 1468 | Structure of a C-type mannose-binding protein complexed with an oligosaccharide. <b>1992</b> , 360, 127-34  | 879 |
| 1467 | Theoretical and practical aspects of antigenized antibodies. <b>1992</b> , 130, 125-50  | 15  |
| 1466 | A bibliography on computational molecular biology and genetics. <b>1992</b> , 16, 245-319   | 2   |
| 1465 | Estimation of accuracy in determining protein backbone conformations from NOE data and empirical probability distributions. <b>1992</b> , 96, 457-472                             |     |
| 1464 | Finding and filling protein cavities using cellular logic operations. <b>1992</b> , 10, 174-7, 163  | 41  |
| 1463 | Representation of noncovalent interactions in protein structures. <b>1992</b> , 10, 96-100, 110   | 6   |
| 1462 | Antigen binding thermodynamics and antiproliferative effects of chimeric and humanized anti-p185HER2 antibody Fab fragments. <b>1992</b> , 31, 5434-41                            | 97  |
| 1461 | Molecular surface calculations on organic compounds. <b>1992</b> , 254, 369-377   | 10  |
| 1460 | Variable and conserved structural elements of trypanosome variant surface glycoproteins. <b>1992</b> , 51, 119-32   | 23  |
| 1459 | The segmented anisotropic refinement of monoclinic papain by the application of the rigid-body TLS model and comparison to bovine ribonuclease A. <b>1992</b> , 48 ( Pt 1), 67-75 | 18  |
| 1458 | Structure determination of monoclinic canine parvovirus. <b>1992</b> , 48 ( Pt 1), 75-88  | 28  |
| 1457 | Effect of cavity-modulating mutations on the stability of Escherichia coli ribonuclease HI. <b>1992</b> , 206, 337-43   | 23  |

|      |  |     |
|------|--|-----|
| 1456 | Calorimetric measurements of thermal denaturation of stefins A and B. Comparison to predicted thermodynamics of stefin-B unfolding. <b>1992</b> , 210, 217-21  | 22  |
| 1455 | Anti-insulin antibody structure and conformation. I. Molecular modeling and mechanics of an insulin antibody. <b>1992</b> , 32, 11-21  | 10  |
| 1454 | Anti-insulin antibody structure and conformation. II. Molecular dynamics with explicit solvent. <b>1992</b> , 32, 23-32  | 23  |
| 1453 | Hydrophobic interaction between globin helices. <b>1992</b> , 32, 477-90   | 13  |
| 1452 | Early assembly pathways of type I collagen. <b>1992</b> , 32, 497-515  | 6   |
| 1451 | Shape distributions of protein topography. <b>1992</b> , 32, 1215-36   | 43  |
| 1450 | Polarization of the nucleic acid bases in aqueous solution. <b>1992</b> , 198, 74-80   | 61  |
| 1449 | MSEED: A program for the rapid analytical determination of accessible surface areas and their derivatives. <b>1992</b> , 13, 1-11  | 134 |
| 1448 | Microscopic models for quantum mechanical calculations of chemical processes in solutions: LD/AMPAC and SCAAS/AMPAC calculations of solvation energies. <b>1992</b> , 13, 199-213                      | 273 |
| 1447 | PM3-SM3: A general parameterization for including aqueous solvation effects in the PM3 molecular orbital model. <b>1992</b> , 13, 1089-1097  | 157 |
| 1446 | Hydrational and intrinsic compressibilities of globular proteins. <b>1993</b> , 33, 11-26  | 150 |
| 1445 | Conformational preference functions for predicting helices in membrane proteins. <b>1993</b> , 33, 255-73  | 36  |
| 1444 | Effect of various frictional models on long-time peptide dynamics. <b>1993</b> , 33, 1423-1429   | 10  |
| 1443 | Refined three-dimensional solution structure of a snake cardiotoxin: analysis of the side-chain organization suggests the existence of a possible phospholipid binding site. <b>1993</b> , 33, 1659-75 | 29  |
| 1442 | Rapid approximation to molecular surface area via the use of Boolean logic and look-up tables. <b>1993</b> , 14, 349-352   | 112 |
| 1441 | Finite element approach to the electrostatics of macromolecules with arbitrary geometries. <b>1993</b> , 14, 484-501   | 67  |
| 1440 | Minimization of empirical energy functions in proteins including hydrophobic surface area effects. <b>1993</b> , 14, 510-521   | 51  |
| 1439 | Calculation of hydrophobic interactions from molecular dynamics, surface areas, and experimental hydrocarbon solubilities. <b>1993</b> , 14, 741-750   | 14  |

|      |   |     |
|------|---|-----|
| 1438 | Improved strategy in analytic surface calculation for molecular systems: Handling of singularities and computational efficiency. <b>1993</b> , 14, 1272-1280                        | 176 |
| 1437 | Epitope analysis using kinetic measurements of antibody binding to synthetic peptides presenting single amino acid substitutions. <b>1993</b> , 6, 71-9                             | 17  |
| 1436 | Texture mapping in molecular graphics. <b>1993</b> , 11, 259-260  |     |
| 1435 | Hydrophobic interactions and CoMFA using hint. <b>1993</b> , 11, 260  |     |
| 1434 | A new approach to the automatic identification of candidates for ligand receptor sites in proteins: (I). Search for pocket regions. <b>1993</b> , 11, 23-9, 42                      | 36  |
| 1433 | Tertiary structure of calcineurin B by homology modeling. <b>1993</b> , 11, 47-52, 45   | 8   |
| 1432 | The molecular surface package. <b>1993</b> , 11, 139-41   | 487 |
| 1431 | Protein dynamics and fluorescence quenching. <b>1993</b> , 18, 3-16   | 20  |
| 1430 | The sequence-immunology correlation revisited: data for cetacean myoglobins and mammalian lysozymes. <b>1993</b> , 37, 408-16   | 8   |
| 1429 | A new approach to analysis and display of local lipophilicity/hydrophilicity mapped on molecular surfaces. <b>1993</b> , 7, 503-14  | 149 |
| 1428 | PROGEN: an automated modelling algorithm for the generation of complete protein structures from the alpha-carbon atomic coordinates. <b>1993</b> , 7, 199-224                       | 9   |
| 1427 | Gaussian neighborhood: a new measure of accessibility for residues of protein molecules. <b>1993</b> , 15, 50-61  | 6   |
| 1426 | Structural energetics of peptide recognition: angiotensin II/antibody binding. <b>1993</b> , 15, 113-20   | 161 |
| 1425 | Successful prediction of the coiled coil geometry of the GCN4 leucine zipper domain by simulated annealing: comparison to the X-ray structure. <b>1993</b> , 15, 133-46             | 66  |
| 1424 | Crystallographic analysis of the interaction between cyclosporin A and the Fab fragment of a monoclonal antibody. <b>1993</b> , 15, 339-48  | 29  |
| 1423 | Perturbation of Trp 138 in T4 lysozyme by mutations at Gln 105 used to correlate changes in structure, stability, solvation, and spectroscopic properties. <b>1993</b> , 15, 401-12 | 17  |
| 1422 | Refined structure of bovine carbonic anhydrase III at 2.0 A resolution. <b>1993</b> , 16, 29-42   | 102 |
| 1421 | Fluoride inhibition of yeast enolase: crystal structure of the enolase-Mg(2+)-F(-)-Pi complex at 2.6 A resolution. <b>1993</b> , 16, 219-25   | 36  |

|      |   |     |
|------|---|-----|
| 1420 | Improved calculations of compactness and a reevaluation of continuous compact units. <b>1993</b> , 16, 293-300  | 17  |
| 1419 | Molecular basis of cooperativity in protein folding. IV. CORE: a general cooperative folding model. <b>1993</b> , 17, 111-23  | 26  |
| 1418 | Crystal structure of TGF-beta 2 refined at 1.8 A resolution. <b>1993</b> , 17, 176-92   | 49  |
| 1417 | Molecular skins: a new concept for quantitative shape matching of a protein with its small molecule mimics. <b>1993</b> , 17, 193-202   | 41  |
| 1416 | Conformational analysis of protein structures derived from NMR data. <b>1993</b> , 17, 232-51   | 64  |
| 1415 | Modeling alpha-helical transmembrane domains: the calculation and use of substitution tables for lipid-facing residues. <b>1993</b> , 2, 55-70  | 127 |
| 1414 | Crevice-forming mutants of bovine pancreatic trypsin inhibitor: stability changes and new hydrophobic surface. <b>1993</b> , 2, 588-96  | 35  |
| 1413 | Prediction of the three-dimensional structures of the nerve growth factor and epidermal growth factor binding proteins (kallikreins) and an hypothetical structure of the high molecular weight complex of epidermal growth factor with its binding protein. <b>1993</b> , 2, 1229-41 | 11  |
| 1412 | Dominant role of local dipoles in stabilizing uncompensated charges on a sulfate sequestered in a periplasmic active transport protein. <b>1993</b> , 2, 1643-7   | 67  |
| 1411 | Comparison of conformational characteristics in structurally similar protein pairs. <b>1993</b> , 2, 1811-26  | 160 |
| 1410 | Tryptophan replacements in the trp aporepressor from Escherichia coli: probing the equilibrium and kinetic folding models. <b>1993</b> , 2, 1853-61   | 42  |
| 1409 | Macromolecular solvation energies derived from small molecule crystal morphology. <b>1993</b> , 2, 1882-9   | 9   |
| 1408 | Amide proton exchange rates of oxidized and reduced Saccharomyces cerevisiae iso-1-cytochrome c. <b>1993</b> , 2, 1966-74   | 52  |
| 1407 | Origins of structural diversity within sequentially identical hexapeptides. <b>1993</b> , 2, 2134-45  | 89  |
| 1406 | Probing weakly polar interactions in cytochrome c. <b>1993</b> , 2, 2187-97   | 15  |
| 1405 | Protein secondary structure conformations and associated hydrophobicity scales. <b>1993</b> , 14, 35-45   | 7   |
| 1404 | Molecular modeling: a tool for predicting anthelmintic activity in vivo. <b>1993</b> , 79, 475-9  | 4   |
| 1403 | Conformational preference of N-acyl urea containing valine residue in DMSO d6. <b>1993</b> , 3, 153-156   | 4   |

|      |  |     |
|------|--|-----|
| 1402 | Efficient catalysis of disulphide bond rearrangements by protein disulphide isomerase. <b>1993</b> , 365, 185-8  | 195 |
| 1401 | The structure of crystalline profilin-beta-actin. <b>1993</b> , 365, 810-6   | 617 |
| 1400 | Molecular basis of crossreactivity and the limits of antibody-antigen complementarity. <b>1993</b> , 365, 859-63   | 157 |
| 1399 | How amino-acid insertions are allowed in an alpha-helix of T4 lysozyme. <b>1993</b> , 361, 561-4   | 106 |
| 1398 | Recognition of a high-affinity phosphotyrosyl peptide by the Src homology-2 domain of p56lck. <b>1993</b> , 362, 87-91   | 501 |
| 1397 | Substrate interactions between trypanothione reductase and N1-glutathionylspermidine disulphide at 0.28-nm resolution. <b>1993</b> , 213, 67-75  | 91  |
| 1396 | The solution structure of the histidine-containing protein (HPr) from <i>Staphylococcus aureus</i> as determined by two-dimensional <sup>1</sup> H-NMR spectroscopy. <b>1993</b> , 216, 205-14 | 39  |
| 1395 | Structure of the bovine eye lens protein gammaB(gammall)-crystallin at 1.47 Å. <b>1993</b> , 49, 223-33  | 36  |
| 1394 | Structural studies of the binding of the anti-ulcer drug sucrose octasulfate to acidic fibroblast growth factor. <b>1993</b> , 1, 27-34  | 88  |
| 1393 | HIV protease: Structure-based design. <b>1993</b> , 1, 49-68   | 18  |
| 1392 | Urea unfolding and stability of gamma-II crystallin. <b>1993</b> , 21, 183-9   |     |
| 1391 | Photo-CIDNP of biopolymers. <b>1993</b> , 25, 345-402  | 148 |
| 1390 | The evolution of proteins from random amino acid sequences. I. Evidence from the lengthwise distribution of amino acids in modern protein sequences. <b>1993</b> , 36, 79-95                   | 38  |
| 1389 | Standard structures in proteins. <b>1993</b> , 60, 201-39  | 114 |
| 1388 | Characterisation of an epitope recognised by a monoclonal antibody against horse alcohol dehydrogenase using peptides synthesised on solid support. <b>1993</b> , 335, 327-30                  | 6   |
| 1387 | Crystal structure of a distal site double mutant of sperm whale myoglobin at 1.6 Å resolution. <b>1993</b> , 320, 13-6   | 8   |
| 1386 | Trifluoromethanesulfonamide anthelmintics. Protonophoric uncouplers of oxidative phosphorylation. <b>1993</b> , 45, 1873-80  | 8   |
| 1385 | Hydration and heat stability effects on protein unfolding. <b>1993</b> , 59, 237-84  | 163 |

|      |   |     |
|------|---|-----|
| 1384 | Hydrophobic characteristics of folded proteins. <b>1993</b> , 59, 57-103  | 92  |
| 1383 | Aspects of protein energetics and dynamics. <b>1993</b> , 60, 73-200  | 60  |
| 1382 | .   | 3   |
| 1381 |  <b>1993</b> , 7, 91-94  |     |
| 1380 | Structure of bovine <b>B</b> -crystallin at 150 K. <b>1993</b> , 89, 2677-2682  | 9   |
| 1379 | Mapping of two "neutralizing" epitopes of a snake curaremimetic toxin by proton nuclear magnetic resonance spectroscopy. <b>1993</b> , 32, 6884-91              | 19  |
| 1378 | .   | 4   |
| 1377 | A Continuum Solvation Model for the AM1 Semi-Empirical Method. <b>1993</b> , 33, 427-434  | 24  |
| 1376 | Thermodynamic characterization of the structural stability of the coiled-coil region of the bZIP transcription factor GCN4. <b>1993</b> , 32, 5491-6            | 186 |
| 1375 | Stability of oxidized Escherichia coli thioredoxin and its dependence on protonation of the aspartic acid residue in the 26 position. <b>1993</b> , 32, 7526-30 | 38  |
| 1374 | Structural basis of amino acid alpha helix propensity. <b>1993</b> , 260, 1637-40   | 448 |
| 1373 | Structures of the noncovalent complexes of human and bovine prothrombin fragment 2 with human PPACK-thrombin. <b>1993</b> , 32, 4727-37                         | 100 |
| 1372 | Thermodynamic analysis of an antibody functional epitope. <b>1993</b> , 32, 6828-35   | 176 |
| 1371 | Molecular shape comparison of angiotensin II receptor antagonists. <b>1993</b> , 36, 1230-8   | 78  |
| 1370 | Crystal structure of the soluble human 55 kd TNF receptor-human TNF beta complex: implications for TNF receptor activation. <b>1993</b> , 73, 431-45            | 994 |
| 1369 | Multigrid solution of the nonlinear Poisson-Boltzmann equation and calculation of titration curves. <b>1993</b> , 65, 48-55                                     | 95  |
| 1368 | Acid stabilization of insulin. <b>1993</b> , 32, 8075-82  | 56  |
| 1367 | Thermodynamics of the glucocorticoid receptor-DNA interaction: binding of wild-type GR DBD to different response elements. <b>1993</b> , 32, 5074-82            | 50  |

|      |   |     |
|------|---|-----|
| 1366 | Molecular dynamics investigations of DNA triple helical models: unique features of the Watson-Crick duplex. <b>1993</b> , 11, 225-44                      | 24  |
| 1365 | Peptide-protein interactions: an overview. <b>1993</b> , 26, 333-63   | 15  |
| 1364 | A study of structural determinants in the interleukin-1 fold. <b>1993</b> , 6, 711-5  | 14  |
| 1363 | Structure and Function of the Photosynthetic Reaction Center of Rhodobacter sphaeroides. <b>1993</b> , 1-12   | 2   |
| 1362 | Structural relationship of bacterial RecA proteins to recombination proteins from bacteriophage T4 and yeast. <b>1993</b> , 259, 1892-6                   | 156 |
| 1361 | An analysis of the fractal properties of the surfaces of globular proteins. <b>1993</b> , 99, 4076-4083   | 31  |
| 1360 | Structure of the regulatory complex of Escherichia coli IIIGlc with glycerol kinase. <b>1993</b> , 259, 673-677   | 210 |
| 1359 | Environmental characteristics of residues in proteins: three-dimensional molecular hydrophobicity potential approach. <b>1993</b> , 11, 483-507           | 37  |
| 1358 | Crystal structure of neocarzinostatin, an antitumor protein-chromophore complex. <b>1993</b> , 262, 1042-6  | 78  |
| 1357 | Blue Copper Oxidases. <b>1993</b> , 40, 121-185   | 51  |
| 1356 | Overall and internal protein dynamics in solution studied by the nonselective proton relaxation. <b>1993</b> , 11, 121-41                                 | 9   |
| 1355 | Modelling alpha-helical transmembrane domains. <b>1993</b> , 21, 36-9   | 9   |
| 1354 | A progress report on the crystallographic studies on the B800-850 antenna complex from Rhodospseudomonas acidophila strain 10050. <b>1993</b> , 21, 39-40 | 1   |
| 1353 | Solvent Exclusion Effect Predicted by the Scaled Particle Theory as an Important Factor of the Hydrophobic Effect. <b>1993</b> , 62, 1782-1793            | 33  |
| 1352 | Protein hydration elucidated by molecular dynamics simulation. <b>1993</b> , 90, 9135-9   | 222 |
| 1351 | On achieving better than 1-A accuracy in a simulation of a large protein: Streptomyces griseus protease A. <b>1993</b> , 90, 8920-4                       | 49  |
| 1350 | Three-dimensional structures of avidin and the avidin-biotin complex. <b>1993</b> , 90, 5076-80   | 537 |
| 1349 | Comparison of the P2 specificity pocket in three human histocompatibility antigens: HLA-A*6801, HLA-A*0201, and HLA-B*2705. <b>1993</b> , 90, 8053-7      | 98  |

|      |   |     |
|------|---|-----|
| 1348 | Crystal structure of yeast TATA-binding protein and model for interaction with DNA. <b>1993</b> , 90, 8174-8  | 134 |
| 1347 | Strategies for differential sensory responses mediated through the same transmembrane receptor.. <b>1993</b> , 12, 1897-1905  | 15  |
| 1346 | Definition and spatial location of mouse interleukin-2 residues that interact with its heterotrimeric receptor.. <b>1993</b> , 12, 5113-5119  | 60  |
| 1345 | References. <b>1994</b> , 251-265   |     |
| 1344 | Macromolecular chelation as an improved mechanism of protease inhibition: structure of the ecotin-trypsin complex.. <b>1994</b> , 13, 1502-1507   | 55  |
| 1343 | Rapid crystallization of T4 lysozyme by intermolecular disulfide cross-linking. <b>1994</b> , 7, 301-7  | 33  |
| 1342 | Toxic shock syndrome toxin-1 complexed with a class II major histocompatibility molecule HLA-DR1. <b>1994</b> , 266, 1870-4   | 266 |
| 1341 | Parallel computing in biomedical research. <b>1994</b> , 265, 902-8   | 37  |
| 1340 | Local polarity analysis: a sensitive method that discriminates between native proteins and incorrectly folded models. <b>1994</b> , 7, 627-31   | 8   |
| 1339 | GRAFTER: a computational aid for the design of novel proteins. <b>1994</b> , 7, 1411-21   | 8   |
| 1338 | Tritium planigraphy of biological systems. <b>1994</b> , 63, 781-796  | 11  |
| 1337 | Hydration and partial compressibility of biological compounds. <b>1994</b> , 51, 89-107; discussion 107-9   | 223 |
| 1336 | Determination of the accessible surface of globular proteins by means of tritium planigraphy. <b>1994</b> , 23, 139-43  | 10  |
| 1335 | Electrostatic complementarity between proteins and ligands. 1. Charge disposition, dielectric and interface effects. <b>1994</b> , 8, 513-25  | 25  |
| 1334 | The effect of physical organic properties on hydrophobic fields. <b>1994</b> , 8, 41-9  | 31  |
| 1333 | Implementation of solvent effect in molecular mechanics Part 3. The first- and second-order analytical derivatives of excluded volume. <b>1994</b> , 311, 305-324   | 2   |
| 1332 | Cyclodextrins, cyclomannins, and cyclogalactins with five and six (1->4)-linked sugar units: A comparative assessment of their conformations and hydrophobicity potential profiles1. <b>1994</b> , 5, 2045-2060 | 55  |
| 1331 | Structure and dynamics of the active site gorge of acetylcholinesterase: synergistic use of molecular dynamics simulation and X-ray crystallography. <b>1994</b> , 3, 188-97                                    | 136 |



|      |  |     |
|------|--|-----|
| 1330 | Do salt bridges stabilize proteins? A continuum electrostatic analysis. <b>1994</b> , 3, 211-26  | 533 |
| 1329 | Slow-folding kinetics of ribonuclease-A by volume change and circular dichroism: evidence for two independent reactions. <b>1994</b> , 3, 638-49                           | 11  |
| 1328 | Protein folding dynamics: the diffusion-collision model and experimental data. <b>1994</b> , 3, 650-68   | 359 |
| 1327 | Modeling studies of the change in conformation required for cleavage of limited proteolytic sites. <b>1994</b> , 3, 757-68   | 174 |
| 1326 | Conservation of solvent-binding sites in 10 crystal forms of T4 lysozyme. <b>1994</b> , 3, 1031-9  | 97  |
| 1325 | Buried waters and internal cavities in monomeric proteins. <b>1994</b> , 3, 1224-35  | 270 |
| 1324 | Optimization of the electrostatic interactions in proteins of different functional and folding type. <b>1994</b> , 3, 1556-69  | 61  |
| 1323 | Sequence determinants of the capping box, a stabilizing motif at the N-termini of alpha-helices. <b>1994</b> , 3, 1741-5   | 109 |
| 1322 | Structural studies of the engrailed homeodomain. <b>1994</b> , 3, 1779-87  | 133 |
| 1321 | Formation of a native-like subdomain in a partially folded intermediate of bovine pancreatic trypsin inhibitor. <b>1994</b> , 3, 1822-32                                   | 116 |
| 1320 | Kinetics and crystal structure of a mutant Escherichia coli alkaline phosphatase (Asp-369-->Asn): a mechanism involving one zinc per active site. <b>1994</b> , 3, 2005-14 | 18  |
| 1319 | A structural model for the prostate disease marker, human prostate-specific antigen. <b>1994</b> , 3, 2033-44  | 65  |
| 1318 | A structural comparison of 21 inhibitor complexes of the aspartic proteinase from Endothia parasitica. <b>1994</b> , 3, 2129-43  | 44  |
| 1317 | Hydrogen exchange in BPTI variants that do not share a common disulfide bond. <b>1994</b> , 3, 2226-32   | 17  |
| 1316 | Dissecting the energetics of an antibody-antigen interface by alanine shaving and molecular grafting. <b>1994</b> , 3, 2351-7  | 78  |
| 1315 | An evaluation of implicit and explicit solvent model systems for the molecular dynamics simulation of bacteriophage T4 lysozyme. <b>1994</b> , 18, 19-33                   | 44  |
| 1314 | Molecular surface representations by sparse critical points. <b>1994</b> , 18, 94-101  | 94  |
| 1313 | Crystallization and structural analysis of bullfrog red cell L-subunit ferritins. <b>1994</b> , 18, 107-18   | 47  |

|      |   |     |
|------|---|-----|
| 1312 | A molecular dynamics approach for the generation of complete protein structures from limited coordinate data. <b>1994</b> , 18, 174-85  | 38  |
| 1311 | Spatial optimization of electrostatic interactions between the ionized groups in globular proteins. <b>1994</b> , 19, 222-9   | 19  |
| 1310 | Structural modeling and electrostatic properties of aspartate transcarbamylase from <i>Saccharomyces cerevisiae</i> . <b>1994</b> , 19, 230-43  | 12  |
| 1309 | Molecular basis of cooperativity in protein folding. V. Thermodynamic and structural conditions for the stabilization of compact denatured states. <b>1994</b> , 19, 291-301  | 116 |
| 1308 | Structure and dynamics of the neutrophil defensins NP-2, NP-5, and HNP-1: NMR studies of amide hydrogen exchange kinetics. <b>1994</b> , 20, 52-67  | 48  |
| 1307 | Estimation of changes in side chain configurational entropy in binding and folding: general methods and application to helix formation. <b>1994</b> , 20, 68-84   | 204 |
| 1306 | Conservation and prediction of solvent accessibility in protein families. <b>1994</b> , 20, 216-26  | 523 |
| 1305 | Polar and nonpolar atomic environments in the protein core: implications for folding and binding. <b>1994</b> , 20, 264-78  | 74  |
| 1304 | Controlling the electron transfer rate between oxymyoglobin and ferricytochrome C by alterations in the myoglobin contact site. The role of histidines and electrostatic and steric interactions in the mechanism of the reaction. <b>1994</b> , 4, 431-449 | 1   |
| 1303 | Potential radioprotective agents. 2. Substituted anilines. <b>1994</b> , 83, 219-21   | 5   |
| 1302 | Structural and physicochemical analysis of the reaction between the anti-lysozyme antibody D1.3 and the anti-idiotopic antibodies E225 and E5.2. <b>1994</b> , 7, 57-62   | 23  |
| 1301 | Buried surface analysis of HIV-1 reverse transcriptase p66/p51 heterodimer and its interaction with dsDNA template/primer. <b>1994</b> , 7, 157-61  | 22  |
| 1300 | High-pressure molecular dynamics of a nucleic acid fragment. <b>1994</b> , 224, 219-224   | 16  |
| 1299 | General parameterization of a reaction field theory combined with the boundary element method. <b>1994</b> , 15, 90-104   | 24  |
| 1298 | On the analytical calculation of van der Waals surfaces and volumes: Some numerical aspects. <b>1994</b> , 15, 507-523  | 85  |
| 1297 | GEPOL: An improved description of molecular surfaces. III. A new algorithm for the computation of a solvent-excluding surface. <b>1994</b> , 15, 1127-1138  | 620 |
| 1296 | On the use of mild hydrophobic interaction chromatography for "method scouting" protein purification strategies in aqueous two-phase systems: a study using model proteins. <b>1994</b> , 44, 626-35  | 14  |
| 1295 | Globular proteins at solid/liquid interfaces. <b>1994</b> , 2, 517-566  | 702 |

|      |   |      |
|------|---|------|
| 1294 | DNurbs: DNA modeled with NURBS. <b>1994</b> , 12, 178-84, 195   | 3    |
| 1293 | WinMGM: a fast CPK molecular graphics program for analyzing molecular structure. <b>1994</b> , 12, 212-8, 198   | 27   |
| 1292 | Computer-aided molecular modeling of the binding site architecture for eight monoclonal antibodies that bind a high potency guanidinium sweetener. <b>1994</b> , 12, 257-66, 289-90 | 16   |
| 1291 | Evaluation of the hydrophilic behaviour of a $\beta$ -casein peptide by molecular dynamics simulation. <b>1994</b> , 189, 511-521   | 1    |
| 1290 | Energetics of interactions of aromatic hydrocarbons with water. <b>1994</b> , 50, 285-91  | 61   |
| 1289 | Thermodynamic prediction of structural determinants of the molten globule state of barnase. <b>1994</b> , 51, 243-51  | 5    |
| 1288 | Spatial and free energy distribution patterns of amino acid residues in water soluble proteins. <b>1994</b> , 51, 327-36  | 8    |
| 1287 | Variation of protein partition coefficients with volume ratio in poly(ethylene glycol)-salt aqueous two-phase systems. <b>1994</b> , 668, 3-11                                      | 11   |
| 1286 | . <b>1994</b> ,   | 1    |
| 1285 | Thermodynamics of unfolding of the all beta-sheet protein interleukin-1 beta. <b>1994</b> , 33, 9327-32   | 45   |
| 1284 | Determination of the monomer-dimer equilibrium of interleukin-8 reveals it is a monomer at physiological concentrations. <b>1994</b> , 33, 12741-5                                  | 153  |
| 1283 | Analysis of electrostatic interactions in ribonuclease A monoclinic crystal. <b>1994</b> , 1206, 55-62  | 2    |
| 1282 | Determination of hydrophobic hydration in protein unfolding by an intrinsic reference state. <b>1994</b> , 1208, 15-21  | 4    |
| 1281 | The design of peptide analogues for improved absorption. <b>1994</b> , 29, 283-291  | 20   |
| 1280 | Crystal structure of the human class II MHC protein HLA-DR1 complexed with an influenza virus peptide. <b>1994</b> , 368, 215-21  | 1431 |
| 1279 | Three-dimensional structure of a human class II histocompatibility molecule complexed with superantigen. <b>1994</b> , 368, 711-8   | 532  |
| 1278 | Structure of the regulatory domains of the Src-family tyrosine kinase Lck. <b>1994</b> , 368, 764-9   | 253  |
| 1277 | The crystal structure of the bacterial chaperonin GroEL at 2.8 Å. <b>1994</b> , 371, 578-86   | 1250 |

|      |   |     |
|------|---|-----|
| 1276 | Solution structure of apocytochrome b562. <b>1994</b> , 1, 30-5   | 109 |
| 1275 | Bio-incorporation of telluromethionine into buried residues of dihydrofolate reductase. <b>1994</b> , 1, 283-4  | 32  |
| 1274 | The crystal structure of human endothelin. <b>1994</b> , 1, 311-9   | 80  |
| 1273 | Parallel evolution in two homologues of phosphorylase. <b>1994</b> , 1, 681-90  | 19  |
| 1272 | Crosslinking of mammalian lectin (galectin-1) by complex biantennary saccharides. <b>1994</b> , 1, 863-70   | 193 |
| 1271 | Solution structure of the ets domain of Fli-1 when bound to DNA. <b>1994</b> , 1, 871-5   | 86  |
| 1270 | The structure and antigenicity of a type C foot-and-mouth disease virus. <b>1994</b> , 2, 123-39  | 239 |
| 1269 | Refinement of gamma delta resolvase reveals a strikingly flexible molecule. <b>1994</b> , 2, 371-84   | 52  |
| 1268 | The structure of a neutralized virus: canine parvovirus complexed with neutralizing antibody fragment. <b>1994</b> , 2, 595-607   | 79  |
| 1267 | Volume changes on protein folding. <b>1994</b> , 2, 641-9   | 491 |
| 1266 | Crystal structures of influenza virus hemagglutinin in complex with high-affinity receptor analogs. <b>1994</b> , 2, 719-31   | 108 |
| 1265 | Refined structures of the active Ser83-->Cys and impaired Ser46-->Asp histidine-containing phosphocarrier proteins. <b>1994</b> , 2, 1203-16  | 19  |
| 1264 | Trimeric structure of a C-type mannose-binding protein. <b>1994</b> , 2, 1227-40  | 279 |
| 1263 | Structure of trypanothione reductase from Crithidia fasciculata at 2.6 A resolution; enzyme-NADP interactions at 2.8 A resolution. <b>1994</b> , 50, 139-54   | 330 |
| 1262 | Error detection in crystallographic models. <b>1994</b> , 50, 900-9   | 1   |
| 1261 | Expression cloning of an equine T-lymphocyte glycoprotein CD2 cDNA. Structure-based analysis of conserved sequence elements. <b>1994</b> , 219, 969-76  | 23  |
| 1260 | Probing the structure of hirudin from Hirudinaria manillensis by limited proteolysis. Isolation, characterization and thrombin-inhibitory properties of N-terminal fragments. <b>1994</b> , 226, 323-33 | 31  |
| 1259 | Implementation of solvent effect in molecular mechanics Part 3. The first- and second-order analytical derivatives of excluded volume. <b>1994</b> , 311, 305-324                                       | 13  |

|      |   |     |     |
|------|---|-----|-----|
| 1258 | NMR study of the positions of His-12 and His-119 in the ribonuclease A-uridine vanadate complex. <b>1994</b> , 67, 331-5  |     | 14  |
| 1257 | Stabilization of intermediate density states in globular proteins by homogeneous intramolecular attractive interactions. <b>1994</b> , 66, 454-66   |     | 11  |
| 1256 | A global model of the protein-solvent interface. <b>1994</b> , 66, 601-14   |     | 142 |
| 1255 | Environmental effects on the protonation states of active site residues in bacteriorhodopsin. <b>1994</b> , 66, 1341-52   |     | 94  |
| 1254 | N9 neuraminidase complexes with antibodies NC41 and NC10: empirical free energy calculations capture specificity trends observed with mutant binding data. <b>1994</b> , 33, 7986-97                                |     | 39  |
| 1253 | Three-dimensional structure of phosphotriesterase: an enzyme capable of detoxifying organophosphate nerve agents. <b>1994</b> , 33, 15001-7   |     | 187 |
| 1252 | Efficient product clearance through exit channels in substrate hydrolysis by acetylcholinesterase. <b>1994</b> , 349, 60-4  |     | 11  |
| 1251 | Volume changes in protein evolution. <i>Journal of Molecular Biology</i> , <b>1994</b> , 236, 1067-78   | 6.5 | 139 |
| 1250 | Crystal structure of a NAD-dependent D-glycerate dehydrogenase at 2.4 Å resolution. <i>Journal of Molecular Biology</i> , <b>1994</b> , 236, 1123-40  | 6.5 | 99  |
| 1249 | Mechanism of allergenic cross-reactions--IV. Evidence for participation of aromatic residues in the ligand binding site of two multi-specific IgE monoclonal antibodies. <b>1994</b> , 31, 537-48                   |     | 18  |
| 1248 | Thermodynamic characterization of an equilibrium folding intermediate of staphylococcal nuclease. <b>1994</b> , 3, 2175-84  |     | 39  |
| 1247 | The prediction and orientation of alpha-helices from sequence alignments: the combined use of environment-dependent substitution tables, Fourier transform methods and helix capping rules. <b>1994</b> , 7, 645-53 |     | 53  |
| 1246 | The role of high performance parallel computing in biological research [molecular structure application].   |     |     |
| 1245 | Studies on free energy calculations. II. A theoretical approach to molecular solvation. <b>1994</b> , 101, 6126-6140  |     | 28  |
| 1244 | Rules for alpha-helix termination by glycine. <b>1994</b> , 264, 1126-30  |     | 260 |
| 1243 | Three-dimensional structure of the muscle fatty-acid-binding protein isolated from the desert locust <i>Schistocerca gregaria</i> . <b>1994</b> , 33, 12378-85  |     | 52  |
| 1242 | Kinetic consequences of the removal of a disulfide bridge on the folding of hen lysozyme. <b>1994</b> , 33, 13038-48  |     | 89  |
| 1241 | . <b>1994</b> ,   |     |     |

|      |  |     |
|------|--|-----|
| 1240 | Detection of an intermediate in the folding of the (beta alpha) <sub>8</sub> -barrel N-(5'-phosphoribosyl)anthranilate isomerase from Escherichia coli. <b>1994</b> , 33, 6350-5     | 40  |
| 1239 | Isothermal titration calorimetric study of the association of hen egg lysozyme and the anti-lysozyme antibody HyHEL-5. <b>1994</b> , 33, 3584-90                                     | 86  |
| 1238 | Three-dimensional structure of the biotin carboxylase subunit of acetyl-CoA carboxylase. <b>1994</b> , 33, 10249-56  | 185 |
| 1237 | Structures of horse liver alcohol dehydrogenase complexed with NAD <sup>+</sup> and substituted benzyl alcohols. <b>1994</b> , 33, 5230-7  | 180 |
| 1236 | Implementation of the solvent effect in molecular mechanics. 1. Model development and analytical algorithm for the solvent-accessible surface area. <b>1994</b> , 3, 303-317         | 18  |
| 1235 | Open "back door" in a molecular dynamics simulation of acetylcholinesterase. <b>1994</b> , 263, 1276-8   | 258 |
| 1234 | Mapping staphylococcal nuclease conformation using an EDTA-Fe derivative attached to genetically engineered cysteine residues. <b>1994</b> , 33, 13625-41                            | 42  |
| 1233 | Refined crystal structure of mitochondrial malate dehydrogenase from porcine heart and the consensus structure for dicarboxylic acid oxidoreductases. <b>1994</b> , 33, 2078-88      | 69  |
| 1232 | Specificity and promiscuity in membrane helix interactions. <b>1994</b> , 27, 157-218  | 168 |
| 1231 | Identification of Short Turn Motifs in Proteins Using Sequence and Structure Fingerprints. <b>1994</b> , 34, 257-269   | 2   |
| 1230 | An evolutionary approach to folding small alpha-helical proteins that uses sequence information and an empirical guiding fitness function. <b>1994</b> , 91, 4436-40                 | 147 |
| 1229 | BACK MATTER. <b>1994</b> , 513-556   |     |
| 1228 | Structural basis of asymmetry in the human immunodeficiency virus type 1 reverse transcriptase heterodimer. <b>1994</b> , 91, 7242-6   | 173 |
| 1227 | The T-to-R transformation in hemoglobin: a reevaluation. <b>1994</b> , 91, 11113-7   | 81  |
| 1226 | Complex flexibility of the transforming growth factor beta superfamily. <b>1995</b> , 92, 5406-10  | 9   |
| 1225 | Molecular volume. <b>1995</b> , 259, 377-95  | 4   |
| 1224 | Molecular Concepts. <b>1995</b> , 15-47  | 15  |
| 1223 | Amide Proton Exchange and Surface Conformation of the Basic Pancreatic Trypsin Inhibitor in Solution: Studies with Two-dimensional Nuclear Magnetic Resonance. <b>1995</b> , 540-558 |     |

1222 Drug design based on receptor modeling using a system BIOCES [E] 1995, 23, 49-81

1221 Protein-protein recognition. 1995, 64, 145-66

97

1220 Structure of the azurin mutant Phe114Ala from Pseudomonas aeruginosa at 2.6 A resolution. 1995, 51, 168-76

12

1219 Structure of the photochemical reaction centre of a spheroidene-containing purple-bacterium, Rhodobacter sphaeroides Y, at 3 A resolution. 1995, 51, 368-79

55

1218 Structure of human diferric lactoferrin refined at 2.2 A resolution. 1995, 51, 629-46

78

1217 Calculation of relative binding affinities of purine nucleoside phosphorylase inhibitors. 1995, 51, 536-40

1

1216 Refined structures at 2 and 2.2 A resolution of two forms of the H-protein, a lipamide-containing protein of the glycine decarboxylase complex. 1995, 51, 1041-51

9

1215 Refined three-dimensional solution structure of insect defensin A. 1995, 3, 435-48

290

1214 Structural comparison of two strains of foot-and-mouth disease virus subtype O1 and a laboratory antigenic variant, G67. 1995, 3, 571-80

68

1213 Electrostatic analysis of TEM1 beta-lactamase: effect of substrate binding, steep potential gradients and consequences of site-directed mutations. 1995, 3, 603-13

56

1212 A role for quaternary structure in the substrate specificity of leucine dehydrogenase. 1995, 3, 693-705

78

1211 The prosegment-subtilisin BPN' complex: crystal structure of a specific 'foldase'. 1995, 3, 907-14

170

1210 Common themes in redox chemistry emerge from the X-ray structure of oilseed rape (Brassica napus) enoyl acyl carrier protein reductase. 1995, 3, 927-38

105

1209 The structure of Pyrococcus furiosus glutamate dehydrogenase reveals a key role for ion-pair networks in maintaining enzyme stability at extreme temperatures. 1995, 3, 1147-58

426

1208 The Thermal Unfolding of Hevein, a Small Disulfide-Rich Protein. 1995, 228, 649-652

1207 Molecular modeling of saccharides, 6. Small-ring cyclodextrins: Their geometries and hydrophobic topographies. 1995, 1995, 929-942

32

1206 Molecular modeling of saccharides, 7. The conformation of sucrose in water: A molecular dynamics approach. 1995, 1995, 1925-1937

70

1205 Molecular modeling of saccharides, 8. Selective 2-O-benylation of sucrose: A facile entry to its 2-deoxy- and 2-keto-derivatives and to sucrosamine. 1995, 1995, 1939-1947

22

|      |  |     |
|------|--|-----|
| 1204 | Occluded molecular surface: analysis of protein packing. <b>1995</b> , 8, 334-44   | 103 |
| 1203 | Conformational analysis of endothelin-1: effects of solvation free energy. <b>1995</b> , 36, 283-301   | 12  |
| 1202 | Relative stability of alternative chair forms and hydroxymethyl conformations of $\beta$ -D-glucopyranose. <b>1995</b> , 276, 219-251  | 174 |
| 1201 | A numerical study on the effective dimension of protein surfaces. <b>1995</b> , 242, 325-332   | 3   |
| 1200 | Optimized atomic radii for quantum dielectric continuum solvation models. <b>1995</b> , 244, 65-74   | 118 |
| 1199 | Electrostatics and diffusion of molecules in solution: simulations with the University of Houston Brownian Dynamics program. <b>1995</b> , 91, 57-95   | 567 |
| 1198 | New methods for the analysis of the protein-solvent interface. <b>1995</b> , 91, 321-329   | 5   |
| 1197 | The double cubic lattice method: Efficient approaches to numerical integration of surface area and volume and to dot surface contouring of molecular assemblies. <b>1995</b> , 16, 273-284         | 632 |
| 1196 | Improved methods for semiempirical solvation models. <b>1995</b> , 16, 422-440   | 110 |
| 1195 | An improved algorithm for the analytical computation of solvent-excluded volume. The treatment of singularities in solvent-accessible surface area and volume functions. <b>1995</b> , 16, 817-842 | 23  |
| 1194 | A rapid method for calculating derivatives of solvent accessible surface areas of molecules. <b>1995</b> , 16, 1038-1044   | 62  |
| 1193 | Computational combinatorial chemistry for de novo ligand design: Review and assessment. <b>1995</b> , 3, 51-84   | 35  |
| 1192 | Analysis of the loop-helix interaction in bundle motif protein structures. <b>1995</b> , 14, 559-66  | 6   |
| 1191 | Ecotin: A most adaptable protease inhibitor. <b>1995</b> , 2, 475-482  | 2   |
| 1190 | Hydration in drug design. 2. Influence of local site surface shape on water binding. <b>1995</b> , 9, 513-20   | 59  |
| 1189 | SMART: a solvent-accessible triangulated surface generator for molecular graphics and boundary element applications. <b>1995</b> , 9, 149-59   | 51  |
| 1188 | The relationship between amide proton chemical shifts and secondary structure in proteins. <b>1995</b> , 6, 227-36   | 109 |
| 1187 | Permeability of lysozyme tetragonal crystals to water. <b>1995</b> , 24, 93  | 26  |



|      |  |     |
|------|--|-----|
| 1186 | Elusive affinities. <b>1995</b> , 21, 30-9   | 157 |
| 1185 | Configurational effects in antibody-antigen interactions studied by microcalorimetry. <b>1995</b> , 21, 83-90  | 69  |
| 1184 | Affinities of phosphorylated substrates for the E. coli tryptophan synthase alpha-subunit: roles of Ser-235 and helix-8' dipole. <b>1995</b> , 21, 130-9   | 9   |
| 1183 | Computational approaches to study protein unfolding: hen egg white lysozyme as a case study. <b>1995</b> , 21, 196-213   | 89  |
| 1182 | Modeling the quinone-B binding site of the photosystem-II reaction center using notions of complementarity and contact-surface between atoms. <b>1995</b> , 21, 214-25                           | 66  |
| 1181 | Dramatic differences in the motions of the mouth of open and closed cytochrome P450BM-3 by molecular dynamics simulations. <b>1995</b> , 21, 237-43  | 56  |
| 1180 | Structural model of the photosynthetic reaction center of Rhodobacter capsulatus. <b>1995</b> , 22, 226-44   | 18  |
| 1179 | The catalytic domain of a bacterial lytic transglycosylase defines a novel class of lysozymes. <b>1995</b> , 22, 245-58  | 61  |
| 1178 | The heat capacity of proteins. <b>1995</b> , 22, 404-12  | 371 |
| 1177 | Determination of the conformation of folding initiation sites in proteins by computer simulation. <b>1995</b> , 23, 129-41   | 40  |
| 1176 | Protein-protein interaction at crystal contacts. <b>1995</b> , 23, 580-7   | 226 |
| 1175 | Mutations of surface residues in Anabaena vegetative and heterocyst ferredoxin that affect thermodynamic stability as determined by guanidine hydrochloride denaturation. <b>1995</b> , 4, 58-64 | 12  |
| 1174 | A comparison of X-ray and NMR structures for human endothelin-1. <b>1995</b> , 4, 75-83  | 30  |
| 1173 | A procedure for the automatic determination of hydrophobic cores in protein structures. <b>1995</b> , 4, 93-102  | 35  |
| 1172 | Thermodynamics of the temperature-induced unfolding of globular proteins. <b>1995</b> , 4, 1315-24   | 44  |
| 1171 | Limited proteolysis of native proteins: the interaction between avidin and proteinase K. <b>1995</b> , 4, 1337-45  | 49  |
| 1170 | Solvent accessibility as a predictive tool for the free energy of inhibitor binding to the HIV-1 protease. <b>1995</b> , 4, 1356-64  | 32  |
| 1169 | A new computational model for protein folding based on atomic solvation. <b>1995</b> , 4, 1402-11  | 31  |

|      |   |      |
|------|---|------|
| 1168 | Volume changes of the molten globule transitions of horse heart ferricytochrome c: a thermodynamic cycle. <b>1995</b> , 4, 1426-9   | 21   |
| 1167 | The optimization of protein-solvent interactions: thermostability and the role of hydrophobic and electrostatic interactions. <b>1995</b> , 4, 1516-27                      | 150  |
| 1166 | A preference-based free-energy parameterization of enzyme-inhibitor binding. Applications to HIV-1-protease inhibitor design. <b>1995</b> , 4, 1881-903                     | 121  |
| 1165 | Denaturant m values and heat capacity changes: relation to changes in accessible surface areas of protein unfolding. <b>1995</b> , 4, 2138-48                               | 1686 |
| 1164 | Homology modeling of an immunoglobulin-like domain in the <i>Saccharomyces cerevisiae</i> adhesion protein alpha-agglutinin. <b>1995</b> , 4, 2168-78                       | 17   |
| 1163 | Mechanism of CDK activation revealed by the structure of a cyclinA-CDK2 complex. <b>1995</b> , 376, 313-20  | 1227 |
| 1162 | The allosteric ligand site in the Vmax-type cooperative enzyme phosphoglycerate dehydrogenase. <b>1995</b> , 2, 69-76   | 214  |
| 1161 | Novel metal-binding proteins by design. <b>1995</b> , 2, 368-73   | 87   |
| 1160 | Structural determinants of the stability of thermolysin-like proteinases. <b>1995</b> , 2, 374-9  | 76   |
| 1159 | A third native one-disulphide intermediate in the folding of bovine pancreatic trypsin inhibitor. <b>1995</b> , 2, 674-9  | 24   |
| 1158 | One-step evolution of a dimer from a monomeric protein. <b>1995</b> , 2, 746-51   | 95   |
| 1157 | Solvent isotope effect and protein stability. <b>1995</b> , 2, 852-5  | 155  |
| 1156 | Pseudospecific docking surfaces on electron transfer proteins as illustrated by pseudoazurin, cytochrome c550 and cytochrome cd1 nitrite reductase. <b>1995</b> , 2, 975-82 | 100  |
| 1155 | Solution structure of a mammalian PCB-binding protein in complex with a PCB. <b>1995</b> , 2, 983-9   | 35   |
| 1154 | Outline structures for the extracellular domains of the fibroblast growth factor receptors. <b>1995</b> , 2, 1068-74  | 17   |
| 1153 | A kinetic explanation for the rearrangement pathway of BPTI folding. <b>1995</b> , 2, 1123-30   | 75   |
| 1152 | Using evolutionary changes to achieve species-specific inhibition of enzyme action--studies with triosephosphate isomerase. <b>1995</b> , 2, 847-55                         | 60   |
| 1151 | Quantification and visualization of molecular surface flexibility. <b>1995</b> , 13, 89-97, 110-1   | 5    |

|      |   |     |
|------|---|-----|
| 1150 | Simulating the folding of small proteins by use of the local minimum energy and the free solvation energy yields native-like structures. <b>1995</b> , 13, 312-22 | 23  |
| 1149 | Detection and geometric modeling of molecular surfaces and cavities using digital mathematical morphological operations. <b>1995</b> , 13, 331-6                  | 29  |
| 1148 | Unambiguous configurational and conformational determination of thuriferic acid. <b>1995</b> , 51, 6343-6348  | 13  |
| 1147 | Protein-protein interactions: a review of protein dimer structures. <b>1995</b> , 63, 31-65   | 444 |
| 1146 | Correlation of intron-exon organisation with the three-dimensional structure in glutamate dehydrogenase. <b>1995</b> , 1247, 231-8                                | 6   |
| 1145 | Multifractal analysis of solvent accessibilities in proteins. <b>1995</b> , 52, 880-887   | 18  |
| 1144 | Protein destabilization at low temperatures. <b>1995</b> , 46, 105-39   | 131 |
| 1143 | The Use of Observed Amino Acid Composition in the Proteins to the Analysis of the Sense and Antisense Strands Of DNA. <b>1995</b> , 32, 1237-1243                 |     |
| 1142 | Global structure-acute toxicity relationships for mice using structural parameter ratios: new approach to molecular design and screening. <b>1995</b> , 3, 15-26  | 2   |
| 1141 | Molecular Similarity in Drug Design. <b>1995</b> ,  | 52  |
| 1140 | Differential scanning calorimetry of proteins. <b>1995</b> , 24, 133-76   | 51  |
| 1139 | Fast and robust computation of molecular surfaces. <b>1995</b> ,  | 56  |
| 1138 | Hydrophobic potential by pairwise surface area sum. <b>1995</b> , 8, 437-42   | 24  |
| 1137 | Continuum Electrostatics Model for an SN2 Reaction in Supercritical Water. <b>1995</b> , 99, 16136-16143  | 36  |
| 1136 | Detection of internal cavities in globular proteins. <b>1995</b> , 8, 1011-5  | 32  |
| 1135 | Functional mapping of the surface residues of human thrombin. <b>1995</b> , 270, 16854-63   | 138 |
| 1134 | Thermodynamics of partly folded intermediates in proteins. <b>1995</b> , 24, 141-65   | 93  |
| 1133 | Evaluating contribution of hydrogen bonding and hydrophobic bonding to protein folding. <b>1995</b> , 259, 538-54   | 70  |

|      |   |      |
|------|---|------|
| 1132 | Crystallographic evidence for dimerization of unliganded tumor necrosis factor receptor. <b>1995</b> , 270, 13303-7   | 144  |
| 1131 | Molecular dynamics simulation of cytochrome b5: implications for protein-protein recognition. <b>1995</b> , 34, 9682-93   | 65   |
| 1130 | Three-dimensional structure of galactose-1-phosphate uridylyltransferase from Escherichia coli at 1.8 A resolution. <b>1995</b> , 34, 11049-61                                | 86   |
| 1129 | Calorimetric studies on the interaction of horse ferricytochrome c and yeast cytochrome c peroxidase. <b>1995</b> , 34, 8398-405  | 52   |
| 1128 | Thermodynamic analysis of the structural stability of the tetrameric oligomerization domain of p53 tumor suppressor. <b>1995</b> , 34, 5309-16                                | 122  |
| 1127 | Analysis of gp39/CD40 interactions using molecular models and site-directed mutagenesis. <b>1995</b> , 34, 9884-92  | 57   |
| 1126 | Analysis of the factor VIIa binding site on human tissue factor: effects of tissue factor mutations on the kinetics and thermodynamics of binding. <b>1995</b> , 34, 10383-92 | 93   |
| 1125 | Proton NMR assignments and solution conformation of RANTES, a chemokine of the C-C type. <b>1995</b> , 34, 5329-42  | 147  |
| 1124 | Side-chain determinants of beta-sheet stability. <b>1995</b> , 34, 5718-24  | 71   |
| 1123 | Three-dimensional structure of butyryl-CoA dehydrogenase from Megasphaera elsdenii. <b>1995</b> , 34, 2163-71   | 97   |
| 1122 | Structure of the tetraheme cytochrome from Desulfovibrio desulfuricans ATCC 27774: X-ray diffraction and electron paramagnetic resonance studies. <b>1995</b> , 34, 12830-41  | 64   |
| 1121 | Classical electrostatics in biology and chemistry. <b>1995</b> , 268, 1144-9  | 2487 |
| 1120 | Protein-peptide interactions. <b>1995</b> , 5, 103-13   | 146  |
| 1119 | Osmotic pressure method to measure salt induced folding/unfolding of bovine serum albumin. <b>1995</b> , 30, 113-31   | 11   |
| 1118 | Principles of protein-protein recognition from structure to thermodynamics. <b>1995</b> , 77, 497-505   | 130  |
| 1117 | Crystal structure of the cys2 activator-binding domain of protein kinase C delta in complex with phorbol ester. <b>1995</b> , 81, 917-24                                      | 606  |
| 1116 | The structure of the G protein heterotrimer Gi alpha 1 beta 1 gamma 2. <b>1995</b> , 83, 1047-58  | 1034 |
| 1115 | Structure of the bacteriophage Mu transposase core: a common structural motif for DNA transposition and retroviral integration. <b>1995</b> , 82, 209-20                      | 208  |

|      |   |     |     |
|------|---|-----|-----|
| 1114 | Crystal structure of the replication terminator protein from <i>B. subtilis</i> at 2.6 Å. <b>1995</b> , 80, 651-60  |     | 83  |
| 1113 | The recognition of parvovirus capsids by antibodies. <b>1995</b> , 6, 219-231   |     | 9   |
| 1112 | The peptide backbone plays a dominant role in protein stabilization by naturally occurring osmolytes. <b>1995</b> , 34, 12884-91  |     | 424 |
| 1111 | Alanine scanning mutagenesis of the alpha-helix 115-123 of phage T4 lysozyme: effects on structure, stability and the binding of solvent. <i>Journal of Molecular Biology</i> , <b>1995</b> , 246, 317-30   | 6.5 | 79  |
| 1110 | The three-dimensional solution structure of human stefin A. <i>Journal of Molecular Biology</i> , <b>1995</b> , 246, 331-43   | 6.5 | 100 |
| 1109 | Crystallographic refinement at 2.3 Å resolution and refined model of the photosynthetic reaction centre from <i>Rhodospseudomonas viridis</i> . <i>Journal of Molecular Biology</i> , <b>1995</b> , 246, 429-57   | 6.5 | 577 |
| 1108 | X-ray structure analysis of the iron-dependent superoxide dismutase from <i>Mycobacterium tuberculosis</i> at 2.0 Å resolution reveals novel dimer-dimer interactions. <i>Journal of Molecular Biology</i> , <b>1995</b> , 246, 531-44                                    | 6.5 | 95  |
| 1107 | Conservation of salt bridges in protein families. <i>Journal of Molecular Biology</i> , <b>1995</b> , 248, 125-35   | 6.5 | 35  |
| 1106 | High resolution crystal structures of amphibian red-cell L ferritin: potential roles for structural plasticity and solvation in function. <i>Journal of Molecular Biology</i> , <b>1995</b> , 248, 949-67   | 6.5 | 127 |
| 1105 | A molecular model for the redox potential difference between thioredoxin and DsbA, based on electrostatics calculations. <i>Journal of Molecular Biology</i> , <b>1995</b> , 249, 376-87  | 6.5 | 67  |
| 1104 | Contribution of individual side-chains to the stability of BPTI examined by alanine-scanning mutagenesis. <i>Journal of Molecular Biology</i> , <b>1995</b> , 249, 388-97   | 6.5 | 75  |
| 1103 | A thermodynamic study of mutant forms of <i>Streptomyces subtilisin</i> inhibitor. III. Replacements of a hyper-exposed residue, Met73. <i>Journal of Molecular Biology</i> , <b>1995</b> , 249, 646-53   | 6.5 | 13  |
| 1102 | Crystal structure of <i>Escherichia coli</i> QOR quinone oxidoreductase complexed with NADPH. <i>Journal of Molecular Biology</i> , <b>1995</b> , 249, 785-99   | 6.5 | 95  |
| 1101 | Algorithms for evaluating the long-range accessibility of protein surfaces. <i>Journal of Molecular Biology</i> , <b>1995</b> , 249, 804-15   | 6.5 | 18  |
| 1100 | Structure, dynamics and energetics of initiation sites in protein folding: I. Analysis of a 1 ns molecular dynamics trajectory of an early folding unit in water: the helix I/loop I-fragment of barnase. <i>Journal of Molecular Biology</i> , <b>1995</b> , 250, 239-57 | 6.5 | 10  |
| 1099 | A continuum model for protein-protein interactions: application to the docking problem. <i>Journal of Molecular Biology</i> , <b>1995</b> , 250, 258-75   | 6.5 | 153 |
| 1098 | X-ray structure of gelonin at 1.8 Å resolution. <i>Journal of Molecular Biology</i> , <b>1995</b> , 250, 368-80   | 6.5 | 40  |
| 1097 | Protein flexibility and adaptability seen in 25 crystal forms of T4 lysozyme. <i>Journal of Molecular Biology</i> , <b>1995</b> , 250, 527-52   | 6.5 | 187 |

|      |  |     |     |
|------|--|-----|-----|
| 1096 | The structure of chloroplast cytochrome c6 at 1.9 Å resolution: evidence for functional oligomerization. <i>Journal of Molecular Biology</i> , <b>1995</b> , 250, 627-47   | 6.5 | 109 |
| 1095 | Refined crystal structure of ferrocytochrome c2 from <i>Rhodospseudomonas viridis</i> at 1.6 Å resolution. <i>Journal of Molecular Biology</i> , <b>1995</b> , 252, 235-47   | 6.5 | 29  |
| 1094 | Thermodynamic mapping of the inhibitor site of the aspartic protease endothiapepsin. <i>Journal of Molecular Biology</i> , <b>1995</b> , 252, 337-50   | 6.5 | 226 |
| 1093 | Conformational properties of four peptides spanning the sequence of hen lysozyme. <i>Journal of Molecular Biology</i> , <b>1995</b> , 252, 483-91  | 6.5 | 112 |
| 1092 | Fluctuation and cross-correlation analysis of protein motions observed in nanosecond molecular dynamics simulations. <i>Journal of Molecular Biology</i> , <b>1995</b> , 252, 492-503  | 6.5 | 332 |
| 1091 | Acid and thermal denaturation of barnase investigated by molecular dynamics simulations. <i>Journal of Molecular Biology</i> , <b>1995</b> , 252, 672-708  | 6.5 | 160 |
| 1090 | Recognizing native folds by the arrangement of hydrophobic and polar residues. <i>Journal of Molecular Biology</i> , <b>1995</b> , 252, 709-20   | 6.5 | 122 |
| 1089 | The 2.0 Å crystal structure of <i>Scapharca</i> tetrameric hemoglobin: cooperative dimers within an allosteric tetramer. <i>Journal of Molecular Biology</i> , <b>1995</b> , 253, 168-86   | 6.5 | 33  |
| 1088 | Refined crystal structure of recombinant murine interferon-beta at 2.15 Å resolution. <i>Journal of Molecular Biology</i> , <b>1995</b> , 253, 187-207   | 6.5 | 44  |
| 1087 | Structure, thermodynamics and cooperativity of the glucocorticoid receptor DNA-binding domain in complex with different response elements. Molecular dynamics simulation and free energy perturbation studies. <i>Journal of Molecular Biology</i> , <b>1995</b> , 253, 453-72 | 6.5 | 39  |
| 1086 | Strange bedfellows: interactions between acidic side-chains in proteins. <i>Journal of Molecular Biology</i> , <b>1995</b> , 254, 96-105   | 6.5 | 63  |
| 1085 | The refined X-ray structure of muconate lactonizing enzyme from <i>Pseudomonas putida</i> PRS2000 at 1.85 Å resolution. <i>Journal of Molecular Biology</i> , <b>1995</b> , 254, 918-41  | 6.5 | 58  |
| 1084 | The three-dimensional solution structure of a constrained peptidomimetic in water and in chloroform. Observation of solvent induced hydrophobic cluster. <b>1995</b> , 359, 113-8  |     | 5   |
| 1083 | Amino acid residue: is it structural or functional?. <b>1995</b> , 375, 162-6  |     | 9   |
| 1082 | On the pH dependence of amide proton exchange rates in proteins. <b>1995</b> , 69, 329-39  |     | 41  |
| 1081 | Potential of mean force calculations of the stacking-unstacking process in single-stranded deoxyribonucleoside monophosphates. <b>1995</b> , 69, 2277-85   |     | 57  |
| 1080 | Molecular dynamics simulations of the glucocorticoid receptor DNA-binding domain in complex with DNA and free in solution. <b>1995</b> , 68, 402-26  |     | 51  |
| 1079 | Structure of water and ionic hydration. <b>1995</b> , 132-210  |     |     |

|      |  |      |
|------|--|------|
| 1078 | 1H NMR solution structure of an active monomeric interleukin-8. <b>1995</b> , 34, 12983-90   | 89   |
| 1077 | Hydrophobic-interaction chromatography. <b>2001</b> , Chapter 8, Unit8.4   | 2    |
| 1076 | Determination of the three-dimensional solution structure of noxiustoxin: analysis of structural differences with related short-chain scorpion toxins. <b>1995</b> , 34, 16563-73  | 77   |
| 1075 | Enthalpic contribution to protein stability: insights from atom-based calculations and statistical mechanics. <b>1995</b> , 47, 231-306  | 146  |
| 1074 | Structural investigation of the antibiotic and ATP-binding sites in kanamycin nucleotidyltransferase. <b>1995</b> , 34, 13305-11   | 155  |
| 1073 | Structural features that stabilize halophilic malate dehydrogenase from an archaebacterium. <b>1995</b> , 267, 1344-6  | 242  |
| 1072 | Tertiary and quaternary structural changes in Gi alpha 1 induced by GTP hydrolysis. <b>1995</b> , 270, 954-60  | 270  |
| 1071 | Energetics of protein structure. <b>1995</b> , 47, 307-425   | 846  |
| 1070 | .  | 24   |
| 1069 | Stabilizing amino acid replacements at position 52 in yeast iso-1-cytochrome c: in vivo and in vitro effects. <b>1995</b> , 34, 7094-102   | 25   |
| 1068 | Design and use of a software framework to obtain information derived from macromolecular structure data. <b>1995</b> ,   |      |
| 1067 | A hot spot of binding energy in a hormone-receptor interface. <b>1995</b> , 267, 383-6   | 1763 |
| 1066 | A geometry-based suite of molecular docking processes. <i>Journal of Molecular Biology</i> , <b>1995</b> , 248, 459-776.5  | 86   |
| 1065 | Structural determinants of protein dynamics: analysis of 15N NMR relaxation measurements for main-chain and side-chain nuclei of hen egg white lysozyme. <b>1995</b> , 34, 4041-55 | 197  |
| 1064 | Noncovalent forces important to the conformational stability of protein structures. <b>1995</b> , 40, 1-34   | 9    |
| 1063 | Role of electrostatic screening in determining protein main chain conformational preferences. <b>1995</b> , 34, 755-64   | 138  |
| 1062 | Three-dimensional structure of bacterial luciferase from <i>Vibrio harveyi</i> at 2.4 Å resolution. <b>1995</b> , 34, 6581-6   | 102  |
| 1061 | Folding of omega-conotoxins. 1. Efficient disulfide-coupled folding of mature sequences in vitro. <b>1996</b> , 35, 15537-46   | 58   |

|      |  |      |
|------|--|------|
| 1060 | Transforming growth factor beta 1: three-dimensional structure in solution and comparison with the X-ray structure of transforming growth factor beta 2. <b>1996</b> , 35, 8517-34                             | 149  |
| 1059 | Solvation energies of amino acid side chains and backbone in a family of host-guest pentapeptides. <b>1996</b> , 35, 5109-24   | 475  |
| 1058 | Theoretical investigation of the dynamics of the active site lid in <i>Rhizomucor miehei</i> lipase. <b>1996</b> , 71, 119-29  | 93   |
| 1057 | Electrostatic properties of cytochrome f: implications for docking with plastocyanin. <b>1996</b> , 71, 64-76  | 52   |
| 1056 | Novel approaches to vaccine development against HBV. <b>1996</b> , 44, 67-73   | 11   |
| 1055 | Reduced surface: An efficient way to compute molecular surfaces. <b>1996</b> , 38, 305-320   | 1616 |
| 1054 | Long-acting growth hormones produced by conjugation with polyethylene glycol. <b>1996</b> , 271, 21969-77  | 191  |
| 1053 | Distal cavity fluctuations in myoglobin: protein motion and ligand diffusion. <b>1996</b> , 35, 1125-36  | 58   |
| 1052 | Dynamical Fluctuating Charge Force Fields: The Aqueous Solvation of Amides. <b>1996</b> , 118, 672-679   | 199  |
| 1051 | Salt effects on the amide hydrogen exchange of bovine pancreatic trypsin inhibitor. <b>1996</b> , 35, 2309-15  | 24   |
| 1050 | An approach to rapid estimation of relative binding affinities of enzyme inhibitors: application to peptidomimetic inhibitors of the human immunodeficiency virus type 1 protease. <b>1996</b> , 39, 705-12    | 41   |
| 1049 | Structure-based understanding of ligand affinity using human thrombin as a model system. <b>1996</b> , 35, 9690-9  | 33   |
| 1048 | Positive and negative cooperativities at subsequent steps of oxygenation regulate the allosteric behavior of multistate sebacylhemoglobin. <b>1996</b> , 35, 3418-25   | 19   |
| 1047 | <sup>13</sup> C NMR spectroscopic and X-ray crystallographic study of the role played by mitochondrial cytochrome b5 heme propionates in the electrostatic binding to cytochrome c. <b>1996</b> , 35, 16378-90 | 77   |
| 1046 | Temperature and pH dependences of hydrogen exchange and global stability for ovomucoid third domain. <b>1996</b> , 35, 171-80  | 97   |
| 1045 | Direct determination of the membrane affinities of individual amino acids. <b>1996</b> , 35, 1803-9  | 73   |
| 1044 | Temperature dependence of the redox potential of rubredoxin from <i>Pyrococcus furiosus</i> : a molecular dynamics study. <b>1996</b> , 35, 13772-9  | 24   |
| 1043 | Structure of 4-chlorobenzoyl coenzyme A dehalogenase determined to 1.8 Å resolution: an enzyme catalyst generated via adaptive mutation. <b>1996</b> , 35, 8103-9  | 156  |



|      |   |     |      |
|------|---|-----|------|
| 1042 | Structural and mutational analysis of affinity-inert contact residues at the growth hormone-receptor interface. <b>1996</b> , 35, 10300-7   |     | 70   |
| 1041 | Molecular dynamics simulations of the bis-intercalated complexes of ditercalinium and Flexi-Di with the hexanucleotide d(GCGCGC) <sub>2</sub> : theoretical analysis of the interaction and rationale for the sequence binding specificity. <b>1996</b> , 39, 4810-24 |     | 19   |
| 1040 | Thermodynamics of ligand binding to acyl-coenzyme A binding protein studied by titration calorimetry. <b>1996</b> , 35, 14118-26  |     | 125  |
| 1039 | Identification of residues critical to the activity of human granulocyte colony-stimulating factor. <b>1996</b> , 35, 9034-41   |     | 44   |
| 1038 | Retention Thermodynamics in Hydrophobic Interaction Chromatography. <b>1996</b> , 35, 2964-2981   |     | 93   |
| 1037 | Effect of immunoglobulin variable region structure on C3b and C4b deposition. <b>1996</b> , 33, 759-68  |     | 16   |
| 1036 | Calculation of Cys 30 delta pKa's and oxidising power for DsbA mutants. <b>1996</b> , 385, 105-8  |     | 26   |
| 1035 | Automatic classification and analysis of alpha alpha-turn motifs in proteins. <i>Journal of Molecular Biology</i> , <b>1996</b> , 255, 235-53   | 6.5 | 108  |
| 1034 | Altered domain closure and iron binding in transferrins: the crystal structure of the Asp60Ser mutant of the amino-terminal half-molecule of human lactoferrin. <i>Journal of Molecular Biology</i> , <b>1996</b> , 256, 352-63                                       | 6.5 | 52   |
| 1033 | An efficient mean solvation force model for use in molecular dynamics simulations of proteins in aqueous solution. <i>Journal of Molecular Biology</i> , <b>1996</b> , 256, 939-48  | 6.5 | 114  |
| 1032 | An evolutionary trace method defines binding surfaces common to protein families. <i>Journal of Molecular Biology</i> , <b>1996</b> , 257, 342-58   | 6.5 | 1030 |
| 1031 | Statistical potentials extracted from protein structures: how accurate are they?. <i>Journal of Molecular Biology</i> , <b>1996</b> , 257, 457-69   | 6.5 | 372  |
| 1030 | Conservation and variability in the structures of serine proteinases of the chymotrypsin family. <i>Journal of Molecular Biology</i> , <b>1996</b> , 258, 501-37  | 6.5 | 127  |
| 1029 | Context dependence of mutational effects in a protein: the crystal structures of the V35I, I47V and V35I/I47V gene V protein core mutants. <i>Journal of Molecular Biology</i> , <b>1996</b> , 259, 148-59  | 6.5 | 20   |
| 1028 | Conformation, protein-carbohydrate interactions and a novel subunit association in the refined structure of peanut lectin-lactose complex. <i>Journal of Molecular Biology</i> , <b>1996</b> , 259, 281-96  | 6.5 | 158  |
| 1027 | Three-dimensional solution structure and backbone dynamics of a variant of human interleukin-3. <i>Journal of Molecular Biology</i> , <b>1996</b> , 259, 524-41   | 6.5 | 61   |
| 1026 | Thermodynamic and structural compensation in "size-switch" core repacking variants of bacteriophage T4 lysozyme. <i>Journal of Molecular Biology</i> , <b>1996</b> , 259, 542-59  | 6.5 | 83   |
| 1025 | Assessment of protein fold predictions from sequence information: the predicted alpha/beta doubly wound fold of the von Willebrand factor type A domain is similar to its crystal structure. <i>Journal of Molecular Biology</i> , <b>1996</b> , 260, 277-85          | 6.5 | 33   |

|      |  |     |     |
|------|--|-----|-----|
| 1024 | High-resolution structures of the ligand binding domain of the wild-type bacterial aspartate receptor. <i>Journal of Molecular Biology</i> , <b>1996</b> , 262, 186-201  | 6.5 | 138 |
| 1023 | Crystal structure of the pyridoxal-5'-phosphate dependent cystathionine beta-lyase from <i>Escherichia coli</i> at 1.83 Å. <i>Journal of Molecular Biology</i> , <b>1996</b> , 262, 202-24   | 6.5 | 342 |
| 1022 | Multiple sequence information for threading algorithms. <i>Journal of Molecular Biology</i> , <b>1996</b> , 262, 314-236.5   |     | 35  |
| 1021 | The mannose-specific bulb lectin from <i>Galanthus nivalis</i> (snowdrop) binds mono- and dimannosides at distinct sites. Structure analysis of refined complexes at 2.3 Å and 3.0 Å resolution. <i>Journal of Molecular Biology</i> , <b>1996</b> , 262, 516-31 | 6.5 | 71  |
| 1020 | Antibody-antigen interactions: contact analysis and binding site topography. <i>Journal of Molecular Biology</i> , <b>1996</b> , 262, 732-45   | 6.5 | 398 |
| 1019 | Protein recognition of adenylate: an example of a fuzzy recognition template. <i>Journal of Molecular Biology</i> , <b>1996</b> , 263, 486-500   | 6.5 | 111 |
| 1018 | Multiple wavelength anomalous diffraction (MAD) crystal structure of rusticyanin: a highly oxidizing cupredoxin with extreme acid stability. <i>Journal of Molecular Biology</i> , <b>1996</b> , 263, 730-51   | 6.5 | 112 |
| 1017 | Structural families in loops of homologous proteins: automatic classification, modelling and application to antibodies. <i>Journal of Molecular Biology</i> , <b>1996</b> , 263, 800-15  | 6.5 | 222 |
| 1016 | Deviations from standard atomic volumes as a quality measure for protein crystal structures. <i>Journal of Molecular Biology</i> , <b>1996</b> , 264, 121-36   | 6.5 | 470 |
| 1015 | Disallowed Ramachandran conformations of amino acid residues in protein structures. <i>Journal of Molecular Biology</i> , <b>1996</b> , 264, 191-8   | 6.5 | 87  |
| 1014 | Conformational changes of three periplasmic receptors for bacterial chemotaxis and transport: the maltose-, glucose/galactose- and ribose-binding proteins. <i>Journal of Molecular Biology</i> , <b>1996</b> , 264, 350-63                                      | 6.5 | 115 |
| 1013 | Hyperthermophile protein folding thermodynamics: differential scanning calorimetry and chemical denaturation of Sac7d. <i>Journal of Molecular Biology</i> , <b>1996</b> , 264, 784-805  | 6.5 | 138 |
| 1012 | The crystal structure of a hyperthermophilic archaeal TATA-box binding protein. <i>Journal of Molecular Biology</i> , <b>1996</b> , 264, 1072-84   | 6.5 | 153 |
| 1011 | The contour-buildup algorithm to calculate the analytical molecular surface. <b>1996</b> , 116, 138-43   |     | 75  |
| 1010 | A model for prion protein dimerisation based on alpha-helical packing. <b>1996</b> , 226, 777-82   |     | 13  |
| 1009 | Crystal structure of an IHF-DNA complex: a protein-induced DNA U-turn. <b>1996</b> , 87, 1295-306  |     | 688 |
| 1008 | . <b>1996</b> , 16, 58-61  |     | 26  |
| 1007 | Including Side Chain Flexibility in Continuum Electrostatic Calculations of Protein Titration. <b>1996</b> , 100, 20156-20163  |     | 106 |

|      |   |                 |
|------|---|-----------------|
| 1006 | Analysis of structural determinants of the stability of thermolysin-like proteases by molecular modelling and site-directed mutagenesis. <b>1996</b> , 9, 1181-9  | 27              |
| 1005 | Parametrized Models of Aqueous Free Energies of Solvation Based on Pairwise Descreening of Solute Atomic Charges from a Dielectric Medium. <b>1996</b> , 100, 19824-19839   | 75 <sup>2</sup> |
| 1004 | A Universal Organic Solvation Model. <b>1996</b> , 61, 8720-8721  | 88              |
| 1003 | Effective Atomic Charge Model for Solvent and Ion Screening Effect in Iterative Calculation and Application to Monte Carlo Simulation. <b>1996</b> , 100, 14520-14525   | 8               |
| 1002 | The 1.5-A resolution crystal structure of bacterial luciferase in low salt conditions. <b>1996</b> , 271, 21956-68  | 99              |
| 1001 | Heparin structure and interactions with basic fibroblast growth factor. <b>1996</b> , 271, 1116-20  | 73 <sup>1</sup> |
| 1000 | Functional mimicry of a protein hormone by a peptide agonist: the EPO receptor complex at 2.8 Å. <b>1996</b> , 273, 464-71  | 567             |
| 999  | Crystal structure of DNA recombination protein RuvA and a model for its binding to the Holliday junction. <b>1996</b> , 274, 415-21   | 151             |
| 998  | Model for Aqueous Solvation Based on Class IV Atomic Charges and First Solvation Shell Effects. <b>1996</b> , 100, 16385-16398  | 335             |
| 997  | Molecular Dynamics Simulations of a Calcium Carbonate/Calcium Sulfonate Reverse Micelle <b>1996</b> , 100, 6637-6648  | 84              |
| 996  | Protein Purification Protocols. <b>1996</b> ,   | 12              |
| 995  | Molecular electrostatic potentials and fields: hydrogen bonding, recognition, reactivity and modelling. <b>1996</b> , 257-296   | 26              |
| 994  | Protein Electrostatics. <b>1996</b> , 2, 315-372  | 24              |
| 993  | Crystal structures of the recombinant kringle 1 domain of human plasminogen in complexes with the ligands epsilon-aminocaproic acid and trans-4-(aminomethyl)cyclohexane-1-carboxylic Acid. <b>1996</b> , 35, 2567-76 | 73              |
| 992  | Protein and Peptide Analysis by Mass Spectrometry. <b>1996</b> ,  | 30              |
| 991  | A Comprehensive Analytical Treatment of Continuum Electrostatics. <b>1996</b> , 100, 1578-1599  | 494             |
| 990  | . <b>1996</b> ,   | 79              |
| 989  | Geometric modeling in CAVE. <b>1996</b> ,   | 2               |

|     |  |      |
|-----|--|------|
| 988 | Computer Methods in Protein Modeling: An Overview. <b>1996</b> , 51-73   |      |
| 987 | Structure and function of the Pseudomonas putida integration host factor. <b>1996</b> , 178, 6319-26   | 34   |
| 986 | Three quaternary structures for a single protein. <b>1996</b> , 93, 7017-21  | 40   |
| 985 | A procedure for the prediction of temperature-sensitive mutants of a globular protein based solely on the amino acid sequence. <b>1996</b> , 93, 13908-13                | 39   |
| 984 | Molecular surfaces and volumes. <b>1996</b> , 239-265  |      |
| 983 | Outline structure of the human L1 cell adhesion molecule and the sites where mutations cause neurological disorders.. <b>1996</b> , 15, 6050-6059                        | 96   |
| 982 | Interfacial behaviour of biomacromolecules. <b>1996</b> , 9-17   | 12   |
| 981 | Structure and stability of hyperstable proteins: glycolytic enzymes from hyperthermophilic bacterium Thermotoga maritima. <b>1996</b> , 48, 181-269                      | 114  |
| 980 | Tertiary Structure Comparison of Bromelain Inhibitor VI from Pineapple Stem with Bovine Pancreatic Trypsin Inhibitor.. <b>1996</b> , 72, 104-107                         | 7    |
| 979 | Three-dimensional structure of recombinant human osteogenic protein 1: structural paradigm for the transforming growth factor beta superfamily. <b>1996</b> , 93, 878-83 | 255  |
| 978 | Finite-difference solution of the Poisson-Boltzmann equation: Complete elimination of self-energy. <b>1996</b> , 17, 1344-51   | 64   |
| 977 | Principles of protein-protein interactions. <b>1996</b> , 93, 13-20  | 2309 |
| 976 | Structural stability of small oligomeric proteins. <b>1996</b> , 459-467   | 6    |
| 975 | Discrimination of common protein folds: application of protein structure to sequence/structure comparisons. <b>1996</b> , 266, 575-98                                    | 43   |
| 974 | Packing at the protein-water interface. <b>1996</b> , 93, 10167-72   | 193  |
| 973 | Molecular electrostatic potentials for large systems. <b>1996</b> , 297-331  | 1    |
| 972 | Sequence-specific DNA-binding dominated by dehydration. <b>1996</b> , 93, 4754-9   | 65   |
| 971 | Crystal structure of the Aequorea victoria green fluorescent protein. <b>1996</b> , 273, 1392-5  | 1891 |

|     |  |     |
|-----|--|-----|
| 970 | A mutational analysis of the binding of two different proteins to the same antibody. <b>1996</b> , 35, 9667-76   | 128 |
| 969 | A model of solvation of polypeptide side chains. Application to angiotensin II. <b>1996</b> , 363, 151-165   | 2   |
| 968 | Analysis of electrostatic and hydrophobic complementarities between trypsin and Cucurbita maxima trypsin inhibitor I using molecular electrostatic potential. <b>1996</b> , 365, 39-45 | 7   |
| 967 | Conformational analysis of pentapeptide sequences matching a proposed recognition motif for lysosomal degradation. <b>1996</b> , 1293, 243-53  | 3   |
| 966 | Effect of transmembrane helix packing on tryptophan and tyrosine environments in detergent-solubilized bacterio-opsin. <b>1996</b> , 15, 281-9   | 9   |
| 965 | Hydrogen exchange in the carbon monoxide complex of soybean leghemoglobin. <b>1996</b> , 237, 212-20   | 14  |
| 964 | Ras and its effectors. <b>1996</b> , 66, 1-41  | 49  |
| 963 | The evolution of an allosteric site in phosphorylase. <b>1996</b> , 4, 463-73  | 16  |
| 962 | Crystal structure of a phosphatase-resistant mutant of sporulation response regulator Spo0F from Bacillus subtilis. <b>1996</b> , 4, 679-90  | 65  |
| 961 | Structures of the extracellular domain of the type I tumor necrosis factor receptor. <b>1996</b> , 4, 1251-62  | 131 |
| 960 | The structure of the C-terminal domain of methionine synthase: presenting S-adenosylmethionine for reductive methylation of B12. <b>1996</b> , 4, 1263-75                              | 106 |
| 959 | The crystal structure of a class II fructose-1,6-bisphosphate aldolase shows a novel binuclear metal-binding active site embedded in a familiar fold. <b>1996</b> , 4, 1303-15         | 100 |
| 958 | Properties of the protein matrix revealed by the free energy of cavity formation. <b>1996</b> , 4, 1517-29   | 52  |
| 957 | Analysis of the effect of local interactions on protein stability. <b>1996</b> , 1, 167-78   | 61  |
| 956 | A database of globular protein structural domains: clustering of representative family members into similar folds. <b>1996</b> , 1, 209-20   | 53  |
| 955 | Molecular dynamics simulations of apocytochrome b562--the highly ordered limit of molten globules. <b>1996</b> , 1, 335-46   | 27  |
| 954 | A study of combined structure/sequence profiles. <b>1996</b> , 1, 451-61   | 40  |
| 953 | Alteration of a model antigen by Au(III) leads to T cell sensitization to cryptic peptides. <b>1996</b> , 26, 279-87   | 74  |

|     |   |      |
|-----|---|------|
| 952 | Design eines nichtpeptidischen Rezeptors als Mimeticum für die Phosphocholin-Bindungsstelle des Antikörpers McPC603. <b>1996</b> , 108, 1816-1819   | 12   |
| 951 | Analytical first derivatives of molecular surfaces with respect to nuclear coordinates. <b>1996</b> , 17, 57-73   | 98   |
| 950 | Patterns in ionizable side chain interactions in protein structures. <b>1996</b> , 24, 439-49   | 25   |
| 949 | Molecular docking using surface complementarity. <b>1996</b> , 25, 120-9  | 61   |
| 948 | Predicting solvent accessibility: higher accuracy using Bayesian statistics and optimized residue substitution classes. <b>1996</b> , 25, 38-47   | 24   |
| 947 | The magnitude of the backbone conformational entropy change in protein folding. <b>1996</b> , 25, 143-56  | 98   |
| 946 | Identification and analysis of long-range electrostatic effects in proteins by computer modeling: aspartate transcarbamylase. <b>1996</b> , 25, 300-14  | 5    |
| 945 | Structural model of the anti-snake-toxin antibody, M alpha 2,3. <b>1996</b> , 26, 9-31  | 11   |
| 944 | Modeling of serpin-protease complexes: antithrombin-thrombin, alpha 1-antitrypsin (358Met-->Arg)-thrombin, alpha 1-antitrypsin (358Met-->Arg)-trypsin, and antitrypsin-elastase. <b>1996</b> , 26, 288-303              | 25   |
| 943 | Prediction and evaluation of side-chain conformations for protein backbone structures. <b>1996</b> , 26, 323-52   | 38   |
| 942 | Seeing double: crystal structures of the type I TNF receptor. <b>1996</b> , 9, 113-7  | 16   |
| 941 | A molecular dynamics study of the three-dimensional model of human synovial fluid phospholipase A2 transition state mimic complexes. <b>1996</b> , 9, 95-102  | 4    |
| 940 | Analysis of electrostatic and hydrophobic complementarities between chymotrypsin and avian ovomucoid third domains using molecular electrostatic potential: Effect of residue replacements. <b>1996</b> , 60, 1081-1091 |      |
| 939 | Energy and energy derivatives for molecular solutes: Perspectives of application to hybrid quantum and molecular methods. <b>1996</b> , 60, 1165-1178   | 13   |
| 938 | Geometrical analysis of the voids in structural models of molten salts. <b>1996</b> , 20, 227-233   | 2    |
| 937 | Characterization of pyridoxal phosphate as an optical label for measuring electrostatic potentials in proteins. <b>1996</b> , 32, 71-9  | 6    |
| 936 | Entropic force and folding of macromolecules. <b>1996</b> , 220, 178-182  | 4    |
| 935 | MOLMOL: a program for display and analysis of macromolecular structures. <b>1996</b> , 14, 51-5, 29-32  | 6340 |

|     |  |    |
|-----|--|----|
| 934 | Cosolute effect on crystallization of two dinucleotide complexes of bovine seminal ribonuclease from concentrated salt solutions. <b>1996</b> , 168, 192-197   | 9  |
| 933 | Torsional effects on the molecular polarizabilities of the benzothiazole (A)-benzobisthiazole (B) oligomer A-B13-A. <b>1996</b> , 14, 245-59, 277              | 14 |
| 932 | Analytically defined surfaces to analyze molecular interaction properties. <b>1996</b> , 14, 341-53, 374-5   | 28 |
| 931 | Triangulating the surface of a molecule. <b>1996</b> , 71, 5-22  | 51 |
| 930 | Volumetric properties of tetraphenylporphine, their metallo-complexes and some substituted tetraphenylporphines in benzene solution. <b>1996</b> , 25, 135-153 | 23 |
| 929 | Refinement and structural analysis of bovine cytochrome b5 at 1.5 Å resolution. <b>1996</b> , 52, 65-76  | 90 |
| 928 | Molecular structure of a proteolytic fragment of TLP20. <b>1996</b> , 52, 1153-60  | 3  |
| 927 | Pitfalls of molecular replacement: the structure determination of an immunoglobulin light-chain dimer. <b>1996</b> , 52, 1058-66                               | 11 |
| 926 | Hydrophobic partitioning of proteins in aqueous two-phase systems. <b>1996</b> , 19, 507-517   | 82 |
| 925 | Computational combinatorial ligand design: application to human alpha-thrombin. <b>1996</b> , 10, 372-96   | 55 |
| 924 | Wavelets and molecular structure. <b>1996</b> , 10, 273-83   | 24 |
| 923 | Identification of the Serratia endonuclease dimer: structural basis and implications for catalysis. <b>1996</b> , 5, 24-33                                     | 50 |
| 922 | The crystal structure of trypanothione reductase from the human pathogen Trypanosoma cruzi at 2.3 Å resolution. <b>1996</b> , 5, 52-61                         | 78 |
| 921 | Folding proteins with a simple energy function and extensive conformational searching. <b>1996</b> , 5, 254-61   | 70 |
| 920 | Computational method for relative binding energies of enzyme-substrate complexes. <b>1996</b> , 5, 348-56  | 30 |
| 919 | On the entropy of protein folding. <b>1996</b> , 5, 507-10   | 66 |
| 918 | Classification of mutations in the human CD40 ligand, gp39, that are associated with X-linked hyper IgM syndrome. <b>1996</b> , 5, 531-4                       | 31 |
| 917 | Structural investigation of the alpha-1-antichymotrypsin: prostate-specific antigen complex by comparative model building. <b>1996</b> , 5, 836-51             | 28 |

|     |  |     |
|-----|--|-----|
| 916 | Protein design automation. <b>1996</b> , 5, 895-903  | 232 |
| 915 | The crystal structure of TGF-beta 3 and comparison to TGF-beta 2: implications for receptor binding. <b>1996</b> , 5, 1261-71  | 127 |
| 914 | Cytochrome c3 from <i>Desulfovibrio gigas</i> : crystal structure at 1.8 A resolution and evidence for a specific calcium-binding site. <b>1996</b> , 5, 1342-54                                   | 74  |
| 913 | Hydrophobic regions on protein surfaces. Derivation of the solvation energy from their area distribution in crystallographic protein structures. <b>1996</b> , 5, 1676-86                          | 29  |
| 912 | Dynamics of ribonuclease A and ribonuclease S: computational and experimental studies. <b>1996</b> , 5, 2104-14  | 20  |
| 911 | Water-mediated protein-DNA interactions: the relationship of thermodynamics to structural detail. <b>1996</b> , 5, 2115-8  | 95  |
| 910 | High-resolution X-ray structure of UDP-galactose 4-epimerase complexed with UDP-phenol. <b>1996</b> , 5, 2149-61   | 83  |
| 909 | Insights into the molecular basis of thermal stability from the structure determination of <i>Pyrococcus furiosus</i> glutamate dehydrogenase. <b>1996</b> , 18, 105-17                            | 48  |
| 908 | The X-ray structures of two mutant crystallin domains shed light on the evolution of multi-domain proteins. <b>1996</b> , 3, 267-74  | 33  |
| 907 | Access of ligands to cavities within the core of a protein is rapid. <b>1996</b> , 3, 516-21   | 90  |
| 906 | A novel mode of carbohydrate recognition in jacalin, a Moraceae plant lectin with a beta-prism fold. <b>1996</b> , 3, 596-603  | 195 |
| 905 | Ras/Rap effector specificity determined by charge reversal. <b>1996</b> , 3, 723-9   | 189 |
| 904 | Crystal structure of a camel single-domain VH antibody fragment in complex with lysozyme. <b>1996</b> , 3, 803-11  | 383 |
| 903 | Crystal structure of a G-protein beta gamma dimer at 2.1A resolution. <b>1996</b> , 379, 369-74  | 714 |
| 902 | Structure of Taq polymerase with DNA at the polymerase active site. <b>1996</b> , 382, 278-81  | 291 |
| 901 | Correlation of drug absorption with molecular surface properties. <b>1996</b> , 85, 32-9   | 317 |
| 900 | Can Hydrophobic Interactions Be Correctly Reproduced by the Continuum Models?. <b>1996</b> , 100, 9955-9959  | 26  |
| 899 | Crystal structure of L-2-haloacid dehalogenase from <i>Pseudomonas</i> sp. YL. An alpha/beta hydrolase structure that is different from the alpha/beta hydrolase fold. <b>1996</b> , 271, 20322-30 | 128 |



|     |  |     |
|-----|--|-----|
| 898 | Structural distribution of dipeptides that are identified to be determinants of intracellular protein stability. <b>1996</b> , 14, 201-10  | 7   |
| 897 | Internal packing conditions and fluctuations of amino acid residues in globular proteins. <b>1996</b> , 13, 627-39   | 8   |
| 896 | The role of Phe-92 in the Ca(2+)-induced conformational transition in the C-terminal domain of calmodulin. <b>1996</b> , 271, 11284-90   | 16  |
| 895 | Relationship between accessibility and reactivity of Lys, Met and Tyr in subtilisins DY and Carlsberg. <b>1996</b> , 377, 653-9  | 2   |
| 894 | Fast protein folding in the hydrophobic-hydrophilic model within three-eighths of optimal. <b>1996</b> , 3, 53-96  | 61  |
| 893 | Constant pressure molecular dynamics simulations of the dodecamers: d(GCGCGCGCGCGC) <sub>2</sub> and r(GCGCGCGCGCGC) <sub>2</sub> . <b>1996</b> , 104, 6052-6057   | 41  |
| 892 | Computed electrostatic potentials in molecules, clusters, solids and biosystems containing transition metals. <b>1996</b> , 3, 457-508   | 1   |
| 891 | Development and parametrization of continuum solvent models. I. Models based on the boundary element method. <b>1996</b> , 104, 6679-6695  | 30  |
| 890 | Computational biochemistry of antibodies and T-cell receptors. <b>1996</b> , 49, 149-260   | 7   |
| 889 | Potentials of mean force for biomolecular simulations: Theory and test on alanine dipeptide. <b>1996</b> , 104, 8639-8648  | 25  |
| 888 | Loop replacement and random mutagenesis of omega-loop D, residues 70-84, in iso-1-cytochrome c. <b>1996</b> , 271, 8633-45   | 20  |
| 887 | Specificity of DnaK for arginine/lysine and effect of DnaJ on the amino acid specificity of DnaK. <b>1996</b> , 271, 15486-90  | 19  |
| 886 | Protein-protein interfaces: architectures and interactions in protein-protein interfaces and in protein cores. Their similarities and differences. <b>1996</b> , 31, 127-52                              | 92  |
| 885 | X-ray crystallography of antibodies. <b>1996</b> , 49, 57-133  | 131 |
| 884 | Structural analysis of monosaccharide recognition by rat liver mannose-binding protein. <b>1996</b> , 271, 663-74  | 133 |
| 883 | A role of the amino acid residue located on the fifth position before the first aspartate-rich motif of farnesyl diphosphate synthase on determination of the final product. <b>1996</b> , 271, 30748-54 | 100 |
| 882 | Identification of determinants in the alpha-subunit of Gq required for phospholipase C activation. <b>1996</b> , 271, 5066-72  | 57  |
| 881 | Hydrophobic regions on protein surfaces: definition based on hydration shell structure and a quick method for their computation. <b>1996</b> , 9, 1121-33  | 44  |

|     |   |     |
|-----|---|-----|
| 880 | Multiple human taste receptor sites: a molecular modeling approach. <b>1996</b> , 21, 425-45  | 13  |
| 879 | Conformational Free Energy Landscape of ApApA from Molecular Dynamics Simulations. <b>1996</b> , 100, 2550-2554   | 33  |
| 878 | Geometric manipulation of flexible ligands. <b>1996</b> , 67-78   | 7   |
| 877 | Modeling Drug Receptor Interactions. <b>1996</b> , 235-336  | 10  |
| 876 | A Continuum Solvation Model Including Electrostriction: Application to the Anisole Hydrolysis Reaction in Supercritical Water. <b>1996</b> , 100, 11165-11174                   | 37  |
| 875 | Improving the Continuum Dielectric Approach to Calculating pKas of Ionizable Groups in Proteins. <b>1996</b> , 100, 17373-17387   | 227 |
| 874 | Hydrophobic interaction chromatography. <b>1996</b> , 59, 151-5   | 2   |
| 873 | Rapid analysis of single-cysteine variants of recombinant proteins. <b>1996</b> , 61, 171-83  | 2   |
| 872 | Structure-based thermodynamic scale of alpha-helix propensities in amino acids. <b>1996</b> , 35, 13681-8   | 110 |
| 871 | Whatever happened to the fun? An autobiographical investigation. <b>1997</b> , 26, 1-25   | 12  |
| 870 | The receptor binding site of human interleukin-3 defined by mutagenesis and molecular modeling. <b>1997</b> , 272, 22630-41   | 26  |
| 869 | Fourier-filtered van der Waals contact surfaces: accurate ligand shapes from protein structures. <b>1997</b> , 10, 851-63   | 11  |
| 868 | Identification of common and distinct residues involved in the interaction of alpha <sub>2</sub> and alpha <sub>s</sub> with adenylyl cyclase. <b>1997</b> , 272, 20619-26      | 36  |
| 867 | Thermodynamic analysis of the interaction between the 0.5beta Fv fragment and the RP135 peptide antigen derived from the V3 loop of HIV-1 gp120. <b>1997</b> , 272, 31407-11    | 5   |
| 866 | Analysis of the quaternary structure, substrate specificity, and catalytic mechanism of valine dehydrogenase. <b>1997</b> , 272, 25105-11                                       | 19  |
| 865 | Characterization of ligand binding of a soluble human insulin-like growth factor I receptor variant suggests a ligand-induced conformational change. <b>1997</b> , 272, 8189-97 | 30  |
| 864 | Molecular modeling of immunoglobulin light chains implicates hydrophobic residues in non-amyloid light chain deposition disease. <b>1997</b> , 10, 1191-7                       | 41  |
| 863 | Probing the role of packing specificity in protein design. <b>1997</b> , 94, 10172-7  | 208 |

|     |   |     |
|-----|---|-----|
| 862 | Parallel algorithms in molecular biology. <b>1997</b> , 232-240   | 6   |
| 861 | The rational design of allosteric interactions in a monomeric protein and its applications to the construction of biosensors. <b>1997</b> , 94, 4366-71   | 172 |
| 860 | Identification of a second aryl phosphate-binding site in protein-tyrosine phosphatase 1B: a paradigm for inhibitor design. <b>1997</b> , 94, 13420-5   | 386 |
| 859 | A homology-based model of Juvenile Hormone Esterase from the crop pest, <i>Heliothis virescens</i> . <b>1997</b> , 655-665  | 3   |
| 858 | Isolation and characterization of multiple-methionine mutants of T4 lysozyme with simplified cores. <b>1997</b> , 8, 851-863  | 7   |
| 857 | Using Molecular Graphics to Analyze Protein Structures. <b>1997</b> , 81-108  |     |
| 856 | Predicting Protein Structure With Probabilistic Models. <b>1997</b> , 447-506   | 24  |
| 855 | Thermodynamics of unfolding for Kazal-type serine protease inhibitors: entropic stabilization of ovomucoid first domain by glycosylation. <b>1997</b> , 36, 2323-31   | 40  |
| 854 | Thermodynamic characterization of the reversible, two-state unfolding of maltose binding protein, a large two-domain protein. <b>1997</b> , 36, 5020-8  | 85  |
| 853 | Exceptionally stable salt bridges in cytochrome P450cam have functional roles. <b>1997</b> , 36, 5402-17  | 91  |
| 852 | Calculation of Absolute and Relative Acidities of Substituted Imidazoles in Aqueous Solvent. <b>1997</b> , 101, 10075-10081   | 147 |
| 851 | Solvation and Solubility of Globular Proteins. <b>1997</b> , 101, 1077-1086   | 22  |
| 850 | Structure-based thermodynamic analysis of HIV-1 protease inhibitors. <b>1997</b> , 36, 6588-96  | 73  |
| 849 | Parametrized Model for Aqueous Free Energies of Solvation Using Geometry-Dependent Atomic Surface Tensions with Implicit Electrostatics. <b>1997</b> , 101, 7147-7157   | 73  |
| 848 | Solution structure of the actinorhodin polyketide synthase acyl carrier protein from <i>Streptomyces coelicolor</i> A3(2). <b>1997</b> , 36, 6000-8   | 129 |
| 847 | Molten globule of human alpha-lactalbumin: hydration, density, and compressibility of the interior. <b>1997</b> , 36, 1882-90   | 73  |
| 846 | Kinetic folding and cis/trans prolyl isomerization of staphylococcal nuclease. A study by stopped-flow absorption, stopped-flow circular dichroism, and molecular dynamics simulations. <b>1997</b> , 36, 6529-38 | 28  |
| 845 | Functionally linked hydration changes in <i>Escherichia coli</i> aspartate transcarbamylase and its catalytic subunit. <b>1997</b> , 36, 10161-7  | 36  |

|     |  |     |
|-----|--|-----|
| 844 | Residue accessibility, hydrogen bonding, and molecular recognition: metal-chelate probing of active site histidines in chymotrypsins. <b>1997</b> , 36, 6896-905   | 33  |
| 843 | Conformational Changes in Spin-Labeled Cephalosporin and Penicillin upon Hydrolysis Revealed by Electron Nuclear Double Resonance Spectroscopy. <b>1997</b> , 119, 12619-12628   | 16  |
| 842 | Structural studies of the Escherichia coli signal transducing protein IIAGlc: implications for target recognition. <b>1997</b> , 36, 16087-96  | 42  |
| 841 | Correlation between disulfide reduction and conformational unfolding in bovine pancreatic trypsin inhibitor. <b>1997</b> , 36, 3728-36   | 19  |
| 840 | Continuum Electrostatic Energies of Macromolecules in Aqueous Solutions. <b>1997</b> , 101, 8098-8106  | 124 |
| 839 | "Designing out" disulfide bonds: thermodynamic properties of 30-51 cystine substitution mutants of bovine pancreatic trypsin inhibitor. <b>1997</b> , 36, 5323-35  | 31  |
| 838 | Study of the Ag <sup>+</sup> Hydration by Means of a Semicontinuum Quantum-Chemical Solvation Model. <b>1997</b> , 101, 4444-4448  | 62  |
| 837 | Molecular Dynamics of Acetylcholinesterase Dimer Complexed with Tacrine. <b>1997</b> , 119, 9513-9522  | 144 |
| 836 | The entropic penalty of ordered water accounts for weaker binding of the antibiotic novobiocin to a resistant mutant of DNA gyrase: a thermodynamic and crystallographic study. <b>1997</b> , 36, 9663-73  | 200 |
| 835 | Probing protein structure by solvent perturbation of NMR spectra: the surface accessibility of bovine pancreatic trypsin inhibitor. <b>1997</b> , 73, 382-96   | 36  |
| 834 | Computation of molecular electrostatics with boundary element methods. <b>1997</b> , 73, 1830-41   | 124 |
| 833 | pKa calculations for class A beta-lactamases: methodological and mechanistic implications. <b>1997</b> , 73, 2416-26   | 53  |
| 832 | The tautomeric state of histidines in myoglobin. <b>1997</b> , 73, 3230-40   | 41  |
| 831 | Temperature dependence of histidine ionization constants in myoglobin. <b>1997</b> , 73, 3241-56   | 33  |
| 830 | Molecular Mechanism of Radiationless Deactivation of Aminoanthraquinones through Intermolecular Hydrogen-Bonding Interaction with Alcohols and Hydroperoxides. <b>1997</b> , 101, 8166-8173  | 88  |
| 829 | Allosteric properties of inosine monophosphate dehydrogenase revealed through the thermodynamics of binding of inosine 5'-monophosphate and mycophenolic acid. Temperature dependent heat capacity of binding as a signature of ligand-coupled conformational equilibria. <b>1997</b> , 36, 10428-38 | 45  |
| 828 | Models for Simulating Molecular Properties in Condensed Systems. <b>1997</b> , 215-248   | 1   |
| 827 | Structure-cytoprotective activity relationship of simple molecules containing an alpha,beta-unsaturated carbonyl system. <b>1997</b> , 40, 1827-34   | 31  |

|     |  |        |
|-----|--|--------|
| 826 | Organophosphorus hydrolase is a remarkably stable enzyme that unfolds through a homodimeric intermediate. <b>1997</b> , 36, 14366-74   | 138    |
| 825 | Surface and electrostatics of cutinases. <b>1997</b> , 284, 130-54   | 24     |
| 824 | Stability of Like and Oppositely Charged Organic Ion Pairs in Aqueous Solution. <b>1997</b> , 119, 12917-12922   | 58     |
| 823 | Molecular Size Based Approach To Estimate Partition Properties for Organic Solutes. <b>1997</b> , 101, 3404-3412   | 86     |
| 822 | A naturally occurring protective system in urea-rich cells: mechanism of osmolyte protection of proteins against urea denaturation. <b>1997</b> , 36, 9101-8   | 409    |
| 821 | Dissection of the pH dependence of inhibitor binding energetics for an aspartic protease: direct measurement of the protonation states of the catalytic aspartic acid residues. <b>1997</b> , 36, 16166-72                       | 63     |
| 820 | Crystal structure of the catalytic domains of adenylyl cyclase in a complex with G $\alpha$ .GTP $\gamma$ S. <b>1997</b> , 278, 1907-16  | 638    |
| 819 | Availability of NHS-biotin labeling to identify free protein lysine revealed by experiment and MD simulation. <b>2018</b> , 557, 46-58   | 3      |
| 818 | Protein-protein interface hot spots prediction based on a hybrid feature selection strategy. <b>2018</b> , 19, 14  | 60     |
| 817 | Conformational flexibility of pore loop-1 gives insights into substrate translocation by the AAA protease FtsH. <b>2018</b> , 204, 199-206   | 5      |
| 816 | A reassessment of entropy convergence in solvation thermodynamics. <b>2018</b> , 269, 119-125  | 5      |
| 815 | Establishment of Constraints on Amyloid Formation Imposed by Steric Exclusion of Globular Domains. <i>Journal of Molecular Biology</i> , <b>2018</b> , 430, 3835-3846  | 6.5 10 |
| 814 | Molecular basis for dengue virus broad cross-neutralization by humanized monoclonal antibody 513. <b>2018</b> , 8, 8449  | 8      |
| 813 | The geometry of protein hydration. <b>2018</b> , 148, 215101   | 24     |
| 812 | Impact of the green tea ingredient epigallocatechin gallate and a short pentapeptide (Ile-Ile-Ala-Glu-Lys) on the structural organization of mixed micelles and the related uptake of cholesterol. <b>2018</b> , 1862, 1956-1963 | 2      |
| 811 | Structural mechanism of AadA, a dual-specificity aminoglycoside adenylyltransferase from. <b>2018</b> , 293, 11481-11490   | 14     |
| 810 | Loop modelling 1.0. <b>2018</b> , 84, 64-68  | 4      |
| 809 | Identification of novel leishmanicidal molecules by virtual and biochemical screenings targeting Leishmania eukaryotic translation initiation factor 4A. <b>2018</b> , 12, e0006160  | 13     |

|     |  |       |
|-----|--|-------|
| 808 | Protein Structural Bioinformatics: An Overview. <b>2019</b> , 445-459  | 9     |
| 807 | Protein Structure Visualization. <b>2019</b> , 520-538   |       |
| 806 | A structure-based model for the prediction of protein-RNA binding affinity. <b>2019</b> , 25, 1628-1645  | 5     |
| 805 | Nonspherical Nanoparticle Shape Stability Is Affected by Complex Manufacturing Aspects: Its Implications for Drug Delivery and Targeting. <b>2019</b> , 8, e1900352                                    | 12    |
| 804 | PEPOP 2.0: new approaches to mimic non-continuous epitopes. <b>2019</b> , 20, 387  | 8     |
| 803 | : Consistent Identification of Plausible Binding Sites Despite the Elusive Nature of Cavities and Grooves in Protein Dynamics. <b>2019</b> , 59, 3506-3518   | 9     |
| 802 | Proteins and Protein Structure. <b>2019</b> , 1-52   |       |
| 801 | A super-Gaussian Poisson-Boltzmann model for electrostatic free energy calculation: smooth dielectric distribution for protein cavities and in both water and vacuum states. <b>2019</b> , 79, 631-672 | 9     |
| 800 | Computational re-design of protein structures to improve solubility. <b>2019</b> , 14, 1077-1088   | 10    |
| 799 | Decreasing the immunogenicity of <i>Erwinia chrysanthemi</i> asparaginase via protein engineering: computational approach. <b>2019</b> , 46, 4751-4761   | 0     |
| 798 | Structural and Thermodynamic Analysis of HIV-1 Fusion Inhibition Using Small gp41 Mimetic Proteins. <i>Journal of Molecular Biology</i> , <b>2019</b> , 431, 3091-3106                                 | 6.5 5 |
| 797 | Even/Odd Alkyl Chain-Length Alternation Regulates Oligothiophene Crystal Structure. <b>2019</b> , 31, 6900-6907  | 12    |
| 796 | Structural basis of the atypical activation mechanism of KRAS. <b>2019</b> , 294, 13964-13972  | 16    |
| 795 | Molecular dynamics simulation of removal of heavy metals with sodium dodecyl sulfate micelle in water. <b>2019</b> , 578, 123613   | 4     |
| 794 | Matched Forest: supervised learning for high-dimensional matched case-control studies. <b>2020</b> , 36, 1570-1576   |       |
| 793 | Prediction of Solubility Parameters of Light Gases in Glassy Polymers on the Basis of Simulation of a Short Segment of a Polymer Chain. <b>2019</b> , 61, 718-732                                      | 0     |
| 792 | Structural insight into conformational dynamics of non-active site mutations in KasA: A <i>Mycobacterium tuberculosis</i> target protein. <b>2019</b> , 720, 144082                                    | 7     |
| 791 | Energy propagation along polypeptide Helix: Experimental data and ab initio zone structure. <b>2019</b> , 185, 104016  | 9     |

|     |   |    |
|-----|---|----|
| 790 | Simulations of Temperature and Pressure Unfolding in Soy Allergen Gly m 4 Using Molecular Modeling. <b>2019</b> , 67, 12547-12557   | 15 |
| 789 | MARTINI-Based Protein-DNA Coarse-Grained HADDOCKing. <b>2019</b> , 6, 102   | 12 |
| 788 | Ellipsoidal Abstract and Illustrative Representations of Molecular Surfaces. <b>2019</b> , 20,  | 1  |
| 787 | Tracing chirality, diameter dependence, and temperature-controlling of single-walled carbon nanotube non-covalent functionalization by biologically compatible peptide: insights from molecular dynamics simulations. <b>2019</b> , 25, 274 | 3  |
| 786 | Forkhead Domains of FOXO Transcription Factors Differ in both Overall Conformation and Dynamics. <b>2019</b> , 8,   | 16 |
| 785 | Structure and Functional Binding Epitope of V-domain Ig Suppressor of T Cell Activation. <b>2019</b> , 28, 2509-2516.e5   | 5  |
| 784 | Residue conservation elucidates the evolution of r-proteins in ribosomal assembly and function. <b>2019</b> , 140, 323-329  | 4  |
| 783 | Less Is More: Coarse-Grained Integrative Modeling of Large Biomolecular Assemblies with HADDOCK. <b>2019</b> , 15, 6358-6367  | 19 |
| 782 | Trimer Protein-Protein Complex Interface Interacting Residue Pairs Prediction Using Deep Learning Approach. <b>2019</b> ,   | 0  |
| 781 | An Allosteric Anti-tryptase Antibody for the Treatment of Mast Cell-Mediated Severe Asthma. <b>2019</b> , 179, 417-431.e19  | 42 |
| 780 | On the opposite effect of guanidinium chloride and guanidinium sulphate on the kinetics of the Diels-Alder reaction. <b>2019</b> , 275, 100-104   | 3  |
| 779 | Models for Antibody Behavior in Hydrophobic Interaction Chromatography and in Self-Association. <b>2019</b> , 108, 1434-1441  | 15 |
| 778 | Effect of thermal and microwave processing on secondary structure of bovine $\beta$ -lactoglobulin: A molecular modeling study. <b>2019</b> , 43, e12898  | 6  |
| 777 | Dual binding mode of "bitter sugars" to their human bitter taste receptor target. <b>2019</b> , 9, 8437   | 21 |
| 776 | Evolutionary coupling analysis identifies the impact of disease-associated variants at less-conserved sites. <b>2019</b> , 47, e94  | 3  |
| 775 | Free enzyme dynamics of CmaA3 and CmaA2 cyclopropane mycolic acid synthases from Mycobacterium tuberculosis: Insights into residues with potential significance in cyclopropanation. <b>2019</b> , 91, 61-71                                | 0  |
| 774 | The breadth of HIV-1 neutralizing antibodies depends on the conservation of key sites in their epitopes. <b>2019</b> , 15, e1007056   | 12 |
| 773 | Protein Structure and Modeling. <b>2019</b> ,   | 0  |

- 772 Dissecting macromolecular recognition sites in ribosome: implication to its self-assembly. **2019**, 16, 1300-1312 5
- 771 A molecular contact theory for simulating polarization: application to dielectric constant prediction. **2019**, 21, 14846-14857 8
- 770 I-PINE web server: an integrative probabilistic NMR assignment system for proteins. **2019**, 73, 213-222 26
- 769 SASCUBE: An Updated Method of Cubes for Calculation of the Intensity of X-Ray Scattering by Biopolymers in Solution. **2019**, 64, 38-48
- 768 Geometric description of self-interaction potential in symmetric protein complexes. **2019**, 6, 64 2
- 767 Significance of Molecular Surfaces and Different Visualization Tools in Drug Designing. **2019**, 4, 1-19
- 766 Crystal Structures of the Full-Length Murine and Human Gasdermin D Reveal Mechanisms of Autoinhibition, Lipid Binding, and Oligomerization. **2019**, 51, 43-49.e4 66
- 765 Why does urea have a different effect on the collapse temperature of PDEAM and PNIPAM?. **2019**, 285, 204-212 5
- 764 Dissecting protein-protein interactions in proteasome assembly: Implication to its self-assembly. **2019**, 32, e2784 1
- 763 Molecular dynamics simulation study of linear, bottlebrush, and star-like amphiphilic block polymer assembly in solution. **2019**, 15, 3987-3998 23
- 762 Optimization and Evaluation of Site-Identification by Ligand Competitive Saturation (SILCS) as a Tool for Target-Based Ligand Optimization. **2019**, 59, 3018-3035 27
- 761 Comparative analysis of the methods used for finding surface energy to investigate protein interaction behavior on chromatographic supports. **2019**, 35, e2828 1
- 760 Salt-containing aqueous two-phase system shows predictable partition of proteins with surface amino acids residues. **2019**, 133, 1182-1186 1
- 759 Experiments and Simulations of Complex Sugar-Based Coil-Brush Block Polymer Nanoassemblies in Aqueous Solution. **2019**, 13, 5147-5162 17
- 758 Characterisation of the absolute accessible volume of porous materials. **2019**, 25, 1075-1087 1
- 757 A Domain Decomposition Method for the Poisson-Boltzmann Solvation Models. **2019**, 41, B320-B350 7
- 756 Structural and functional impact of non-synonymous SNPs in the CST complex subunit TEN1: structural genomics approach. **2019**, 39, 15
- 755 Effects of Selective Substitution of Cysteine Residues on the Conformational Properties of Chlorotoxin Explored by Molecular Dynamics Simulations. **2019**, 20, 0



|     |  |    |
|-----|--|----|
| 754 | XGBPRH: Prediction of Binding Hot Spots at Protein?RNA Interfaces Utilizing Extreme Gradient Boosting. <b>2019</b> , 10,   | 12 |
| 753 | The Light and Dark Sides of Virtual Screening: What Is There to Know?. <b>2019</b> , 20,   | 71 |
| 752 | Accelerating the computation of triangulated molecular surfaces with OpenMP. <b>2019</b> , 75, 3426-3470   | 2  |
| 751 | Interactive visualization of biomolecules' dynamic and complex properties. <b>2019</b> , 227, 1725-1739  | 1  |
| 750 | Molecular dynamics of carbon nanohorns and their complexes with cisplatin in aqueous solution. <b>2019</b> , 89, 167-177   | 12 |
| 749 | Effect of pH and Molecular Length on the Structure and Dynamics of Short Poly(acrylic acid) in Dilute Solution: Detailed Molecular Dynamics Study. <b>2019</b> , 123, 4204-4219  | 23 |
| 748 | Studies on the Interaction between Poly-Phosphane Gold(I) Complexes and Dihydrofolate Reductase: An Interplay with Nicotinamide Adenine Dinucleotide Cofactor. <b>2019</b> , 20, | 1  |
| 747 | Complex Behavior of Phosphatidylcholine-Phosphatidic Acid Bilayers and Monolayers: Effect of Acyl Chain Unsaturation. <b>2019</b> , 35, 5944-5956                                | 13 |
| 746 | Free Energy Calculations Based on Coupling Proximal Distribution Functions and Thermodynamic Cycles. <b>2019</b> , 15, 2649-2658   | 3  |
| 745 | DG-GL: Differential geometry-based geometric learning of molecular datasets. <b>2019</b> , 35, e3179   | 34 |
| 744 | Distinct molecular assembly of homologous peroxiredoxins from <i>Pyrococcus horikoshii</i> and <i>Thermococcus kodakaraensis</i> . <b>2019</b> , 166, 89-95                      | 3  |
| 743 | FUNDAMENTAL PRINCIPLES GOVERNING SOLVENTS USE. <b>2019</b> , 11-77   |    |
| 742 | Molecular Dynamics Simulations of 2-Aminopurine-Labeled Dinucleoside Monophosphates Reveal Multiscale Stacking Kinetics. <b>2019</b> , 123, 2291-2304                            | 3  |
| 741 | Morphometric Approach to Many-Body Correlations in Hard Spheres. <b>2019</b> , 122, 068004   | 11 |
| 740 | Cooperative DNA binding by proteins through DNA shape complementarity. <b>2019</b> , 47, 8874-8887   | 8  |
| 739 | A theoretical, dynamical evaluation method of the steric hindrance in nitroxide radicals using transition states of model reactions. <b>2019</b> , 9, 20339                      | 2  |
| 738 | Exit Regions of Cavities in Proteins. <b>2019</b> ,  | 2  |
| 737 | Computational evaluation of the effect of processing on the trypsin and alpha-amylase inhibitor from Ragi ( <i>Eleusine coracana</i> ) seed. <b>2019</b> , 1, e12064             | 0  |

|     |  |    |
|-----|--|----|
| 736 | Molecular dynamics simulations suggest stabilizing mutations in a de novo designed protein. <b>2019</b> , 32, 317-329  | 4  |
| 735 | Advances in Small and Wide-Angle X-Ray Scattering from Proteins and Macromolecular Solutions. <b>2019</b> , 1-39   |    |
| 734 | The Poisson-Boltzmann model for implicit solvation of electrolyte solutions: Quantum chemical implementation and assessment via Sechenov coefficients. <b>2019</b> , 151, 224111   | 20 |
| 733 | Fitting PB1-p62 filaments model structure into its electron microscopy based on an improved genetic algorithm. <b>2019</b> , 1   |    |
| 732 | Solvent-accessible surfaces of proteins and nucleic acids. <b>2019</b> , 125-129   |    |
| 731 | TMP-SSurface: A Deep Learning-Based Predictor for Surface Accessibility of Transmembrane Protein Residues. <b>2019</b> , 9, 640  | 5  |
| 730 | Structure and role for active site lid of lactate monooxygenase from Mycobacterium smegmatis. <b>2019</b> , 28, 135-149  | 10 |
| 729 | Thermodynamic Evaluation of the Interaction Driven by Hydrophobic Bonding in the Aqueous Phase. <b>2019</b> , 108, 173-177   | 1  |
| 728 | Aprotinin interacts with substrate-binding site of human dipeptidyl peptidase III. <b>2019</b> , 37, 3596-3606   | 2  |
| 727 | Investigation of deleterious effects of nsSNPs in the POT1 gene: a structural genomics-based approach to understand the mechanism of cancer development. <b>2019</b> , 120, 10281-10294  | 25 |
| 726 | Energy Exchange Network Model Demonstrates Protein Allosteric Transition: An Application to an Oxygen Sensor Protein. <b>2019</b> , 123, 768-775   | 14 |
| 725 | Analysis of solvent-exposed and buried co-crystallized ligands: a case study to support the design of novel protein-protein interaction inhibitors. <b>2019</b> , 24, 551-559  | 11 |
| 724 | TargetDBP: Accurate DNA-Binding Protein Prediction Via Sequence-Based Multi-View Feature Learning. <b>2020</b> , 17, 1419-1429   | 17 |
| 723 | Molecular Modeling of Surfactant Micellization Using Solvent-Accessible Surface Area. <b>2019</b> , 35, 2443-2450  | 22 |
| 722 | In Silico Structure-Based Prediction of ReceptorLigand Binding Affinity: Current Progress and Challenges. <b>2019</b> , 109-175  | 2  |
| 721 | Beta-complex versus Alpha-complex: Similarities and Dissimilarities. <b>2020</b> , 26, 1686-1701   | 1  |
| 720 | Trehalose Limits Fragment Antibody Aggregation and Influences Charge Variant Formation in Spray-Dried Formulations at Elevated Temperatures. <b>2019</b> , 16, 349-358   | 4  |
| 719 | Improving prediction of protein secondary structure, backbone angles, solvent accessibility and contact numbers by using predicted contact maps and an ensemble of recurrent and residual convolutional neural networks. <b>2019</b> , 35, 2403-2410 | 84 |

|                 |   |    |
|-----------------|---|----|
| 7 <sup>18</sup> | Study of phase behavior of 2,6-lutidine, 2,6-lutidine-N-oxide and water mixture using UNIQUAC model with interaction parameters determined by molecular simulations. <b>2019</b> , 671, 110-118 | 1  |
| 7 <sup>17</sup> | Dissecting water binding sites at protein-protein interfaces: a lesson from the atomic structures in the Protein Data Bank. <b>2019</b> , 37, 1204-1219   | 5  |
| 7 <sup>16</sup> | Global phosphoproteomic analysis of Ebola virions reveals a novel role for VP35 phosphorylation-dependent regulation of genome transcription. <b>2020</b> , 77, 2579-2603                       | 6  |
| 7 <sup>15</sup> | An engineered ultra-high affinity Fab-Protein G pair enables a modular antibody platform with multifunctional capability. <b>2020</b> , 29, 141-156   | 3  |
| 7 <sup>14</sup> | RMSD analysis of structures of the bacterial protein FimH identifies five conformations of its lectin domain. <b>2020</b> , 88, 593-603   | 4  |
| 7 <sup>13</sup> | Small protein-protein interfaces rich in electrostatic are often linked to regulatory function. <b>2020</b> , 38, 3260-3279   | 3  |
| 7 <sup>12</sup> | Graph coloring: a novel heuristic based on trailing path properties, perspective and applications in structured networks. <b>2020</b> , 24, 603-625   | 2  |
| 7 <sup>11</sup> | Intrinsically smooth discretisation of Connolly's solvent-excluded molecular surface. <b>2020</b> , 118, e1644384   | 9  |
| 7 <sup>10</sup> | Molecular dynamics study of the behaviour of surfactant Triton X-100 in the extraction process of Cd <sup>2+</sup> . <b>2020</b> , 739, 136920  | 1  |
| 7 <sup>09</sup> | Preferred conformations of lipooligosaccharides and oligosaccharides of <i>Moraxella catarrhalis</i> . <b>2020</b> , 30, 86-94  | 4  |
| 7 <sup>08</sup> | The Role of Electrostatics and Folding Kinetics on the Thermostability of Homologous Cold Shock Proteins. <b>2020</b> , 60, 546-561   | 2  |
| 7 <sup>07</sup> | A novel near-infrared fluorescent probe for detection of early-stage A $\beta$ protofibrils in Alzheimer's disease. <b>2020</b> , 56, 1625-1628   | 15 |
| 7 <sup>06</sup> | Effect of the Solute Cavity on the Solvation Energy and its Derivatives within the Framework of the Gaussian Charge Scheme. <b>2020</b> , 41, 922-939   | 33 |
| 7 <sup>05</sup> | Do sequence neighbours of intrinsically disordered regions promote structural flexibility in intrinsically disordered proteins?. <b>2020</b> , 209, 107428                                      | 2  |
| 7 <sup>04</sup> | Effect of sodium thiocyanate and sodium perchlorate on poly(N-isopropylacrylamide) collapse. <b>2019</b> , 22, 189-195  | 4  |
| 7 <sup>03</sup> | PBCAVE: Program for exact classification of the mesh points of a protein with possible internal cavities and its application to Poisson-Boltzmann equation solution. <b>2020</b> , 250, 107003  |    |
| 7 <sup>02</sup> | Analysis of a preQ1-I riboswitch in effector-free and bound states reveals a metabolite-programmed nucleobase-stacking spine that controls gene regulation. <b>2020</b> , 48, 8146-8164         | 11 |
| 7 <sup>01</sup> | The hydrophobic effect: is water afraid, or just not that interested?. <b>2020</b> , 6, 1   | 4  |

|     |  |    |
|-----|--|----|
| 700 | RLDOCK: A New Method for Predicting RNA-Ligand Interactions. <b>2020</b> , 16, 7173-7183   | 8  |
| 699 | Characterization of tau binding by gosuranemab. <b>2020</b> , 146, 105120  | 18 |
| 698 | Mapping molecular electrostatic potential (MESP) for fulleropyrrolidine and its derivatives. <b>2020</b> , 52, 1   | 16 |
| 697 | Comprehensive Physico-Chemical Characterization of a Serotonin Inclusion Complex with 2-Hydroxypropyl- $\beta$ -Cyclodextrin. <b>2020</b> , 49, 915-944  | 4  |
| 696 | Molecular insights into inclusion complex formation between $\beta$ and $\gamma$ -cyclodextrins and rosmarinic acid. <b>2020</b> , 314, 113802   | 22 |
| 695 | Precise parallel volumetric comparison of molecular surfaces and electrostatic isopotentials. <b>2020</b> , 15, 11   | 1  |
| 694 | Molecular Sparse Representation by a 3D Ellipsoid Radial Basis Function Neural Network via L1 Regularization. <b>2020</b> , 60, 6054-6064  | 0  |
| 693 | Analyzing the Relationship Between the Activation of the Edema Factor and Its Interaction With Calmodulin. <b>2020</b> , 7, 586544   |    |
| 692 | Considerations for Achieving Maximized DNA Recovery in Solid-Phase DNA-Encoded Library Synthesis. <b>2020</b> , 22, 649-655  |    |
| 691 | The de Rham-Hodge Analysis and Modeling of Biomolecules. <b>2020</b> , 82, 108   | 6  |
| 690 | Systematic Investigation of the Data Set Dependency of Protein Stability Predictors. <b>2020</b> , 60, 4772-4784   | 12 |
| 689 | Computational Assessment of the Molecular Structure and Properties for High Energy Density Fuel. <b>2020</b> , 124, 6660-6666  | 1  |
| 688 | Molecular Dynamics Simulation of the Diffusion Dynamics of Linear DNA Fragments in Dilute Solution with the Parmbsc1 Force Field and Comparison with Experimental Data and Theoretical Models. <b>2020</b> , 53, 6135-6150 |    |
| 687 | Using physical features of protein core packing to distinguish real proteins from decoys. <b>2020</b> , 29, 1931-1944  | 1  |
| 686 | The Human LL-37(17-29) antimicrobial peptide reveals a functional supramolecular structure. <b>2020</b> , 11, 3894   | 27 |
| 685 | Hit-to-lead and lead optimization binding free energy calculations for G protein-coupled receptors. <b>2020</b> , 10, 20190128   | 4  |
| 684 | Multi-models in predicting RNA solvent accessibility exhibit the contribution from none-sequential attributes and providing a globally stable modeling strategy. <b>2020</b> , 205, 104100                                 | 0  |
| 683 | Sampling of the conformational landscape of small proteins with Monte Carlo methods. <b>2020</b> , 10, 18211   | 7  |

|     |   |    |
|-----|---|----|
| 682 | A Visual Differential Analysis of Structural Features of Internal Cavities in Two Chiral Forms of Diphenylalanine Nanotubes. <b>2020</b> , 65, 374-380                      | 5  |
| 681 | Allosteric Inhibition of Adenylyl Cyclase Type 5 by G-Protein: A Molecular Dynamics Study. <b>2020</b> , 10,  | 2  |
| 680 | Pathway of orientational symmetry breaking in crystallization of short n-alkane droplets: A molecular dynamics study. <b>2020</b> , 153, 084903                             | 0  |
| 679 | Structure of the Plasmodium falciparum PfSERA5 pseudo-zymogen. <b>2020</b> , 29, 2245-2258  | 2  |
| 678 | Valence optimization and angle improvement for molecular surface remeshing. <b>2020</b> , 36, 2355-2368   | 1  |
| 677 | Effect of Poly(vinyl butyral) Comonomer Sequence on Adhesion to Amorphous Silica: A Coarse-Grained Molecular Dynamics Study. <b>2020</b> , 12, 47879-47890                  | 5  |
| 676 | Assembly intermediates of orthoreovirus captured in the cell. <b>2020</b> , 11, 4445  | 13 |
| 675 | ADD Force Field for Sugars and Polyols: Predicting the Additivity of Protein-Osmolyte Interaction. <b>2020</b> , 124, 7779-7790   | 3  |
| 674 | Random Coils of Proteins Situated Between a Beta Strand and an Alpha Helix Demonstrate Decreased Solvent Accessibility. <b>2020</b> , 39, 308-317                           | 3  |
| 673 | Myosin dynamics during relaxation in mouse soleus muscle and modulation by 2'-deoxy-ATP. <b>2020</b> , 598, 5165-5182   | 7  |
| 672 | Oligosaccharide Binding and Thermostability of Two Related AA9 Lytic Polysaccharide Monoxygenases. <b>2020</b> , 59, 3347-3358  | 11 |
| 671 | Is water a good solvent for the denatured state of globular proteins?. <b>2020</b> , 759, 137949  | 1  |
| 670 | Structural Insights into Ceftobiprole Inhibition of Pseudomonas aeruginosa Penicillin-Binding Protein 3. <b>2020</b> , 64,  | 7  |
| 669 | Calculation of higher protonation states and of a new resting state for vanadium chloroperoxidase using QM/MM, with an Atom-in-Molecules analysis. <b>2020</b> , 99, 107624 | 1  |
| 668 | Understanding the protein sequence and structural adaptation in extremophilic organisms through machine learning techniques. <b>2020</b> , 307-314                          |    |
| 667 | Systematic approach for wettability prediction using molecular dynamics simulations. <b>2020</b> , 16, 4299-4310  | 5  |
| 666 | Shape effect on non-covalent dimer stability using classic scaled particle theory. <b>2020</b> , 743, 137176  | 3  |
| 665 | Caspase-1 Engages Full-Length Gasdermin D through Two Distinct Interfaces That Mediate Caspase Recruitment and Substrate Cleavage. <b>2020</b> , 53, 106-114.e5             | 42 |

|     |  |    |
|-----|--|----|
| 664 | How Spherical Are Gaseous Low Charged Dendrimer Ions: A Molecular Dynamics/Ion Mobility Study?. <b>2020</b> ,  | 2  |
| 663 | Improving the binding affinity estimations of protein-ligand complexes using machine-learning facilitated force field method. <b>2020</b> , 34, 817-830  | 7  |
| 662 | Molecular Dynamics Simulations in Statistical Physics: Theory and Applications. <b>2020</b> ,  | 5  |
| 661 | Immunoinformatics. <b>2020</b> ,   | 1  |
| 660 | Structure-based discovery of a small-molecule inhibitor of methicillin-resistant virulence. <b>2020</b> , 295, 5944-5959   | 9  |
| 659 | Determining the Mesh Size of Polymer Solutions via the Pore Size Distribution. <b>2020</b> , 53, 2568-2581   | 5  |
| 658 | Analytical calculation of the solvent-accessible surface area and its nuclear gradients by stereographic projection: A general approach for molecules, polymers, nanotubes, helices, and surfaces. <b>2020</b> , 41, 1464-1479 | 4  |
| 657 | A Grid Map Based Approach to Identify Nonobvious Ligand Design Opportunities in 3D Protein Structure Ensembles. <b>2020</b> , 60, 2178-2188  | 2  |
| 656 | Protein-metallodrugs interactions: Effects on the overall protein structure and characterization of Au, Ru and Pt binding sites. <b>2020</b> , 163, 970-976  | 8  |
| 655 | Comparative studies on ion-pair energetic, distribution among three domains of life: Archaea, eubacteria, and eukarya. <b>2020</b> , 88, 865-873   | 0  |
| 654 | Why small proteins tend to have high denaturation temperatures. <b>2020</b> , 22, 16258-16266  | 4  |
| 653 | Disulfide Bonds Affect the Binding Sites of Human $\alpha$ -Defensin Type 3 on Negatively Charged Lipid Membranes. <b>2020</b> , 124, 2088-2100  | 7  |
| 652 | Analyses of protein cores reveal fundamental differences between solution and crystal structures. <b>2020</b> , 88, 1154-1161  | 2  |
| 651 | Using Polar Ion-Pairs to Control Drug Delivery to the Airways of the Lungs. <b>2020</b> , 17, 1482-1490  | 2  |
| 650 | Application of the ESMACS Binding Free Energy Protocol to a Multi-Binding Site Lactate Dehydrogenase A Ligand Dataset. <b>2020</b> , 3, 1900194  | 7  |
| 649 | Molecular dynamics simulation on the dissolution process of Kaempferol cluster. <b>2020</b> , 304, 112779  | 1  |
| 648 | Structural and dynamic origins of ESR lineshapes in spin-labeled GB1 domain: the insights from spin dynamics simulations based on long MD trajectories. <b>2020</b> , 10, 957  | 3  |
| 647 | Gas separation properties of aromatic polyimides with bulky groups. Comparison of experimental and simulated results. <b>2020</b> , 602, 117959  | 10 |

|     |  |    |
|-----|--|----|
| 646 | MGOS: A library for molecular geometry and its operating system. <b>2020</b> , 251, 107101   | 1  |
| 645 | Structure-Based Design of Small Peptide Ligands to Inhibit Early-Stage Protein Aggregation Nucleation. <b>2020</b> , 60, 3304-3314   | 3  |
| 644 | Sodium-salt adduct fullerenes prevent self-association and amyloid fibril formation: molecular dynamics approach. <b>2020</b> , 18, 335-347                                    | 1  |
| 643 | On the Thermal Stability of O-Methylguanine-DNA Methyltransferase from Archaeon by Molecular Dynamics Simulations. <b>2020</b> , 60, 2138-2154                                 | 3  |
| 642 | Effects of the Hydrophobicity of Key Residues on the Characteristics and Stability of Glucose Oxidase on a Graphene Surface. <b>2020</b> , 6, 1899-1908                        | 5  |
| 641 | Molecular dynamics simulations identify the regions of compromised thermostability in SazCA. <b>2021</b> , 89, 375-388   | 4  |
| 640 | Machine learning meets mechanistic modelling for accurate prediction of experimental activation energies. <b>2021</b> , 12, 1163-1175  | 28 |
| 639 | Simulation of differential structure and dynamics of disulfide bond isoforms of conopeptide AuIB in presence of human $\alpha$ 7 nAChR. <b>2021</b> , 113, e24183              |    |
| 638 | Investigation on structural properties of winter flounder antifreeze protein in interaction with clathrate hydrate by molecular dynamics simulation. <b>2021</b> , 152, 106267 | 5  |
| 637 | Evaluation of acridinedione analogs as potential SARS-CoV-2 main protease inhibitors and their comparison with repurposed anti-viral drugs. <b>2021</b> , 128, 104117          | 56 |
| 636 | Temperature dependent aggregation mechanism and pathway of lysozyme: By all atom and coarse grained molecular dynamics simulation. <b>2021</b> , 103, 107816                   | 1  |
| 635 | Insulin binding to the analytical antibody sandwich pair OXI-005 and HUI-018: Epitope mapping and binding properties. <b>2021</b> , 30, 485-496                                | 0  |
| 634 | The magnitude of macromolecular crowding caused by Dextran and Ficoll for the conformational stability of globular proteins. <b>2021</b> , 322, 114969                         | 4  |
| 633 | Atomic insights into the sintering process of polycyclic aromatic hydrocarbon clusters. <b>2021</b> , 38, 1181-1188  | 4  |
| 632 | Techniques assisting peptide vaccine and peptidomimetic design. Sidechain exposure in the SARS-CoV-2 spike glycoprotein. <b>2021</b> , 128, 104124                             | 7  |
| 631 | Structure-based mechanisms: On the way to apply alcohol dehydrogenases/reductases to organic-aqueous systems. <b>2021</b> , 168, 412-427                                       | 3  |
| 630 | Guest-occupiable space in the crystalline solid state: a simple rule-of-thumb for predicting occupancy. <b>2021</b> , 50, 735-749  | 14 |
| 629 | Evaluation of the performances of different atomic charge and nonelectrostatic models in the finite-difference Poisson-Boltzmann approach. <b>2021</b> , 121, e26560           | 4  |

|     |   |    |
|-----|---|----|
| 628 | Cyclically parallelized treecode for fast computations of electrostatic interactions on molecular surfaces. <b>2021</b> , 260, 107742   | 0  |
| 627 | Origin of heat capacity increment in DNA folding: The hydration effect. <b>2021</b> , 1865, 129774  | 5  |
| 626 | Adaptive nanopores: A bioinspired label-free approach for protein sequencing and identification. <b>2021</b> , 14, 328-333  | 5  |
| 625 | Modulation of granulocyte colony stimulating factor conformation and receptor binding by methionine oxidation. <b>2020</b> ,  | 1  |
| 624 | Computational driven molecular dynamics simulation of keratinocyte growth factor behavior at different pH conditions. <b>2021</b> , 23, 100514                                    | 4  |
| 623 | Molecular Dynamics Simulation to Uncover the Mechanisms of Protein Instability During Freezing. <b>2021</b> , 110, 2457-2471  | 8  |
| 622 | Chemical functionality at the liquid surface of pure unsaturated fatty acids.   |    |
| 621 | A novel P38 $\beta$ MAPK activator Bruceine A exhibits potent anti-pancreatic cancer activity. <b>2021</b> , 19, 3437-3450  | 3  |
| 620 | C-phycoyanin as a highly attractive model system in protein crystallography: unique crystallization properties and packing-diversity screening. <b>2021</b> , 77, 224-236         | 3  |
| 619 | Structural Principles of the Flavivirus Particle Organization and of Its Conformational Changes. <b>2021</b> , 290-302  | 1  |
| 618 | Solvent Accessibility of Residues Undergoing Pathogenic Variations in Humans: From Protein Structures to Protein Sequences. <b>2020</b> , 7, 626363                               | 15 |
| 617 | Analysis of the Schwarz Domain Decomposition Method for the Conductor-like Screening Continuum Model. <b>2021</b> , 59, 769-796   |    |
| 616 | Effect of substitutions on the electronic properties of acetylsalicylic acid. <b>2021</b> , 53, 1   | 1  |
| 615 | Propedia: a database for protein-peptide identification based on a hybrid clustering algorithm. <b>2021</b> , 22, 1   | 40 |
| 614 | The function of peptide-mimetic anionic groups and salt bridges in the antimicrobial activity and conformation of cationic amphiphilic copolymers.. <b>2021</b> , 11, 22044-22056 | 3  |
| 613 | A Theoretical Approach to the Fluorophilicity of Ions via the Gibbs Energy of Ion Transfer at the Fluorous Solvent/Water Interface. <b>2021</b> ,                                 | 1  |
| 612 | On the estimation of the molecular inaccessible volume and the molecular accessible surface of a ligand in protein-ligand systems.  | 2  |
| 611 | Structure elements can be predicted using the contact volume among protein residues. <b>2021</b> , 18, 50-59  |    |



|     |   |    |
|-----|---|----|
| 610 | Seeing the PDB. <b>2021</b> , 296, 100742   | 4  |
| 609 | Molecular dynamics simulations and functional studies reveal that hBD-2 binds SARS-CoV-2 spike RBD and blocks viral entry into ACE2 expressing cells. <b>2021</b> ,                                   | 7  |
| 608 | On regularization of charge singularities in solving the Poisson-Boltzmann equation with a smooth solute-solvent boundary. <b>2021</b> , 18, 1370-1405  | 3  |
| 607 | Three-dimensional structure of human cyclooxygenase (hCOX)-1. <b>2021</b> , 11, 4312  | 10 |
| 606 | Insights into the Thermal Response of a Poly(ethylene oxide)-poly(propylene oxide)-poly(ethylene oxide) Triblock Polymer in Water. <b>2021</b> , 125, 2167-2173                                       | 1  |
| 605 | Structural and thermodynamic analyses of human TMED1 (p24 <sup>h</sup> ) Golgi dynamics.  |    |
| 604 | Monolayer Structures of Supramolecular Antagonistic Salt Aggregates. <b>2021</b> , 125, 2351-2359   | 1  |
| 603 | DLAB - Deep learning methods for structure-based virtual screening of antibodies.   | 3  |
| 602 | A base measure of precision for protein stability predictors: structural sensitivity. <b>2021</b> , 22, 88  | 8  |
| 601 | DeepCys: Structure-based multiple cysteine function prediction method trained on deep neural network: Case study on domains of unknown functions belonging to COX2 domains. <b>2021</b> , 89, 745-761 | 1  |
| 600 | Crystal structure of a photosynthetic LH1-RC in complex with its electron donor HiPIP. <b>2021</b> , 12, 1104   | 1  |
| 599 | Role of the Enzymatic Environment in the Reactivity of the Au-C <sup>N</sup> C Anticancer Complexes. <b>2021</b> , 60, 3181-3195  | 2  |
| 598 | Binding the needle in the haystack—will natural products fit for purpose in the treatment of cryptosporidiosis? A theoretical perspective. 1-14   |    |
| 597 | Modulation of post-powerstroke dynamics in myosin II by 2'-deoxy-ADP. <b>2021</b> , 699, 108733   | 0  |
| 596 | Influence of spatial structure on protein damage susceptibility: a bioinformatics approach. <b>2021</b> , 11, 4938  |    |
| 595 | Rotational dynamics of proteins in nanochannels: Role of solvent's local viscosity. <b>2021</b> ,   | 1  |
| 594 | The influences of surface polar unit density on the water dispersity of nanoparticles. <b>2021</b> , 325, 115241  | 1  |
| 593 | Dielectric continuum methods for quantum chemistry. <b>2021</b> , 11, e1519   | 31 |

|     |  |    |
|-----|--|----|
| 592 | Coupling Monte Carlo, Variational Implicit Solvation, and Binary Level-Set for Simulations of Biomolecular Binding. <b>2021</b> , 17, 2465-2478  | 1  |
| 591 | Accurate prediction of inter-protein residue-residue contacts for homo-oligomeric protein complexes. <b>2021</b> , 22,   | 11 |
| 590 | TMP- SSurface2: A Novel Deep Learning-Based Surface Accessibility Predictor for Transmembrane Protein Sequence. <b>2021</b> , 12, 656140   | 3  |
| 589 | Epitope Mapping of Exposed Tegument and Alimentary Tract Proteins Identifies Putative Antigenic Targets of the Attenuated Schistosome Vaccine. <b>2020</b> , 11, 624613  | 5  |
| 588 | Benefits of Ion Mobility Separation and Parallel Accumulation-Serial Fragmentation Technology on timsTOF Pro for the Needs of Fast Photochemical Oxidation of Protein Analysis. <b>2021</b> , 6, 10352-10361                       | 4  |
| 587 | Applications and Specifics of SAXS. <b>2021</b> , 137-195  |    |
| 586 | Marker residue types at the structural regions of transmembrane alpha-helical and beta-barrel interfaces. <b>2021</b> , 89, 1145-1157  |    |
| 585 | Three Simple Properties Explain Protein Stability Change upon Mutation. <b>2021</b> , 61, 1981-1988  | 5  |
| 584 | Rational thermostabilisation of four-helix bundle dimeric de novo proteins. <b>2021</b> , 11, 7526   | 2  |
| 583 | Abundance Imparts Evolutionary Constraints of Similar Magnitude on the Buried, Surface, and Disordered Regions of Proteins. <b>2021</b> , 8, 626729  | 0  |
| 582 | Comprehensive Study on Enhancing Low-Quality Position-Specific Scoring Matrix with Deep Learning for Accurate Protein Structure Property Prediction: Using Bagging Multiple Sequence Alignment Learning. <b>2021</b> , 28, 346-361 | 2  |
| 581 | Protein Cold Denaturation in Implicit Solvent Simulations: A Transfer Free Energy Approach. <b>2021</b> , 125, 5222-5232   | 3  |
| 580 | Cancer-causing BRCA2 missense mutations disrupt an intracellular protein assembly mechanism to disable genome maintenance. <b>2021</b> , 49, 5588-5604   | 8  |
| 579 | Role of the C4 protein PepYLCV in viral symptom determinant: In silico approach. <b>2021</b> , 741, 012055   |    |
| 578 | LanCLs add glutathione to dehydroamino acids generated at phosphorylated sites in the proteome. <b>2021</b> , 184, 2680-2695.e26   | 6  |
| 577 | Molecular Dynamics Simulations of Human Beta-Defensin Type 3 Crossing Different Lipid Bilayers. <b>2021</b> , 6, 13926-13939   | 3  |
| 576 | Localization atomic force microscopy. <b>2021</b> , 594, 385-390   | 20 |
| 575 | VoroContacts: a tool for the analysis of interatomic contacts in macromolecular structures. <b>2021</b> ,  | 0  |

|     |   |    |
|-----|---|----|
| 574 | RosettaSurf - a surface-centric computational design approach.  |    |
| 573 | Analyzing the similarity of protein domains by clustering Molecular Surface Maps. <b>2021</b> , 99, 114-114   | 0  |
| 572 | Broken symmetry between RNA enantiomers in a crystal lattice. <b>2021</b> , 49, 12535-12539   |    |
| 571 | Structural analysis of mammalian protein phosphorylation at a proteome level. <b>2021</b> , 29, 1219-1229.e3  | 2  |
| 570 | Deamidation of the human eye lens protein $\beta$ -crystallin accelerates oxidative aging.  |    |
| 569 | Networks of Networks: An Essay on Multi-Level Biological Organization. <b>2021</b> , 12, 706260   | 7  |
| 568 | Cryo-EM structures of human coagulation factors V and Va. <b>2021</b> , 137, 3137-3144  | 5  |
| 567 | Predicted Coronavirus Nsp5 Protease Cleavage Sites in the Human Proteome: A Resource for SARS-CoV-2 Research.   |    |
| 566 | The effect of temperature and ligand structure on the solubility of gold nanoparticles.   |    |
| 565 | Prediction of protein-protein interaction sites through eXtreme gradient boosting with kernel principal component analysis. <b>2021</b> , 134, 104516   | 10 |
| 564 | Assessing the performances of different continuum solvation models for the calculation of hydration energies of molecules, polymers and surfaces: a comparison between the SMD, VASPsol and FDPB models. <b>2021</b> , 140, 1 | 6  |
| 563 | Atomic Level Investigations of Early Aggregation of Tau43 in Water I. Conformational Propensity of Monomeric Tau43. <b>2021</b> , 42, 1134-1142   |    |
| 562 | Molecular characterization and functional annotation of a hypothetical protein (TDB29877.1) from probiotic bacteria <i>Lactobacillus acidophilus</i> : an in-silico approach.   |    |
| 561 | Structures of full-length VanR from <i>Streptomyces coelicolor</i> in both the inactive and activated states. <b>2021</b> , 77, 1027-1039   | 0  |
| 560 | Molecular dynamics investigation of membrane fouling in organic solvents. <b>2021</b> , 632, 119329   | 3  |
| 559 | Accurate Estimation of Solvent Accessible Surface Area for Coarse-Grained Biomolecular Structures with Deep Learning. <b>2021</b> , 125, 9490-9498  | 0  |
| 558 | Multiscale Water Dynamics on Protein Surfaces: Protein-Specific Response to Surface Ions. <b>2021</b> , 125, 8673-8681  | 4  |
| 557 | Proline Isomerization Regulates the Phase Behavior of Elastin-Like Polypeptides in Water. <b>2021</b> , 125, 9751-9756  | 4  |

|     |   |   |
|-----|---|---|
| 556 | Limited Evidence for a Relationship between HIV-1 Glycan Shield Features in Early Infection and the Development of Neutralization Breadth. <b>2021</b> , 95, e0079721               | 2 |
| 555 | Structure-Property Relationship on the Example of Gas Separation Characteristics of Poly(Arylene Ether Ketone)s and Poly(Diphenylene Phtalide). <b>2021</b> , 11,                   | 0 |
| 554 | Visual Analysis of Large-Scale Protein-Ligand Interaction Data. <b>2021</b> , 40, 394-408   | 1 |
| 553 | The Structural and Dynamical Properties of the Hydration of SNase Based on a Molecular Dynamics Simulation. <b>2021</b> , 26,   | 2 |
| 552 | Quantitative Description of Surface Complementarity of Antibody-Antigen Interfaces. <b>2021</b> , 8, 749784   | 0 |
| 551 | In silico identification of new anti-SARS-CoV-2 agents from bioactive phytocompounds targeting the viral spike glycoprotein and human TLR4. <b>2021</b> , 18,                       | 3 |
| 550 | Inclusion of Levodopa into $\beta$ -Cyclodextrin: A Comprehensive Computational Study. <b>2021</b> , 6, 23814-23825   | 0 |
| 549 | Searching Geometric Patterns in Protein Binding Sites and Their Application to Data Mining in Protein Kinase Structures. <b>2021</b> ,  | 0 |
| 548 | RPocket: an intuitive database of RNA pocket topology information with RNA-ligand data resources. <b>2021</b> , 22, 428   | 2 |
| 547 | DLAB-Deep learning methods for structure-based virtual screening of antibodies. <b>2021</b> ,   | 8 |
| 546 | Generalizing Continuum Solvation in Crystal to Nonaqueous Solvents: Implementation, Parametrization, and Application to Molecules and Surfaces. <b>2021</b> , 17, 6432-6448         | 0 |
| 545 | Biocompatibility of 2D silicon nitride: interaction at the nano-bio interface. <b>2021</b> , 8, 095404  | 2 |
| 544 | Explicit-solvent molecular dynamics simulations revealed conformational regain and aggregation inhibition of I113T SOD1 by Himalayan bioactive molecules. <b>2021</b> , 339, 116798 | 9 |
| 543 | Binding free energy calculation of human beta defensin 3 with negatively charged lipid bilayer using free energy perturbation method. <b>2021</b> , 277, 106662                     | 1 |
| 542 | Computational modeling of protein conformational changes - Application to the opening SARS-CoV-2 spike. <b>2021</b> , 444, 110591   | 2 |
| 541 | Molecular dynamics study of CDC25B mutant causing the activity decrease of CDC25B. <b>2021</b> , 109, 108030  | 0 |
| 540 | Adsorption of Lysozyme on Silica and Aluminosilicate Adsorbents. <b>2021</b> , 95, 188-192  | 1 |
| 539 | Feasibility of Predicting Static Dielectric Constants of Polymer Materials: A Density Functional Theory Method. <b>2021</b> , 13,   | 2 |

|     |   |     |
|-----|---|-----|
| 538 | Allosteric inhibition of SARS-CoV-2 3CL protease by colloidal bismuth subcitrate. <b>2021</b> , 12, 14098-14102         | 5   |
| 537 | ATAC-seq reveals megabase-scale domains of a bacterial nucleoid.  | 2   |
| 536 | Processing and analysis of CASP3 protein structure predictions. <b>1999</b> , 37, 22-29                                 | 46  |
| 535 | Linear extrapolation method of analyzing solvent denaturation curves. <b>2000</b> , 41, 1-7                             | 208 |
| 534 | Calorimetry as an analytical tool in biochemistry and biology. <b>1976</b> , 23, 1-159                                  | 88  |
| 533 | Acquisition and interpretation of hydrogen exchange data from peptides, polymers, and proteins. <b>1982</b> , 28, 1-113 | 62  |
| 532 | Simplified Models for Understanding and Predicting Protein Structure. 57-80   | 9   |
| 531 | Solvents, interfaces and protein structure. <b>1977</b> , 23-45   | 7   |
| 530 | Quantitative Structure-Property Relationships. 1314-1335  | 2   |
| 529 | Prediction of Protein Structure Through Evolution. 1789-1811  | 5   |
| 528 | Sequence and Structure of Proteins. 43-86   | 1   |
| 527 | Tools for Protein Technologies. 325-344   | 7   |
| 526 | Docking enzyme-inhibitor complexes using a preference-based free-energy surface. <b>1996</b> , 25, 403-19               | 209 |
| 525 | A $\mathbb{S}$ hape from the Voronoi Diagram of Atoms for Protein Structure Analysis. <b>2006</b> , 101-110             | 3   |
| 524 | Implicit Solvent Electrostatics in Biomolecular Simulation. <b>2006</b> , 263-295                                       | 24  |
| 523 | Contemporary topics in polymeric materials for biomedical applications. <b>1996</b> , 1-51                              | 82  |
| 522 | Smooth surfaces for multi-scale shape representation. <b>1995</b> , 391-412   | 18  |
| 521 | Computation of Protein Geometry and Its Applications: Packing and Function Prediction. <b>2007</b> , 181-206            | 2   |

|     |   |    |
|-----|---|----|
| 520 | Transfer RNA: crystal structures. <b>1981</b> , 83-112  | 3  |
| 519 | Electrostatic Interactions Associated with Effector Binding to Hemoglobin. <b>1982</b> , 231-241  | 3  |
| 518 | The Folding, Stability and Dynamics of T4 Lysozyme: A Perspective Using Nuclear Magnetic Resonance. <b>1993</b> , 258-304                   | 16 |
| 517 | Predicting Protein Function from Surface Properties. <b>2009</b> , 167-186  | 3  |
| 516 | Atomistic vs. Continuous Representations in Molecular Biology. <b>1999</b> , 146-155  | 2  |
| 515 | Modeling The Effect of Solvation on Structure, Reactivity, and Partitioning of Organic Solutes: Utility in Drug Design. <b>1999</b> , 51-72 | 10 |
| 514 | Solubility. <b>1996</b> , 11-60   | 68 |
| 513 | The GOR Method for Predicting Secondary Structures in Proteins. <b>1989</b> , 417-465   | 37 |
| 512 | Human procathepsin D: three-dimensional model and isolation. <b>1995</b> , 362, 273-8   | 11 |
| 511 | Structural constraints on residue substitution. <b>1992</b> , 14, 231-49  | 3  |
| 510 | Molecular Structure and Protein Variation within and among Populations. <b>1978</b> , 39-100  | 32 |
| 509 | The Structure and Dynamics of Water in Globular Proteins. <b>1982</b> , 387-426   | 14 |
| 508 | X-ray Fiber Diffraction. <b>1982</b> , 3-44   | 6  |
| 507 | Modeling Side Chains in Peptides and Proteins with the Locally Enhanced Sampling/Simulated Annealing Method. <b>1994</b> , 1-41             | 2  |
| 506 | Multiple-Start Monte Carlo Docking of Flexible Ligands. <b>1994</b> , 71-108  | 10 |
| 505 | Molecular Dynamics Studies of Protein and Peptide Folding and Unfolding. <b>1994</b> , 193-230  | 15 |
| 504 | Protein Folding. <b>1980</b> , 43-100   | 6  |
| 503 | Comments on some present and future problems in protein structure. <b>1984</b> , 27, 1-24   | 2  |

|     |   |    |
|-----|---|----|
| 502 | Hydrogen bonding and exchange in oxymyoglobin. <b>1984</b> , 27, 305-22   | 2  |
| 501 | Structure of the Reaction Center from Rhodobacter sphaeroides R-26 and 2.4.1. <b>1988</b> , 5-11  | 18 |
| 500 | Thermodynamic strategies for rational protein and drug design. <b>1995</b> , 7, 219-41  | 10 |
| 499 | Synthetic Protein Surface Domains as Bioactive Stationary Phases. <b>1993</b> , 277-312   | 1  |
| 498 | Molecular Interactions in Hydrophobic Chromatography. <b>1993</b> , 333-359   | 2  |
| 497 | Short Peptide Vaccine Design and Development: Promises and Challenges. <b>2015</b> , 1-14   | 2  |
| 496 | Improving the Accuracy of Fitted Atomic Models in Cryo-EM Density Maps of Protein Assemblies Using Evolutionary Information from Aligned Homologous Proteins. <b>2016</b> , 1415, 193-209     | 3  |
| 495 | CX, DPX, and PCW: Web Servers for the Visualization of Interior and Protruding Regions of Protein Structures in 3D and 1D. <b>2017</b> , 1484, 301-309  | 2  |
| 494 | Protein Hydration. <b>1988</b> , 127-154  | 3  |
| 493 | Protein Hydration. <b>1993</b> , 437-465  | 5  |
| 492 | Hydrophobic Interaction Chromatography. <b>1998</b> , 461-467   | 1  |
| 491 | What can we learn from highly connected beta-rich structures for structural interface design?. <b>2008</b> , 474, 235-53  | 2  |
| 490 | Using Machine Learning in Accuracy Assessment of Knowledge-Based Energy and Frequency Base Likelihood in Protein Structures. <b>2020</b> , 572-584  | 1  |
| 489 | The crystal structures of complexes formed between lysozyme and antibody fragments. <b>1996</b> , 75, 301-19  | 15 |
| 488 | Continuum Electrostatic Analysis of Proteins. <b>2014</b> , 135-163   | 5  |
| 487 | Predicting Protein-Protein Interactions with Weighted PSSM Histogram and Random Forests. <b>2015</b> , 326-335  | 1  |
| 486 | Miyazawa-Jernigan Contact Potentials and Carter-Wolfenden Vapor-to-Cyclohexane and Water-to-Cyclohexane Scales as Parameters for Calculating Amino Acid Pair Distances. <b>2016</b> , 358-365 | 1  |
| 485 | Modeling of Membrane Proteins. <b>2019</b> , 371-451  | 2  |

|     |  |   |
|-----|--|---|
| 484 | Visual Analysis of Biomolecular Surfaces. <b>2008</b> , 237-255  | 5 |
| 483 | Manifoldization of $\mathbb{R}^3$ Shapes by Topology Operators. <b>2008</b> , 505-511  | 4 |
| 482 | A Novel Fuzzy Decision Tree Based Method for Detecting Protein Active Sites. <b>2012</b> , 51-60   | 1 |
| 481 | Top-Down Approach for Protein Binding Sites Prediction Based on Fuzzy Pattern Trees. <b>2013</b> , 325-334   | 1 |
| 480 | Fast and Accurate Calculation of Protein Depth by Euclidean Distance Transform. <b>2013</b> , 7821, 304-316  | 4 |
| 479 | A Supervised Approach to 3D Structural Classification of Proteins. <b>2013</b> , 326-335   | 3 |
| 478 | X-Ray Photoelectron Spectroscopic Studies of Hemocyanin and Superoxide Dismutase. <b>1977</b> , 172-179  | 1 |
| 477 | The Conformation of Glucagon. <b>1983</b> , 37-56  | 5 |
| 476 | Recent Developments in Molecular Graphics. <b>1988</b> , 17-30   | 4 |
| 475 | Structure-Odor Relationships. <b>1994</b> , 9-56   | 3 |
| 474 | Protein folding and unfolding. <b>1977</b> , 24, 282-305   | 2 |
| 473 | Influences of solvent water on the transition state affinity of enzymes, protein folding, and the composition of the genetic code. <b>1980</b> , 32, 43-61 | 2 |
| 472 | Calculation of Hydrodynamic Parameters: US-SOMO. <b>2016</b> , 169-193   | 2 |
| 471 | Three-Dimensional Models of Molecular Structures and Chemical Properties. <b>1989</b> , 675-690  | 1 |
| 470 | Predicting ADME Properties of Chemicals. <b>2016</b> , 1-37  | 2 |
| 469 | Computer Molecular Modelling and Graphic Design. <b>1988</b> , 173-204   | 3 |
| 468 | Molecular basis for the extensibility of elastin. <b>2003</b> , 561-573  | 2 |
| 467 | Visualization Techniques for Science and Engineering. <b>1989</b> , 499-546  | 5 |



|     |  |    |
|-----|--|----|
| 466 | Techniques and Applications of Langevin Dynamics Simulations. <b>1994</b> , 85-138   | 24 |
| 465 | Time scales and fluctuations of protein dynamics: metmyoglobin in aqueous solution. <b>1993</b> , 168-193  | 1  |
| 464 | Structure and Dynamics of Water in Confined Geometry. <b>1994</b> , 307-336  | 10 |
| 463 | Approaches to the Characterisation of Tertiary and Supramolecular Protein Structures by Combination of Protein Chemistry and Mass Spectrometry. <b>1998</b> , 17-43                        | 7  |
| 462 | Variational Methods for Biomolecular Modeling. <b>2017</b> , 181-221   | 1  |
| 461 | Integrated In Silico-In Vitro Identification and Optimization of Bone Morphogenic Protein-2 Armpit Epitope as Its Antagonist Binding Site. <b>2020</b> , 39, 703-710                       | 4  |
| 460 | Accessible Surface Areas of Nucleic Acids and Their Relation to Folding, Conformational Transition, and Protein Recognition. <b>1979</b> , 331-350   | 3  |
| 459 | Predictions of Protein Secondary and Tertiary Structure. <b>1994</b> , 203-232   | 1  |
| 458 | A Model for the Molten Globule State of CTF Generated Using Molecular Dynamics. <b>1993</b> , 525-532  | 3  |
| 457 | The Effects of Local Environments on the Pattern of Amino-Acid Substitution in Homologous Proteins: the Role of Side-Chain to Main-Chain Van Der Waals Interactions. <b>1994</b> , 405-412 | 1  |
| 456 | Applications of Crystallographic Databases in Molecular Design. <b>1990</b> , 261-281  | 2  |
| 455 | X-Ray Structure of Proteins. <b>1977</b> , 403-590   | 27 |
| 454 | THE RELATIONSHIP OF GENE STRUCTURE TO PROTEIN STRUCTURE. <b>1982</b> , 35-54   | 1  |
| 453 | Antigenic Comparison of Animal Lysozymes. <b>1974</b> , 127-141  | 15 |
| 452 | Structure and Chemistry of Lysozyme: pH-Rate Profile, Calorimetric Studies, and Computations on Exposure to Solvent. <b>1974</b> , 251-267   | 3  |
| 451 | Nanosecond Fluorescence Spectroscopy. <b>1984</b> , 181-290  | 3  |
| 450 | E. coli Thioredoxin Stability Is Greatly Enhanced by Substitution of Aspartic Acid 26 by Alanine. <b>1990</b> , 449-456  | 7  |
| 449 | Opposite Surfaces of the Cdc15 F-BAR Domain Create a Membrane Platform That Coordinates Cytoskeletal and Signaling Components for Cytokinesis. <b>2020</b> , 33, 108526                    | 6  |

|     |   |     |
|-----|---|-----|
| 448 | Nuclear magnetic resonance studies of sperm whale myoglobin specifically enriched with <sup>13</sup> C in the methionine methyl groups.. <b>1976</b> , 251, 7452-7460   | 63  |
| 447 | Titration behavior of individual tyrosine residues of myoglobins from sperm whale, horse, and red kangaroo.. <b>1976</b> , 251, 5187-5194   | 30  |
| 446 | Bacillus subtilis alkaline phosphatases III and IV. Cloning, sequencing, and comparisons of deduced amino acid sequence with Escherichia coli alkaline phosphatase three-dimensional structure.. <b>1991</b> , 266, 1077-1084 | 69  |
| 445 | A model for the Ca <sup>2+</sup> -induced conformational transition of troponin C. A trigger for muscle contraction.. <b>1986</b> , 261, 2638-2644  | 240 |
| 444 | A molecular model of the inducer binding domain of the galactose repressor of Escherichia coli.. <b>1994</b> , 269, 13825-13835   | 17  |
| 443 | Pseudomonas exotoxin A mutants. Replacement of surface-exposed residues in domain III with cysteine residues that can be modified with polyethylene glycol in a site-specific manner.. <b>1994</b> , 269, 13398-13404         | 33  |
| 442 | The 1.9 Å x-ray structure of a closed unliganded form of the periplasmic glucose/galactose receptor from Salmonella typhimurium.. <b>1994</b> , 269, 8931-8936  | 95  |
| 441 | Electrostatic interactions in sperm whale myoglobin. Site specificity, roles in structural elements, and external electrostatic potential distributions.. <b>1985</b> , 260, 14070-14082                                      | 26  |
| 440 | Structure at the active site of an acylenzyme of alpha-chymotrypsin and implications for the catalytic mechanism. An electron nuclear double resonance study.. <b>1994</b> , 269, 4577-4586                                   | 11  |
| 439 | Catalytic conformation of carboxypeptidase A. Structure of a true enzyme reaction intermediate determined by electron nuclear double resonance.. <b>1994</b> , 269, 4587-4595   | 22  |
| 438 | Structure of an immunoglobulin Fab fragment specific for poly(dG).poly(dC).. <b>1994</b> , 269, 3605-3614   | 23  |
| 437 | Structure of an immunoglobulin Fab fragment specific for triple-stranded DNA.. <b>1994</b> , 269, 3615-3622   | 28  |
| 436 | Molecular anatomy of the antibody binding site.. <b>1983</b> , 258, 14433-14437   | 97  |
| 435 | The structure of protein-protein recognition sites.. <b>1990</b> , 265, 16027-16030   | 638 |
| 434 | Molecular model of the extracellular lectin-like domain in CD69.. <b>1994</b> , 269, 32457-32463  | 22  |
| 433 | Conformational stability and activity of ribonuclease T1 with zero, one, and two intact disulfide bonds.. <b>1988</b> , 263, 11820-11825  | 338 |
| 432 | The crystal structure of muscle phosphoglucomutase refined at 2.7-angstrom resolution.. <b>1992</b> , 267, 6322-6337  | 65  |
| 431 | L-Arabinose-binding protein-sugar complex at 2.4 Å resolution. Stereochemistry and evidence for a structural change.. <b>1981</b> , 256, 13213-13217  | 49  |

|     |   |     |
|-----|---|-----|
| 430 | Characterization of the antigenic sites on the refined 3-A resolution structure of mouse testicular lactate dehydrogenase C4.. <b>1987</b> , 262, 13155-13162   | 32  |
| 429 | The cDNA sequences encoding two components of the polymeric fraction of the intracellular hemoglobin of <i>Glycera dibranchiata</i> .. <b>1990</b> , 265, 21843-21851   | 11  |
| 428 | The structure of human lymphotoxin (tumor necrosis factor-beta) at 1.9-A resolution.. <b>1992</b> , 267, 2119-2122  | 142 |
| 427 | Alanine scanning mutagenesis identifies surface amino acids on domain II of <i>Pseudomonas</i> exotoxin required for cytotoxicity, proper folding, and secretion into periplasm. <b>1992</b> , 267, 23427-23433 | 16  |
| 426 | Structural evolution of an enzyme specificity. The structure of rat carboxypeptidase A2 at 1.9-A resolution.. <b>1991</b> , 266, 24606-24612  | 35  |
| 425 | Crystal structure of the lysine-, arginine-, ornithine-binding protein (LAO) from <i>Salmonella typhimurium</i> at 2.7-A resolution.. <b>1991</b> , 266, 23893-23899  | 67  |
| 424 | Mapping and molecular modeling of a recognition domain for lysosomal enzyme targeting.. <b>1991</b> , 266, 23365-23372  | 59  |
| 423 | Enzymatic properties of mutant <i>Escherichia coli</i> tryptophan synthase alpha-subunits.. <b>1991</b> , 266, 20205-20212  | 20  |
| 422 | Inaccessibility of tryptophan residues of recombinant human renin to quenching agents.. <b>1987</b> , 262, 10570-10573  |     |
| 421 | The effect of heme-linked ionizable groups on cyanide binding to methemoglobin.. <b>1986</b> , 261, 10576-10581   | 8   |
| 420 | Implications of protein folding. Additivity schemes for volumes and compressibilities.. <b>1988</b> , 263, 4159-4165  | 50  |
| 419 | The Structure of Tumor Necrosis Factor- $\beta$ at 2.6 Å Resolution. <b>1989</b> , 264, 17595-17605   | 389 |
| 418 | Structural Studies of Mutants of T4 Lysozyme That Alter Hydrophobic Stabilization. <b>1989</b> , 264, 16059-16066   | 60  |
| 417 | Conformational stability and mechanism of folding of ribonuclease T1. <b>1989</b> , 264, 11614-11620  | 60  |
| 416 | Conformational stability and activity of ribonuclease T1 and mutants. <b>1989</b> , 264, 11621-11625  | 57  |
| 415 | Immunogenicity of Synthetic Peptides Corresponding to Flexible and Antibody-accessible Segments of Mouse Lactate Dehydrogenase (LDH)-C4. <b>1989</b> , 264, 10513-10519   | 18  |
| 414 | Comparison of the crystal structures and intersubunit interactions of human immunodeficiency and Rous sarcoma virus proteases.. <b>1990</b> , 265, 10492-10496  | 93  |
| 413 | Electrostatic interactions during electron transfer reactions between c-type cytochromes and flavodoxin.. <b>1985</b> , 260, 5568-5573  | 62  |

|     |  |     |
|-----|--|-----|
| 412 | Stomach lysozymes of ruminants. II. Amino acid sequence of cow lysozyme 2 and immunological comparisons with other lysozymes.. <b>1984</b> , 259, 11617-11625  | 37  |
| 411 | A putative glutathione-binding site in T4 glutaredoxin investigated by site-directed mutagenesis. <b>1991</b> , 266, 16105-16112   | 46  |
| 410 | Refined x-ray structure of papain.E-64-c complex at 2.1-A resolution. <b>1991</b> , 266, 14771-14777   | 63  |
| 409 | Rotational motions in myoglobin assessed by carbon 13 relaxation measurements at two magnetic field strengths.. <b>1975</b> , 250, 2238-2242   | 31  |
| 408 | Solvent accessibility in folded proteins. Studies of hydrogen exchange in trypsin. <b>1975</b> , 250, 432-439  | 34  |
| 407 | Two-Angstrom Crystal Structure of Oxidized Chromatium High Potential Iron Protein. <b>1974</b> , 249, 4212-4225  | 187 |
| 406 | Conformational Studies on a Glycosylated Bovine Pancreatic Ribonuclease. <b>1973</b> , 248, 3566-3572  | 49  |
| 405 | Amino Acid Sequence Studies on Bobwhite Quail Egg White Lysozyme. <b>1972</b> , 247, 2905-2916   | 67  |
| 404 | Structural and thermodynamic analysis of compensating mutations within the core of chicken egg white lysozyme.. <b>1992</b> , 267, 10842-10849   | 122 |
| 403 | The 2.3-A resolution structure of the maltose- or maltodextrin-binding protein, a primary receptor of bacterial active transport and chemotaxis.. <b>1991</b> , 266, 5202-5219   | 415 |
| 402 | Thermodynamics of lipid-protein association. The free energy of association of lecithin with reduced and carboxymethylated apolipoprotein A-II from human plasma high density lipoprotein.. <b>1981</b> , 256, 9849-9854 | 31  |
| 401 | Dephosphorylation of rabbit skeletal muscle phosphorylase kinase. Evidence against the operation of the second-site phosphorylation mechanism of regulation.. <b>1981</b> , 256, 3213-3217                               | 32  |
| 400 | Substrate specificity of eukaryotic signal peptidase. Site-saturation mutagenesis at position -1 regulates cleavage between multiple sites in human pre (delta pro) apolipoprotein A-II.. <b>1988</b> , 263, 2070-2078   | 62  |
| 399 | Intramolecular interactions of amino groups in 13C reductively methylated hen egg-white lysozyme.. <b>1982</b> , 257, 2894-2900  | 48  |
| 398 | Topographic antigenic determinants recognized by monoclonal antibodies to sperm whale myoglobin.. <b>1982</b> , 257, 3189-3198   | 105 |
| 397 | Solution structure of GRO/melanoma growth stimulatory activity determined by 1H NMR spectroscopy. <b>1994</b> , 269, 32909-32915   | 42  |
| 396 | Urea and Guanidine Hydrochloride Denaturation of Ribonuclease, Lysozyme, Chymotrypsin, and b-Lactoglobulin. <b>1974</b> , 249, 5388-5393   | 642 |
| 395 | Specificity of the Escherichia coli chaperone DnaK (70-kDa heat shock protein) for hydrophobic amino acids.. <b>1993</b> , 268, 24074-24077  | 34  |

|     |   |    |
|-----|---|----|
| 394 | Heavy chain position 50 is a determinant of affinity and specificity for the anti-digoxin antibody 26-10.. <b>1993</b> , 268, 21739-21747   | 24 |
| 393 | Three-dimensional structure of isonicotinimidylated liver alcohol dehydrogenase.. <b>1983</b> , 258, 5537-5547  | 31 |
| 392 | The multicopper-enzyme ascorbate oxidase. <b>1996</b> , 151-197   | 3  |
| 391 | Multidimensional Global Optimization and Robustness Analysis in the Context of Protein-Ligand Binding. <b>2020</b> , 16, 4669-4684  | 5  |
| 390 | Charge Anisotropy of Nitrogen: Where Chemical Intuition Fails. <b>2020</b> , 16, 4443-4453  | 5  |
| 389 | A chemoproteomic portrait of the oncometabolite fumarate. <b>2019</b> , 15, 391-400   | 37 |
| 388 | Domain interactions reveal auto-inhibition of the deubiquitinating enzyme USP19 and its activation by HSP90 in the modulation of huntingtin aggregation. <b>2020</b> , 477, 4295-4312 | 2  |
| 387 | Protein features identification for machine learning-based prediction of protein-protein interactions.  | 1  |
| 386 | The Human LL-37(17-29) Antimicrobial Peptide Reveals a Functional Supramolecular Nanostructure.   | 2  |
| 385 | Assembly intermediates of orthoreovirus captured in the cell.   | 1  |
| 384 | Modeling the Opening SARS-CoV-2 Spike: an Investigation of its Dynamic Electro-Geometric Properties.  | 1  |
| 383 | The functional landscape of the human phosphoproteome.  | 3  |
| 382 | Less is more: Coarse-grained integrative modeling of large biomolecular assemblies with HADDOCK.  | 1  |
| 381 | The potential of hexatungstotellurate(VI) to induce a significant entropic gain during protein crystallization. <b>2017</b> , 4, 734-740  | 27 |
| 380 | The B-shape and B-complex for three-dimensional spheres. <b>2006</b> ,  | 1  |
| 379 | The thermal unfolding of hevein, a small disulfide-rich protein. <b>1995</b> , 228, 649-52  | 11 |
| 378 | Insights into thermal stability from a comparison of the glutamate dehydrogenases from <i>Pyrococcus furiosus</i> and <i>Thermococcus litoralis</i> . <b>1995</b> , 229, 688-95       | 88 |
| 377 | Method for recovery of enteric viruses from estuarine sediments with chaotropic agents. <b>1983</b> , 46, 379-85  | 40 |

|     |  |    |
|-----|--|----|
| 376 | Molecular cloning, structural analysis, and expression in Escherichia coli of a chitinase gene from Enterobacter agglomerans. <b>1997</b> , 63, 834-9  | 87 |
| 375 | Structure and function of gas vacuoles. <b>1972</b> , 36, 1-32   | 81 |
| 374 | Antibodies against active-site peptides common to glucosyltransferases of mutans streptococci. <b>1993</b> , 61, 4814-7  | 10 |
| 373 | Primate antibody response to immunotoxin: serological and computer-aided analysis of epitopes on a truncated form of Pseudomonas exotoxin. <b>1994</b> , 62, 5055-65   | 20 |
| 372 | Antibodies against a synthetic peptide of the poliovirus replicase protein: reaction with native, virus-encoded proteins and inhibition of virus-specific polymerase activities in vitro. <b>1982</b> , 43, 969-78 | 36 |
| 371 | Antigenic heterogeneity of a foot-and-mouth disease virus serotype in the field is mediated by very limited sequence variation at several antigenic sites. <b>1994</b> , 68, 1407-17                               | 89 |
| 370 | Inner-View of Nanomaterial Incited Protein Conformational Changes: Insights into Designable Interaction. <b>2018</b> , 2018, 9712832   | 29 |
| 369 | Immobilized metal-ion affinity chromatography. <b>2002</b> ,   | 2  |
| 368 | Implicit Solvent Models. <b>2001</b> ,   | 10 |
| 367 | Driving Forces for Protein Adsorption at Solid Surfaces. <b>2003</b> ,   | 4  |
| 366 | Blind testing cross-linking/mass spectrometry under the auspices of the 11 critical assessment of methods of protein structure prediction (CASP11). <b>2016</b> , 1, 24  | 12 |
| 365 | Fibronectin unfolding revisited: modeling cell traction-mediated unfolding of the tenth type-III repeat. <b>2008</b> , 3, e2373  | 40 |
| 364 | Prodepth: predict residue depth by support vector regression approach from protein sequences only. <b>2009</b> , 4, e7072  | 33 |
| 363 | Generating triangulated macromolecular surfaces by Euclidean Distance Transform. <b>2009</b> , 4, e8140  | 82 |
| 362 | Computational protein design: validation and possible relevance as a tool for homology searching and fold recognition. <b>2010</b> , 5, e10410   | 16 |
| 361 | Characterization of protein-protein interaction interfaces from a single species. <b>2011</b> , 6, e21053  | 30 |
| 360 | Bound water at protein-protein interfaces: partners, roles and hydrophobic bubbles as a conserved motif. <b>2011</b> , 6, e24712   | 48 |
| 359 | Bioinformatic analysis of pathogenic missense mutations of activin receptor like kinase 1 ectodomain. <b>2011</b> , 6, e26431  | 12 |

|     |  |     |
|-----|--|-----|
| 358 | Extent of structural asymmetry in homodimeric proteins: prevalence and relevance. <b>2012</b> , 7, e36688  | 44  |
| 357 | The structure of human microplasmin in complex with textilinin-1, an aprotinin-like inhibitor from the Australian brown snake. <b>2013</b> , 8, e54104   | 17  |
| 356 | Prediction of S-glutathionylation sites based on protein sequences. <b>2013</b> , 8, e55512  | 33  |
| 355 | Maximum allowed solvent accessibilities of residues in proteins. <b>2013</b> , 8, e80635   | 190 |
| 354 | Integrating structure to protein-protein interaction networks that drive metastasis to brain and lung in breast cancer. <b>2013</b> , 8, e81035  | 26  |
| 353 | New conformational state of NHERF1-CXCR2 signaling complex captured by crystal lattice trapping. <b>2013</b> , 8, e81904   | 7   |
| 352 | Structural and functional studies of a phosphatidic acid-binding antifungal plant defensin MtDef4: identification of an RGFRRR motif governing fungal cell entry. <b>2013</b> , 8, e82485            | 89  |
| 351 | Cyclotide structure-activity relationships: qualitative and quantitative approaches linking cytotoxic and anthelmintic activity to the clustering of physicochemical forces. <b>2014</b> , 9, e91430 | 15  |
| 350 | Cyanuric acid hydrolase from <i>Azorhizobium caulinodans</i> ORS 571: crystal structure and insights into a new class of Ser-Lys dyad proteins. <b>2014</b> , 9, e99349                              | 8   |
| 349 | Can natural proteins designed with 'inverted' peptide sequences adopt native-like protein folds?. <b>2014</b> , 9, e107647   | 7   |
| 348 | How structure defines affinity in protein-protein interactions. <b>2014</b> , 9, e110085   | 46  |
| 347 | LucY: A Versatile New Fluorescent Reporter Protein. <b>2015</b> , 10, e0124272   | 3   |
| 346 | On the Effect of Sodium Chloride and Sodium Sulfate on Cold Denaturation. <b>2015</b> , 10, e0133550   | 3   |
| 345 | To Hit or Not to Hit, That Is the Question - Genome-wide Structure-Based Druggability Predictions for <i>Pseudomonas aeruginosa</i> Proteins. <b>2015</b> , 10, e0137279                             | 7   |
| 344 | Structure Based Thermostability Prediction Models for Protein Single Point Mutations with Machine Learning Tools. <b>2015</b> , 10, e0138022   | 40  |
| 343 | Analyses of the Sequence and Structural Properties Corresponding to Pentapeptide and Large Palindromes in Proteins. <b>2015</b> , 10, e0139568   | 2   |
| 342 | Comparing Residue Clusters from Thermophilic and Mesophilic Enzymes Reveals Adaptive Mechanisms. <b>2016</b> , 11, e0145848  | 17  |
| 341 | Effect of the Crystal Environment on Side-Chain Conformational Dynamics in Cyanovirin-N Investigated through Crystal and Solution Molecular Dynamics Simulations. <b>2017</b> , 12, e0170337         | 5   |

|     |   |    |
|-----|---|----|
| 340 | The Weighted Mean Curvature Derivative of a Space-Filling Diagram. <b>2020</b> , 8, 51-67   | 2  |
| 339 | Structural changes in thyroid hormone receptor-beta by T3 binding and L330S mutational interactions. <b>2020</b> , 7, 27-40                               | 1  |
| 338 | Alpha influenza virus infiltration prediction using virus-human protein-protein interaction network. <b>2020</b> , 17, 3109-3129                          | 8  |
| 337 | Thermodynamic Principle Revisited: Theory of Protein Folding. <b>2015</b> , 06, 37-48   | 3  |
| 336 | Ben-Naim's Pitfall Don Quixote's Windmill. <b>2013</b> , 03, 13-21  | 3  |
| 335 | Divide-and-conquer strategy for large-scale Eulerian solvent excluded surface. <b>2018</b> , 18, 299-329  | 2  |
| 334 | Calculated Accessibilities and Nucleophilicities of Linear and Cyclic Amines for Carbon Dioxide Absorption Reactions. <b>2011</b> , 32, 2813-2816         | 4  |
| 333 | Protein subunit interfaces: heterodimers versus homodimers. <b>2005</b> , 1, 28-39  | 38 |
| 332 | Insight into gene fusion from molecular dynamics simulation of fused and un-fused IGPS (Imidazole Glycerol Phosphate Synthetase). <b>2006</b> , 1, 99-104 | 4  |
| 331 | Structural inferences for Cholera toxin mutations in <i>Vibrio cholerae</i> . <b>2011</b> , 6, 1-9  | 8  |
| 330 | HIV-1 envelope accessible surface and polarity: clade, blood, and brain. <b>2011</b> , 6, 48-56   | 5  |
| 329 | Insights from the structural analysis of protein heterodimer interfaces. <b>2011</b> , 6, 137-43  | 14 |
| 328 | Accommodation of profound sequence differences at the interfaces of eubacterial RNA polymerase multi-protein assembly. <b>2012</b> , 8, 6-12              | 2  |
| 327 | Prediction of temperature factors from protein sequence. <b>2013</b> , 9, 134-40  | 5  |
| 326 | Comparative Modeling of Protein Structure-Progress and Prospects. <b>1989</b> , 94, 79-84   | 8  |
| 325 | Effect of peptide group-water interaction on $\beta$ -structure conformation. <b>1988</b> , 4, 79-85  | 1  |
| 324 | Hydrophobic contribution to the free energy of complexation of aromatic ligands with DNA. <b>2009</b> , 25, 133-141                                       | 6  |
| 323 | Atomic structures of fibrillar segments of hIAPP suggest tightly mated $\beta$ -sheets are important for cytotoxicity. <b>2017</b> , 6,                   | 76 |



|     |   |    |
|-----|---|----|
| 322 | Structure-based inhibitors of amyloid beta core suggest a common interface with tau. <b>2019</b> , 8,   | 34 |
| 321 | Comprehensive fitness maps of Hsp90 show widespread environmental dependence. <b>2020</b> , 9,  | 18 |
| 320 | A dynamic charge-charge interaction modulates PP2A:B56 substrate recruitment. <b>2020</b> , 9,  | 18 |
| 319 | Enhancement of conformational B-cell epitope prediction using CluSMOTE. <b>2020</b> , 6, e275   | 3  |
| 318 | Prediction of Hydration Structures. <b>2021</b> , 139-162   |    |
| 317 | Hydration Layer Around Proteins. <b>2021</b> , 83-104   |    |
| 316 | Insights from the Interfaces of Corona Viral Proteins: Homomers Versus Heteromers. <b>2021</b> , 14, 1613-1631  |    |
| 315 | In Silico Analysis of Novel Titin Non-Synonymous Missense Variants Detected by Targeted Next Generation Sequencing in a Cohort of Romanian Index Patients with Hypertrophic Cardiomyopathy. <b>2021</b> , 31, 565-571 | 0  |
| 314 | Molecular dynamics simulation study of gold nanosheet as drug delivery vehicles for anti-HIV-1 aptamers. <b>2021</b> , 95, 107595   | 1  |
| 313 | The crystal structure of vaccinia virus protein E2 and perspectives on the prediction of novel viral protein folds.   |    |
| 312 | Spotlight onto surfactant-steam-bitumen interfacial behavior via molecular dynamics simulation. <b>2021</b> , 11, 19660   | 9  |
| 311 | Structural and thermodynamic analyses of human TMED1 (p24 <sup>fl</sup> ) Golgi dynamics. <b>2021</b> , 192, 72-72  | 0  |
| 310 | Loops around the Heme Pocket Have a Critical Role in the Function and Stability of DyP from. <b>2021</b> , 22,  | 1  |
| 309 | Evaluation of SARS-CoV-2 main protease and inhibitor interactions using dihedral angle distributions and radial distribution function. <b>2021</b> , 7, e08220  | 1  |
| 308 | Comprehensive Identification of Deleterious Missense VUS Variants Based on Their Impact on TP53 Structural Stability. <b>2021</b> , 22,   | 0  |
| 307 | Structure Prediction of Binding Sites of MHC Class II Molecules based on the Crystal of HLA-DRB1 and Global Optimization. <b>2000</b> , 157-189   |    |
| 306 | Sequence and Structure of Proteins. <b>2001</b> , 43-86   |    |
| 305 | Tools for Protein Technologies. <b>2001</b> , 325-344   |    |

304 Accessible Surface.

303 Mathematics and Molecular Neurobiology. **2002**, 31-60

302 Protein Structure and Stability: Database-derived Potentials and Prediction.

301 Molecular Surface and Volume.

300 Molecular Models: Visualization.

299 Quantitative StructureProperty Relationships (QSPR).

298 Molecular Surfaces and Solubility.

297 Protein Structure Prediction in 1D, 2D, and 3D.

296 Computer Graphics and Molecular Modeling.

295 Physical Properties and Atmospheric Reactivity of Aqueous Sea Salt Micro-Aerosols. **2003**, 277-293

294 References. **2004**,

293 Improved Maintenance of Molecular Surfaces Using Dynamic Graph Connectivity. **2005**, 401-413 2

292 Protein Simulation Using Fast Volume Preservation. **2006**, 308-315

291 Geometric Modeling of Nano Structures with Periodic Surfaces. **2006**, 343-356 2

290 Solvent effects on biomolecular dynamics simulations: A comparison between TIP3P, SPC and SPC/E water models acting on the Glucocorticoid receptor DNA-binding domain. **2006**, 123-135

289 Molecular Dynamics Study on the Activation Mechanism of p47phox in the Auto-Inhibited Form. **2006**, 5, 81-92

288 The Protein as a Supermolecule: The Architecture of a  $\beta$  Barrel. 235-309

287 Protein-protein interaction: an analysis by computer simulation. **1991**, 161, 237-49; discussion 250-2 2

- 286 Influence of local structure on the location of antigenic determinants in tobacco mosaic virus protein. **1986**, 119, 76-92 3
- 285 BioBrowser Visualization of and Access to Macro-Molecular Structures. **2008**, 257-273 1
- 284 Nuclear magnetic resonance studies of mobility in proteins. **1983**, 93, 310-28 2
- 283 Non-invasive techniques in the study of cataract development at the metabolic and protein molecular level. **1984**, 106, 248-65
- 282 Protein Folding: Energetics.
- 281 Proteins: Computational Analysis.
- 280 The Shape and Complex for Analysis of Molecular Structures. **2009**, 47-66 2
- 279 Creating Datasets. **2009**, 27-64
- 278 Tools and Techniques. **2009**, 65-77
- 277 Solvent Effects and Chemical Reactivity. **2009**, 1 1
- 276 Basic Principles of Protein-Protein Interaction. **2009**, 1-19
- 275 References. **2009**, 303-335
- 274 Identifying the nature of the interface in protein-protein complexes. **2010**,
- 273 Wrapping as a Selectivity Filter for Molecular Targeted Therapy: Preliminary Evidence. **2010**, 97-115
- 272 Macromolecular Crystallographic Computing. **2010**, 1-36
- 271 Chromatography, Hydrophobic Interaction. 1
- 270 Method for Protein Active Sites Detection Based on Fuzzy Decision Trees. **2011**, 143-150 1
- 269 Biomolecular Recognition. **2012**, 1-50 0

268 Background. **2012**, 5-25

267 Introduction. **2013**, 1-15

266 Alpha Complexes. **2014**, 33-39

265 Crystalline-State Reaction and Reaction Cavity. **2014**, 5-18

264 Hemoglobin Interaction in Sickle Cell Fibers: Theoretical Approaches to the Molecular Contacts. **1976**, 389-407

263 ACTIVATION, ACTION AND INHIBITION OF TRYPSIN AS DEDUCED FROM THE THREEDIMENSIONAL STRUCTURES OF TRYPSINOGEN, TRYPSIN AND THEIR COMPLEXES WITH THE BASIC PANCREATIC TRYPSIN INHIBITOR. **1978**, 15-34

262 Strategy for Pure Hydrophobic Chromatography. **1978**, 357-362

1

261 MYOGLOBIN AS A MODEL OF PROTEIN FOLDING. **1981**, 133-149

260 Is It Possible to Deduce the Interaction Between Two Proteins from Their Three-Dimensional Structure?. **1981**, 199-211

259 PREDICTION OF TERTIARY STRUCTURES IN GLOBULAR PROTEINS: SOME ESSENTIAL PARAMETERS. **1981**, 151-167

258 Evolving Nucleotide Binding Surfaces. **1981**, 415-422

257 Protein Folding - Pages 522-556. **1982**, 522-556

256 Serology and Immunochemistry of Plant Viruses - Pages 206-267. **1982**, 206-267

255 Packing Densities and Iron-Sulfur Proteins. **1982**, 361-364

254 REFERENCES. **1984**, 230-294

253 Fine Specificity of Monoclonal Anti-Lysozyme Antibodies and the Three-Dimensional Structure of a Lysozyme-Antibody Complex. **1987**, 219-226

252 New Ways to Look at Old Proteins. **1987**, 3-19

251 Theoretical studies of protein structure. **1988**, 21-26

250 Synthetic Peptides as Immunogens. **1988**, 93-106

249 The use of neutrons to show how proteins work. **1988**, 46, 63-78

248 PROTEIN CONFORMATIONAL PREDICTION. **1990**, 135-145

247 An Approach to the Design of Anti-Influenza Agents. **1990**, 61-74

1

246 Preferred Interaction Patterns from Crystallographic Databases. **1990**, 229-253

1

245 Visualization Techniques and Windowing Interfaces: KGNRAF, XWIB and REMOTE. **1990**, 1021-1090

244 Beziehungen Zwischen Struktur und Geruch. **1990**, 11-56

243 Interactive Visualization Techniques for Chemistry: KGNRAF, XWIB and REMOTE. **1991**, 1139-1190

242 Physicochemical Basis of Hydrophobic Interaction Chromatography. **1992**, 443-480

1

241 Patterns in Secondary Structure Packing Database for Prediction. **1992**, 127-140

240 Molecular Dynamics Computer Modelling and Protein Engineering. **1992**, 123-152

239 Structural Properties of Proteins Predicted by Neural Networks. **1992**, 293-304

238 Principles of Protein Protein Recognition in Protease-Inhibitor and Antigen-Antibody Complexes. **1993**, 103-114

237 Response : Alpha Helix Propensity of Amino Acids. **1993**, 262, 917-918

1

236 Molecular Dynamics Simulation of a DNA Binding Protein free and in Complex with DNA. **1994**, 441-456

1

235 Protein-Protein Recognition: An Analysis by Docking Simulation. **1994**, 331-337

234 Identical mutations at corresponding positions in two homologous proteins with nonidentical effects. **1994**, 269, 11196-11200

6

233 Molecular surface comparisons. **1995**, 163-186

- 232 Screening Three-Dimensional Databases for Lead Finding. **1995**, 111-128
- 231 An Anti-Idiotypic Antibody as a Functional Mirror Image of a Viral Antigen. **1997**, 341-345
- 230 The Structure and Thermodynamics of Antibody-Protein Antigen Interactions. **1997**, 37-50
- 229 . **1997**,
- 228 Three-Dimensional Structure of Neocarzinostatin. **1997**, 109-128
- 227 Incorporation of solvation energy contributions for energy refinement and folding of proteins. **1997**, 270-283
- 226 Molecular Modeling of Ligand and Mutation Sites of the Type A Domains of Human von Willebrand Factor and Their Relevance to von Willebrand's Disease. **1998**, 91, 2032-2044
- 225 Chapter 3 Electrostatic effects in proteins: Experimental and computational approaches. **1999**, 61-97
- 224 Graphics Native Approach to Identifying Surface Atoms of Macromolecules. **2015**, 85-97
- 223 Computational Chemistry: From the Hydrogen Molecule to Nanostructures. **2015**, 1-17
- 222 Prediction of Lysine Acetylation Sites in Porcine Pancreas Lipase Modified by the Ionic Liquids Using Molecular Dynamics Simulations. **2015**, 365-379
- 221 The Biomolecular Interface as a Selectivity Filter for Drug-Based Targeted Therapy. **2015**, 175-192
- 220 Myoglobin. 1-8
- 219 Parallel Computing of the Adaptive N-Body Treecode Algorithm for Solving Boundary Integral Poisson-Boltzmann Equation. **2016**, 82-89
- 218 Cancer: Viruses, Attractors, Fractals. **2016**, 93-124
- 217 Epistructural Selectivity Filters for Molecular Targeted Therapy. **2016**, 217-237
- 216 Molecular Fields to Assess Recognition Forces and Property Spaces?. **2016**, 0
- 215 Multiwavelet Boundary Element Method for Cavities Admitting Many NURBS Patches. **2016**, 06, 69-93 2

214 Blind testing cross-linking/mass spectrometry under the auspices of the 11th critical assessment of methods of protein structure prediction (CASP11).

213 Crystal structure and RNA-binding properties of an Hfq homolog from the deep-branching Aquificae: Conservation of the lateral RNA-binding mode.

212 The relationship between relative solvent accessible surface area (rASA) and irregular structures in protean segments (ProSs). **2016**, 12, 381-387

211 Protein Features Identification for Machine Learning-Based Prediction of Protein-Protein Interactions. **2017**, 305-317

1

210 Sweep Dynamics (SD) plots: Computational identification of selective sweeps to monitor the adaptation of influenza A viruses.

209 Salt-bridge Networks within Globular and Disordered Proteins [Characterizing Trends for Designable Interactions.

208 Interactome INSIDER: a multi-scale structural interactome browser for genomic studies.

2

207 Vermont: a multi-perspective visual interactive platform for mutational analysis.

206 Effects of Force Fields on the Conformational and Dynamic Properties of Amyloid  $\beta$ (1-40) Dimer Explored by Replica Exchange Molecular Dynamics Simulations.

205 Tools and Techniques. **2018**, 75-94

204 Creating Datasets for Bioinformation. **2018**, 33-73

203 Introduction. **2018**, 1-14

202 Identifying G protein-coupled receptor dimers from crystal packings.

201 An accurate and robust algorithm for solvent-excluded surface computation.

200 Extreme Amyloid Polymorphism in Staphylococcus aureus Virulent PSM Peptides.

199 Computer Processing of Chemical Structure Information. 43-119

198 PEPOP: new approaches to mimic non-continuous epitopes.

197 A Volumetric Survey of Cavities and Electrostatic Patterns in Protein-RNA Binding Sites. **2019**,

- 196 Phylogenetic, sequence and structural analysis of Insulin superfamily proteins reveals an indelible link between evolution and structure-function relationship.
- 195 Structure-Based Discovery of a Novel Small-Molecule Inhibitor of Methicillin-Resistant *S. aureus*.
- 194 A physics-based energy function allows the computational redesign of a PDZ domain. 1
- 193 Allosteric inhibition of adenylyl cyclase type 5 by G-protein: a molecular dynamics study.
- 192 The Amphibian Antimicrobial Peptide Uperin 3.5 is a Cross-~~β~~Cross-~~β~~Chameleon Functional Amyloid. 1
- 191 Preparing For the Next Pandemic: Learning Wild Mutational Patterns At Scale For Analyzing Sequence Divergence In Novel Pathogens.
- 190 Molecular insights into the interaction of 5-fluorouracil and FeO nanoparticles with beta-casein: An experimental and theoretical study. **2021**, 267, 120538 1
- 189 Post-translational insertion of boron in proteins to probe and modulate function. **2021**, 17, 1245-1261 4
- 188 Theoretical and Experimental Conformational Analysis of Some Synthetic and Natural Peptides. **1983**, 209-225
- 187 Conformational Fluctuations and Enzymatic Activity. **1983**, 271-282
- 186 Application of Meta Learning to B-Cell Conformational Epitope Prediction. **2020**, 2131, 375-397
- 185 Free Energy Calculation Methods Used in Computer Simulations. **2020**, 137-188
- 184 Aggregation of methacrylate-based ternary biomimetic antimicrobial polymers in solution. **2020**, 33, 064003 2
- 183 Residues at the interface between zinc binding and winged helix domains of human RECQ1 play a significant role in DNA strand annealing activity. **2021**, 49, 11834-11854 2
- 182 Influence of spatial structure on protein damage susceptibility  $\Delta$  a bioinformatics approach.
- 181 Engineering of Cytolethal Distending Toxin B by Its Reducing Immunogenicity and Maintaining Stability as a New Drug Candidate for Tumor Therapy; an In Silico Study. **2021**, 13, 1
- 180 Thermostabilization mechanisms in thermophilic versus mesophilic three-helix bundle proteins. **2022**, 43, 197-205
- 179 DNA steric accessibility for water molecules and ions in the case of B-D transition. **1989**, 5, 66-70 1



|     |  |     |
|-----|--|-----|
| 178 | Hydrophobicity maps and docking of molecular fragments with solvation. <b>2000</b> , 145-169   | 0   |
| 177 | Figures for 6, References for 6. 6030-6032   |     |
| 176 | 5.1.3 Results. 351-356   |     |
| 175 | 5.1.4 References for 5.1. 413-414  |     |
| 174 | Real-Time Triangulation of Molecular Surfaces. <b>2007</b> , 55-67   | 2   |
| 173 | Structural asymmetry along protein sequences and co-translational folding.   |     |
| 172 | A 3D Structural Interactome to Explore the Impact of Evolutionary Divergence, Population Variation, and Small-molecule Drugs on SARS-CoV-2-Human Protein-Protein Interactions. |     |
| 171 | X-ray Diffraction Studies of $\Phi$ 1-Dinitrophenyl-Ribonuclease-S. <b>1973</b> , 248, 5291-5298   | 14  |
| 170 | Genetic engineering in the Precambrian: structure of the chicken triosephosphate isomerase gene. <b>1985</b> , 5, 3497-3506  | 15  |
| 169 | Insights into the functional architecture of the catalytic center of a maize beta-glucosidase Zm-p60.1. <b>2001</b> , 127, 973-85  | 10  |
| 168 | Macromolecular chelation as an improved mechanism of protease inhibition: structure of the ecotin-trypsin complex. <b>1994</b> , 13, 1502-7                                    | 14  |
| 167 | Nobel lecture. The photosynthetic reaction centre from the purple bacterium <i>Rhodospseudomonas viridis</i> . <b>1989</b> , 8, 2149-70  | 133 |
| 166 | Strategies for differential sensory responses mediated through the same transmembrane receptor. <b>1993</b> , 12, 1897-905   | 8   |
| 165 | Definition and spatial location of mouse interleukin-2 residues that interact with its heterotrimeric receptor. <b>1993</b> , 12, 5113-9                                       | 14  |
| 164 | Outline structure of the human L1 cell adhesion molecule and the sites where mutations cause neurological disorders. <b>1996</b> , 15, 6050-9                                  | 45  |
| 163 | The outline structure of the T-cell alpha beta receptor. <b>1988</b> , 7, 3745-55  | 172 |
| 162 | Correlation of exons with structural domains in alcohol dehydrogenase. <b>1984</b> , 3, 1307-10  | 30  |
| 161 | Location of 'continuous' antigenic determinants in the protruding regions of proteins. <b>1986</b> , 5, 409-13   | 77  |

|     |   |    |
|-----|---|----|
| 160 | Variable domain-linked oligosaccharides of a human monoclonal IgG: structure and influence on antigen binding. <b>1999</b> , 338 ( Pt 2), 529-38  | 16 |
| 159 | Thermodynamic and kinetic analysis of the Escherichia coli thioredoxin-C' fragment complementation system. <b>1999</b> , 339 ( Pt 3), 721-7   | 4  |
| 158 | Crystal structure of the anti-(carcinoembryonic antigen) single-chain Fv antibody MFE-23 and a model for antigen binding based on intermolecular contacts. <b>2000</b> , 346 Pt 2, 519-28 | 15 |
| 157 | Structural studies on the ribbon-to-helix transition in profilin: actin crystals. <b>1995</b> , 68, 12S-17S; discussion 17S-18S   | 8  |
| 156 | Degradation of C1-inhibitor by plasmin: implications for the control of inflammatory processes. <b>1997</b> , 3, 385-96   | 5  |
| 155 | Combining sequence and structural profiles for protein solvent accessibility prediction. <b>2008</b> , 7, 195-202   | 2  |
| 154 | Scatter-search with support vector machine for prediction of relative solvent accessibility. <b>2013</b> , 12, 52-63  | 3  |
| 153 | Effect of monovalent salt concentration and peptide secondary structure in peptide-micelle binding.. <b>2021</b> , 11, 36836-36849  | 3  |
| 152 | Evidence for an N-halohistidyl Intermediate in the Catalytic Cycle of Vanadium Chloroperoxidase (VCPO) and an Artificial Enzyme derived from VCPO: A Computational Investigation.         |    |
| 151 | Molecular modeling piloted analysis for semicarbazone derivative of curcumin as a potent Abl-kinase inhibitor targeting colon cancer. <b>2021</b> , 11, 506                               | 0  |
| 150 | A 3D structural SARS-CoV-2-human interactome to explore genetic and drug perturbations. <b>2021</b> , 18, 1477-1488   | 3  |
| 149 | Investigation of microcystin conformation and binding towards PPP1 by molecular dynamics simulation. <b>2021</b> , 109766   | 0  |
| 148 | Molecular dynamics study of the effects of static and oscillating electric fields in ovalbumin. <b>2022</b> , 75, 102911  | 4  |
| 147 | Structure of recombinantly expressed cockroach Lili-Mip protein in glycosylated and deglycosylated forms.. <b>2021</b> , 1866, 130064   | 0  |
| 146 | Probing In Silico the Benzimidazole Privileged Scaffold for the Development of Drug-like Anti-RSV Agents.. <b>2021</b> , 14,  | 0  |
| 145 | Supramolecular assembly of protein building blocks: from folding to function.. <b>2022</b> , 9, 4   | 2  |
| 144 | Atomistic mechanism of leptin and leptin-receptor association.. <b>2022</b> , 1-18  | 1  |
| 143 | Identification of Anticancer and Anti-inflammatory Drugs from Drug-target Interaction Descriptors by Machine Learning... <b>2022</b> , 19,  |    |

|     |  |    |
|-----|--|----|
| 142 | Data set and fitting dependencies when estimating protein mutant stability: Toward simple, balanced, and interpretable models.. <b>2022,</b>                   | 0  |
| 141 | A Rationalization of the Effect That TMAO, Glycine, and Betaine Exert on the Collapse of Elastin-like Polypeptides.. <b>2022, 12,</b>                          |    |
| 140 | Rare by Natural Selection: Disulfide-Bonded Supramolecular Antimicrobial Peptides.. <b>2022,</b>   | 0  |
| 139 | Structural basis for continued antibody evasion by the SARS-CoV-2 receptor binding domain. <b>2022,</b><br>375,  | 15 |
| 138 | The crystal structure of vaccinia virus protein E2 and perspectives on the prediction of novel viral protein folds.. <b>2022, 103,</b>                         | 0  |
| 137 | Molecular descriptors suggest stapling as a strategy for optimizing membrane permeability of cyclic peptides.. <b>2022, 156, 065101</b>                        |    |
| 136 | Advanced computational tools for quantitative analysis of protein-nucleic acid interfaces. <b>2022, 163-180</b>  |    |
| 135 | Identification of the SARS-CoV-2 surface therapeutic targets and drugs using molecular modeling methods for inhibition the virus entry.. <b>2022, 132488</b>   | 1  |
| 134 | Weak formulations of the nonlinear Poisson-Boltzmann equation in biomolecular electrostatics. <b>2022, 126065</b>  | 1  |
| 133 | HBD-2 binds SARS-CoV-2 RBD and blocks viral entry: Strategy to combat COVID-19.. <b>2022, 103856</b>   | 1  |
| 132 | Continuous and Discrete Radius Functions on Voronoi Tessellations and Delaunay Mosaics. <b>2022,</b><br>67, 811  | 0  |
| 131 | PM3 Method based QSAR Study of the Derivatives of Thiadiazole and Quinoxaline for Antiepileptic Activity using Topological Descriptors. <b>2022, 7, 99-110</b> |    |
| 130 | Docking effects of curcuminoid ligands on protein L stability using molecular dynamics simulation with temperature variations. <b>2022,</b>                    |    |
| 129 | Impact of drug aggregation on the structural and dynamic properties of Triton X-100 micelles.. <b>2022,</b>  | 1  |
| 128 | Accurate prediction of immunoglobulin proteins using machine learning model. <b>2022, 29, 100885</b>   | 3  |
| 127 | Structural and functional determinants inferred from deep mutational scans.  |    |
| 126 | Can the Jigsaw Puzzle Model of Protein Folding Re-assemble a Hydrophobic Core?. <b>2022,</b>   | 0  |
| 125 | Extended DeepILST for Various Thermodynamic States and Applications in Coarse-Graining.. <b>2022,</b>  | 1  |

|     |  |   |
|-----|--|---|
| 124 | Simulation analysis of selective alanine mutation effect on stability of human prion protein.. <b>2022</b> , 1-11  |   |
| 123 | Towards optimal boundary integral formulations of the Poisson-Boltzmann equation for molecular electrostatics.. <b>2022</b> ,  | 2 |
| 122 | Capturing a Crucial 'Disorder-to-Order Transition' at the Heart of the Coronavirus Molecular Pathology-Triggered by Highly Persistent, Interchangeable Salt-Bridges.. <b>2022</b> , 10,              | 0 |
| 121 | RosettaSurf-A surface-centric computational design approach.. <b>2022</b> , 18, e1009178   | 0 |
| 120 | The implication of holocytochrome c synthase mutation in Korean familial hypoplastic amelogenesis imperfecta.. <b>2022</b> , 1   | 0 |
| 119 | Pressure-sensitive conversions between Cassie and Wenzel wetting states on a nanocorrugated surface. <b>2022</b> , 128, 1  | 0 |
| 118 | Molecular Dynamics Calculations of Partial Molar Volumes of Amino Acids in Aqueous Solutions.  |   |
| 117 | Deamidation of the human eye lens protein $\beta$ -crystallin accelerates oxidative aging.. <b>2022</b> ,  | 2 |
| 116 | Probing RNA structures and functions by solvent accessibility: an overview from experimental and computational perspectives.. <b>2022</b> ,  | 1 |
| 115 | Coarse-Grained Molecular Dynamics Simulations of Paclitaxel-Loaded Polymeric Micelles.. <b>2022</b> ,  | 0 |
| 114 | Comparative Analysis of SARS-CoV-2 Variants of Concern, Including Omicron, Highlights Their Common and Distinctive Amino Acid Substitution Patterns, Especially at the Spike ORF.. <b>2022</b> , 14, | 5 |
| 113 | HIV-1 infections with multiple founders associate with the development of neutralization breadth.. <b>2022</b> , 18, e1010369  | 1 |
| 112 | In Silico and In Vitro Evaluations of Fluorophoric Thiazolo-[2,3-b]quinazolinones as Anti-cancer Agents Targeting EGFR-TKD.. <b>2022</b> , 1   |   |
| 111 | Probing Site-Selective Conjugation Chemistries for the Construction of Homogeneous Synthetic Glycodendriproteins.. <b>2022</b> , e202200020  |   |
| 110 | Predicted coronavirus Nsp5 protease cleavage sites in the human proteome.. <b>2022</b> , 23, 25  | 3 |
| 109 | Inferring bound structure and residue specific contributions to binding energetics in the Intrinsically Disordered Protein, CcdA.  | 1 |
| 108 | Electrostatic free energies carry structural information on nucleic acid molecules in solution.. <b>2022</b> , 156, 134201   | 0 |
| 107 | Mutation in Eth A protein of Mycobacterium tuberculosis conferred drug tolerance against enthinoamide in Mycobacterium smegmatis mc155.. <b>2022</b> , 98, 107677                                    | 0 |

|     |   |   |
|-----|---|---|
| 106 | NSAID solubilisation promotes morphological transitions in Triton X-114 surfactant micelles. <b>2022</b> , 356, 119050  | 1 |
| 105 | A multi-objective approach for the protein structure prediction problem. <b>2021</b> ,  |   |
| 104 | Predicting Protein-Peptide Complex Structures by Accounting for Peptide Flexibility and the Physicochemical Environment.. <b>2021</b> ,   | 1 |
| 103 | Evolutionary conservation of protein dynamics: insights from all-atom molecular dynamics simulations of 'peptidase' domain of Spt16.. <b>2021</b> , 1-13  | 0 |
| 102 | Machine learning activation energies of chemical reactions.   | 0 |
| 101 | X-ray diffraction and Density Functional Theory based structural analyses of 2-phenyl-4-(prop-2-yn-1-yl)-1,2,4-triazolone. <b>2021</b> , 12, 459-468  |   |
| 100 | Label-Free Higher Order Structure and Dynamic Investigation Method of Proteins in Solution Using an Enzymatic Reactor Coupled to Electrospray High-Resolution Mass Spectrometry Detection.. <b>2021</b> ,           |   |
| 99  | Capturing a crucial Disorder-to-order transition at the heart of the coronavirus molecular pathology triggered by highly persistent, interchangeable salt-bridges.  |   |
| 98  | Probing Allosteric Hsp70 Inhibitors by Molecular Modelling Studies to Expedite the Development of Novel Combined F508del CFTR Modulators.. <b>2021</b> , 14,  | 1 |
| 97  | Electrostatic Interactions Contribute to the Overall Structural Stability in Small Interfaces of Corona Viral Spike Glycoproteins. <b>2022</b> , 15, 433-444  |   |
| 96  | Modified Cyclodextrins: Rosmarinic acid inclusion complexes as functional food ingredients show improved operations (solubility, stability and antioxidant activity). <b>2022</b> , 107731                          | 1 |
| 95  | Energy Landscapes for Base-Flipping in a Model DNA Duplex.. <b>2022</b> ,   | 0 |
| 94  | Investigation of the physico-chemical interaction of ct-DNA with Anticancer Glycine Derivative of Pt-complex by applying docking and MD simulation methods and multi-spectroscopic techniques. <b>2022</b> , 133115 | 1 |
| 93  | Distal Mutations Shape Substrate-Binding Sites during Evolution of a Metallo-Oxidase into a Laccase. 5022-5035  |   |
| 92  | Molecular Face. <b>2022</b> , 375-390   | 1 |
| 91  | Data_Sheet_1.PDF. <b>2019</b> ,   |   |
| 90  | Data_Sheet_1.pdf. <b>2020</b> ,   |   |
| 89  | Table_1.CSV. <b>2021</b> ,  |   |

|    |  |   |
|----|--|---|
| 88 | Table_2.CSV. <b>2021</b> ,   |   |
| 87 | Overlapping synthetic peptides as a tool to map protein-protein interactions FSH as a model system of nonadditive interactions.. <b>2022</b> , 130153              | 0 |
| 86 | Reductive site-selective atypical $\gamma$ -type/N <sub>2</sub> -C <sub>2</sub> cleavage allows C-terminal protein amidation.. <b>2022</b> , 8, eabl8675           | 0 |
| 85 | Contribution of hydrophobic interactions to protein mechanical stability.. <b>2022</b> , 20, 1946-1956   | 0 |
| 84 | OUP accepted manuscript.   | 0 |
| 83 | fastDRH: a webserver to predict and analyze protein-ligand complexes based on molecular docking and MM/PB(GB)SA computation.. <b>2022</b> ,                        | 5 |
| 82 | Genome interpretation using in silico predictors of variant impact.. <b>2022</b> , 1   | 0 |
| 81 | Modulation of Human Transthyretin Stability by the Mutations at Histidine 88 Studied by Free Energy Simulation.. <b>2022</b> ,                                     | 0 |
| 80 | Nanoporous SiO <sub>x</sub> plasma polymer films as carrier for liquid-infused surfaces.   |   |
| 79 | Mechanics of Biosurfactant Aided Liquid Phase Exfoliation of 2D Materials. <b>2022</b> , 100098  |   |
| 78 | A Non-Bornian Approach to the Standard Gibbs Energy of Ion Transfer at the Oil   Water Interface. <b>2022</b> , 68, 3-14   |   |
| 77 | Structure-based interface engineering methodology in designing a thermostable amylose-forming transglucosylase. <b>2022</b> , 102074                               | 1 |
| 76 | The Effect of Ethanol on Mutant Human Prion Protein using Molecular Dynamics Simulations. <b>2022</b> ,  |   |
| 75 | Glucosylation mechanism of resveratrol through the mutant Q345F sucrose phosphorylase from the organism Bifidobacterium adolescentis: a computational study.       | 0 |
| 74 | A comparative analysis of machine learning classifiers for predicting protein-binding nucleotides in RNA sequences. <b>2022</b> , 20, 3195-3207                    |   |
| 73 | RPpocket: An RNA-Protein Intuitive Database with RNA Pocket Topology Resources. <b>2022</b> , 23, 6903   | 1 |
| 72 | MoloVol: an easy-to-use program for analyzing cavities, volumes and surface areas of chemical structures. <b>2022</b> , 55,  | 5 |
| 71 | Towards a transferable nonelectrostatic model for continuum solvation: The electrostatic and nonelectrostatic energy correction model. <b>2022</b> , 43, 1372-1387 |   |

- 70 Some Clues about Enzymes from Psychrophilic Microorganisms. **2022**, 10, 1161 ○
- 69 Curvature and temperature-dependent thermal interface conductance between nanoscale-gold and water. 1
- 68 Molecular dynamics of fibric acids. **2022**, 13, 186-195
- 67 Investigation of the conformation of human prion protein in ethanol solution using molecular dynamics simulations. 1-10
- 66 Core packing of well-defined X-ray and NMR structures is the same. **2022**, 31,
- 65 A Process for the Design and Development of Novel Bone Morphogenetic Protein-7 (BMP-7) Mimetics With an Example: THR-184. 13, ○
- 64 Prediction of allosteric druggable pockets of cyclin-dependent kinases. **2022**, 23, 1
- 63 Molecular models of hematite, goethite, kaolinite, and quartz: Surface terminations, ionic interactions, nano topography, and water coordination. **2022**, 650, 129585 ○
- 62 SHREC 2022: Protein-ligand binding site recognition. **2022**, 107, 20-31 1
- 61 Automated prediction of site and sequence of protein modification with ATRP initiators. ○
- 60 Free energy simulations to study mutational effect of a conserved residue, Trp24, on stability of human serum retinol-binding protein. 1-11
- 59 On the Molecular Driving Force of Protein-Protein Association. **2022**, 2, 240-247
- 58 Micro-electron diffraction structure of the aggregation-driving N-terminus of Drosophila neuronal protein Orb2A reveals amyloid-like  $\beta$ -sheets. **2022**, 102396 ○
- 57 Modeling protein structure as a stable static equilibrium. **2022**, 106,
- 56 Molecular simulations of fluoxetine in hydrated lipid bilayers, as well as in aqueous solutions containing  $\beta$ -cyclodextrin. **2022**, 117, 108305
- 55 Technology development to evaluate the effectiveness of viscosity reducing excipients. **2022**, 626, 122204 ○
- 54 INN: Interfaced neural networks as an accessible meshless approach for solving interface PDE problems. **2022**, 470, 111588 ○
- 53 Convergence of a diffuse interface Poisson-Boltzmann (PB) model to the sharp interface PB model: A unified regularization formulation. **2023**, 436, 127501 ○

- 52 Explaining Small Molecule Binding Specificity with Volumetric Representations of Protein Binding Sites. **2022**, 17-45 ○
- 51 Computational Study on the Dynamics of Mycobacterium Tuberculosis RNA Polymerase Assembly. **2022**, 61-79 ○
- 50 Large Variability and Complexity of Isothermal Solubility for a Series of Redox-Active Phenothiazines. ○
- 49 Simple and high-precision DFT-QSPR prediction of enthalpy of combustion for sesquiterpenoid high-energy-density fuels. **2023**, 332, 126157 ○
- 48 EISA-Score: Element Interactive Surface Area Score for Protein-Ligand Binding Affinity Prediction. **2022**, 62, 4329-4341 1
- 47 Automated prediction of site and sequence of protein modification with ATRP initiators. **2022**, 17, e0274606 ○
- 46 Alternating one-phase and two-phase crystallization mechanisms in octahedral patchy colloids. **2022**, 157, 134501 ○
- 45 Protein Redesign and Engineering Using Machine Learning. **2022**, 247-282 ○
- 44 Machine Learning Approaches to Improve Prediction of Target-Drug Interactions. **2022**, 21-96 ○
- 43 Molecular dynamics simulations and solid-state nuclear magnetic resonance spectroscopy measurements of Cβ bond order parameters and effective correlation times in a POPC-GM3 bilayer. **2022**, 24, 25588-25601 ○
- 42 The influence of saturation on the surface structure of mixed fatty acid-on-water aerosol: a molecular dynamics study. ○
- 41 Coarse-Graining ddCOSMO through an Interface between Tinker and the ddX Library. **2022**, 126, 8827-8837 ○
- 40 Multi-model predictive analysis of RNA solvent accessibility based on modified residual attention mechanism. ○
- 39 Comparative analyses and molecular videography of MD simulations on WT human SOD1. **2022**, 1217, 113929 ○
- 38 Quantifying In Situ Structural Stabilities of Human Blood Plasma Proteins Using a Novel Iodination Protein Stability Assay. 1
- 37 Analysis of Residue Interface Preference in Protein-DNA Complexes and Its Application in Recognition of Binding Interface. **2022**, 10, 47-54 ○
- 36 Molecular Dynamics Simulations of Rhodamine B Zwitterion Diffusion in Polyelectrolyte Solutions. **2022**, 126, 10256-10272 ○
- 35 The impact of genetically controlled splicing on exon inclusion and protein structure. ○



|    |   |   |
|----|---|---|
| 34 | HBD-2 variants and SARS-CoV-2: New insights into inter-individual susceptibility. 13,   | 0 |
| 33 | Number of Hydrogen Bonds per Unit Solvent Accessible Surface Area: A Descriptor of Functional States of Proteins.   | 0 |
| 32 | IRAA : A statistical tool for investigating a protein-protein interaction interface from multiple structures. <b>2023</b> , 32,   | 0 |
| 31 | MUG: a mutation overview of GPCR subfamily A17 receptors. <b>2022</b> ,   | 0 |
| 30 | A Structure-Based Mechanism for the Denaturing Action of Urea, Guanidinium Ion and Thiocyanate Ion. <b>2022</b> , 11, 1764  | 0 |
| 29 | Human Transaldolase and Cross-Reactive Viral Epitopes Identified by Autoantibodies of Multiple Sclerosis Patients. <b>1999</b> , 163, 4027-4032   | 4 |
| 28 | Valproate Coenzyme-A Conjugate Blocks Opening of Receptor Binding Domains in the Spike Trimer of SARS-CoV-2 through an Allosteric Mechanism. <b>2023</b> ,  | 1 |
| 27 | Computing the Volume, Surface Area, Mean, and Gaussian Curvatures of Molecules and Their Derivatives.   | 0 |
| 26 | The Relevance of Cavity Creation for Several Phenomena Occurring in Water. <b>2023</b> , 3, 57-65   | 0 |
| 25 | CAT-Site: Predicting Protein Binding Sites Using a Convolutional Neural Network. <b>2023</b> , 15, 119  | 0 |
| 24 | Non-enzymatic glycation of human angiogenin: Effects on enzymatic activity and binding to hRI and DNA. <b>2022</b> ,  | 0 |
| 23 | ProtRAP: Predicting Lipid Accessibility Together with Solvent Accessibility of Proteins in One Run.   | 0 |
| 22 | Structure of a 28.5 kDa duplex-embedded G-quadruplex system resolved to 7.4 Å resolution with cryo-EM.  | 0 |
| 21 | PCV2 Uptake by Porcine Monocytes Is Strain-Dependent and Is Associated with Amino Acid Characteristics on the Capsid Surface.   | 0 |
| 20 | Structure and Behavior of Oxide-Coated Aluminum in Contact with Acidic and Alkaline Aqueous Solutions-A Reactive Molecular Dynamics Simulation Study. <b>2023</b> , 127, 2493-2507                              | 0 |
| 19 | A computational strategy for therapeutic development against superoxide dismutase (SOD1) amyloid formation: effect of polyphenols on the various events in the aggregation pathway. <b>2023</b> , 25, 6232-6246 | 0 |
| 18 | Assessing the functional impact of protein binding site definition.   | 0 |
| 17 | Mutational scan inferred binding energetics and structure in intrinsically disordered protein CcdA. <b>2023</b> , 32,   | 0 |

- 16 Prediction of hydrophilic and hydrophobic hydration structure of protein by neural network optimized using experimental data. **2023**, 13, ○
- 15 Improving enzymatic performance of antioxidant enzyme catalase in combination with [Mn (phen)<sub>2</sub> Cl.H<sub>2</sub>O]Cl<sub>2</sub> complex. **2023**, 37, ○
- 14 Intrinsic Dynamics of the ClpXP Proteolytic Machine Using Elastic Network Models. **2023**, 8, 7302-7318 1
- 13 Quantification of the atomic surfaces and volumes of a metal cluster based on the molecular surface model. **2023**, 98, 045704 ○
- 12 Linear scaling computation of forces for the domain-decomposition linear Poisson-Boltzmann method. **2023**, 158, 104105 ○
- 11 Heterogeneous and Allosteric Role of Surface Hydration for Protein-Ligand Binding. **2023**, 19, 1875-1887 ○
- 10 An AKT1-and TRIM21-mediated phosphodegron controls proteasomal degradation of HuR enabling cell survival under heat shock. **2023**, 26, 106307 ○
- 9 Effects of Terahertz Radiation on the Aggregation of Alzheimer's A $\beta$ 2 Peptide. **2023**, 24, 5039 ○
- 8 Molecular basis of sulfolactate synthesis by sulfolactaldehyde dehydrogenase from *Rhizobium leguminosarum*. ○
- 7 RPFlex: A Coarse-Grained Network Model for RNA Pocket Flexibility Study. **2023**, 24, 5497 ○
- 6 Lipocalin 2  $\mu$ mutation screen and serum levels in patients with anorexia nervosa or obesity and in lean individuals. 14, ○
- 5 An Affordable Topography-Based Protocol for Assigning a Residue's Character on a Hydropathy (PARCH) Scale. ○
- 4 Nanodisc-embedded cytochrome P450 P3A4 binds diverse ligands by distributing conformational dynamics to its flexible elements. **2023**, 244, 112211 ○
- 3 Combining QM/MM Calculations with Classical Mining Minima to Predict Protein-Ligand Binding Free Energy. ○
- 2 In silico characterization of nanoparticles. **2023**, 25, 13228-13243 ○
- 1 An updated dataset and a structure-based prediction model for protein-RNA binding affinity. ○